

12-2015

# Control of thermoforming process parameters to manufacture surfaces with pin-based tooling

Vijay Sarthy Mysore Sreedhara  
Clemson University, vsreedh@clemson.edu

Follow this and additional works at: [https://tigerprints.clemson.edu/all\\_theses](https://tigerprints.clemson.edu/all_theses)

 Part of the [Mechanical Engineering Commons](#)

---

## Recommended Citation

Sreedhara, Vijay Sarthy Mysore, "Control of thermoforming process parameters to manufacture surfaces with pin-based tooling" (2015). *All Theses*. 2258.

[https://tigerprints.clemson.edu/all\\_theses/2258](https://tigerprints.clemson.edu/all_theses/2258)

This Thesis is brought to you for free and open access by the Theses at TigerPrints. It has been accepted for inclusion in All Theses by an authorized administrator of TigerPrints. For more information, please contact [kokeefe@clemson.edu](mailto:kokeefe@clemson.edu).

CONTROL OF THERMOFORMING PROCESS PARAMETERS TO  
MANUFACTURE SURFACES WITH PIN-BASED TOOLING

---

A Thesis  
Presented to  
the Graduate School of  
Clemson University

---

In Partial Fulfillment  
of the Requirements for the Degree  
Master of Science  
Mechanical Engineering

---

by  
Vijay Sarthy Mysore Sreedhara  
December 2015

---

Accepted by:  
Dr. Gregory Mocko, Committee Chair  
Dr. Joshua Summers, Committee Member  
Dr. Hongseok Choi, Committee Member

## ABSTRACT

Many manufacturing processes used to mass produce parts rely on expensive and time consuming tooling. These processes include sheet metal forming, injection molding, casting, and thermoforming. The time invested in design and development of tooling can be justified for high-production volumes. However, for low-volume production and customized products, the tooling investment cannot be amortized. Flexible tooling has been developed to address the needs of smaller production volumes. Reconfigurable pin tooling is an example of flexible tooling that relies on a matrix of adjustable-height pins to produce approximate surfaces. A key challenge in pin-based tooling is achieving accurate high quality surfaces due to the undulations caused by the pins in mimicking the desired shape. This research studies the effects of process parameters on surface quality. A testbed pin tool and thermoformer are fabricated to support this research. The pin tool comprises of a 10 by 10 matrix of square pins. Each pin measures 0.25 inch by 0.25 inch by 2.5 inches and is actuated manually using screws. Twenty-one exploratory and thirty-two shape specific experiments were conducted with 12 inch by 12 inch polystyrene sheets to check the feasibility of producing undulation-free surfaces. The parameters that influence the quality of the surfaces are heating time, sheet thickness, and sheet to fixture distance. Surface quality is measured by conformance with respect to the tool and the intensity of undulations. The surface-reproducibility and the measurement-repeatability errors were determined to be  $\pm 0.0045$  mm and  $\pm 0.00027$  mm respectively. The surface quality can be improved by reducing intensity of undulations by controlling the process parameters. The

quality of thermoformed surfaces using the pin tool is a function of heating time and the intended shape.

## DEDICATION

I dedicate this thesis to my late grandfather Mr. Sreenivasa Iyengar who is my role model, and to my family for supporting me throughout this journey.

## ACKNOWLEDGEMENTS

I would like to thank everybody who helped me through the journey of completing this thesis.

Firstly, I would like to express my earnest gratitude to my advisor Dr. Gregory Mocko for his knowledge, support, and guidance throughout my masters, making it a great learning experience. I would like to convey my heartfelt thanks to Dr. Joshua Summers and Dr. Hongseok Choi for being on my committee, guiding me, and encouraging me through this journey.

I would like to express my gratitude to all the lab members of Clemson Engineering Design Applications and Research (CEDAR), especially the ones in EIB 136- Rahul Renu, Zach Satterfield, Anthony Garland, Sebastian Barner, Maddison Maddox, Shubhamkar Kulkarni, and Varun Kumar Singh to name a few, for their good hearted humor, knowledge, and thoughtfulness during this journey.

I would like to acknowledge the Mechanical Engineering department which gave me financial support and the opportunities to serve as grading and lab assistants. I would also like to thank the administrative staff of the Mechanical Engineering department for all their help throughout this program.

I am grateful to Dr. Vincent Ervin, Dr. Eleanor Jenkins, Dr. Hyesuk Lee, and Dr. Qingshan Chen from the Mathematical Sciences department for giving me the opportunity to serve as grading assistant for their courses.

I also would like to thank my apartment mates, both former and current, Sumanth Ram, Pratik Khurana, Mit Dave, Achyut Jamadagni, Nakul Ravikumar, and Rishwanth Surapaneni for making me feel at home away from home.

Last but not the least, I would like to thank my parents and my grandmother for their love, belief, and support throughout my life.

## TABLE OF CONTENTS

	<u>Page</u>
Abstract.....	ii
Dedication.....	iv
Acknowledgements.....	v
Table of Contents.....	vii
List of tables.....	x
List of tables (continued) .....	xi
List of figures.....	xii
List of figures (continued) .....	xiii
List of figures (continued) .....	xiv
List of figures (continued) .....	xv
Chapter 1: Introduction.....	1
1.1 Flexibility and Reconfigurability.....	1
1.2 Motivation.....	1
1.3 Research objectives .....	3
1.4 Outline of the thesis:.....	5
Chapter 2: Literature review .....	6
2.1 Pin actuators in the HCI domain.....	6
2.2 Pin actuators in the manufacturing domain .....	9
2.3 Key conclusions from this chapter .....	19
Chapter 3: Experimental setup.....	22
3.1 Thermoforming Process.....	22



Table of Contents (Continued)

	<u>Page</u>
3.2 Application of the pin-tool to thermoforming and experimentation .....	24
3.3 Qualitative Analysis of the initial experiments .....	27
3.4 Key conclusions from this chapter .....	40
Chapter 4: Shape specific experimentation.....	42
4.1 Quantifying quality of the surfaces.....	42
4.2 Surface Reproducibility of the thermoformer.....	43
4.3 Shape specific experimentation .....	49
4.4 Comparison of produced surfaces with the desired surface .....	51
4.5 Key conclusions from this chapter .....	81
Chapter 5: Conclusions and future work .....	83
5.1 Conclusions .....	83
5.2 Future research directions.....	85
Chapter 6: References .....	88
Appendices.....	93
Appendix A: Summary of the pin actuation techniques in manufacturing.....	94
Appendix B: Aligner.....	96
Appendix C: Osada's Radom point generator [43]: matlab code .....	99
Appendix D: Coarse alignment and registration ON CloudCompare® .....	102
D.1 Opening the point clouds .....	102
D.2 Orientation and 3-point registration.....	103
D.3 Trimming the aligned cloud.....	106

Table of Contents (Continued)

	<u>Page</u>
D.4 Sub-sampling and registration .....	108
D.5 Comparing the clouds .....	110
Appendix E: Hypotheses tests .....	114
E.1 Hypotheses test for Reproducibility .....	114
E.2 Hypotheses test for repeatability of registration .....	116

## LIST OF TABLES

<u>Table</u>	<u>Page</u>
Table 2.1: Summary of pin actuator user interfaces in HCI .....	7
Table 2.2: Key learnings from the literature review .....	20
Table 3.1: Design variables in experiments .....	28
Table 3.2: Summary of experiment conditions.....	29
Table 3.3: Qualitative evaluation rubric for surface quality .....	30
Table 3.4: Surface quality rating for each experiment.....	30
Table 4.1: Cloud to cloud distances for reproducibility .....	45
Table 4.2: Design variables for shape specific experiments.....	50
Table 4.3: DOE variables for each shape.....	51
Table 4.4: Repeatability of registration .....	54
Table 4.5: Horizontal surface point cloud to point cloud distance comparison.....	59
Table 4.6: Inclined surface point cloud to point cloud distance comparison.....	63
Table 4.7: Concave surface point cloud to point cloud distance comparison.....	67
Table 4.8: Convex surface point cloud to point cloud distance comparison .....	71
Table 4.9: Standard deviations for individual shapes .....	76
Table 4.10: One way ANOVA table.....	77
Table 4.11: LSD calculations table.....	79
Table.A.1: Summary of the pin actuation techniques in manufacturing .....	94
Table E.1: Comparison of surfaces with benchmark surface for reproducibility.....	114

List of Tables (Continued)

<u>Table</u>	<u>Page</u>
Table E.2: Pairwise mean differences.....	115
Table E.3: Comparison of surfaces for repeatability of registration.....	116
Table E.4: Pairwise standard deviation differences.....	117

## LIST OF FIGURES

<u>Figure</u>	<u>Page</u>
Figure 1.1: Pin-art toy .....	2
Figure 1.2: Limitations of the pin tool .....	4
Figure 2.1: Pin actuators as user interfaces: (a) FEELEX [9], (b) Digital Clay [11], and (c) inFORM [12] .....	8
Figure 2.2: Anstead’s leaf-spring forming tool [13] .....	9
Figure 2.3: 50 by 50 pin matrix comprising of 1mm pins [19] .....	11
Figure 2.4: Hexagonal pin with square pinhead [25] .....	13
Figure 2.5: Pin-tool with the interpolator .....	15
Figure 2.6: (a) Round pin heads, and (b) Square pin heads [33] .....	17
Figure 2.7: Machinable screw pin tooling [35] .....	18
Figure 3.1: Stage by stage representation of the thermoforming process .....	23
Figure 3.2: Reconfigurable pin tool .....	24
Figure 3.3: Experimental Setup; 1. Heating element, 2. Frame, 3. Pin-tool location, 4. Vacuum chamber .....	25
Figure 3.4: Schematic representation of the experimental process .....	26
Figure 3.5: Parabolic shape produced (a) with the interpolator and (b) without the interpolator .....	31
Figure 3.6: Parabolic shape produced (a) Heating time of 5 minutes, (b) Heating time of 4 minutes. ....	31

List of Figures (Continued)

<u>Figure</u>	<u>Page</u>
Figure 3.7: Ordinal Logistic regression: Rating vs Heating time, material thickness, and vacuum .....	34
Figure 3.8: Ordinal Logistic regression: Rating vs Heating time, and material thickness.....	35
Figure 3.9: Ordinal Logistic regression: Rating vs Heating time, and vacuum.....	36
Figure 3.10: (a) A parabolic shape and (b) a parabolic bowl.....	37
Figure 3.11: Different shapes produced to understand the capabilities of the pin tool .....	39
Figure 4.1: Conformance of the produced surface with respect to the tool.....	43
Figure 4.2: Registered surfaces in CloudCompare® .....	44
Figure 4.3: Distance between plastic sheet and the pin tool .....	50
Figure 4.4: Schematic representation of registered surfaces .....	52
Figure 4.5: Actuated shape for the horizontal surface .....	58
Figure 4.6: Template for horizontal shape.....	58
Figure 4.7: Horizontal surface: Intensity of undulations versus heating time .....	61
Figure 4.8: Actuated shape for the inclined surface .....	62
Figure 4.9: Template for inclined shape .....	62
Figure 4.10: Inclined surface: Intensity of undulations versus heating time .....	64
Figure 4.11: Actuated shape for the concave parabolic surface .....	65

List of Figures (Continued)

<u>Figure</u>	<u>Page</u>
Figure 4.12: Template for concave shape .....	66
Figure 4.13: Concave surface: Intensity of undulations versus heating time .....	68
Figure 4.14: Actuated shape for the parabolic convex surface .....	69
Figure 4.15: Template for convex shape.....	70
Figure 4.16: Convex surface: Intensity of undulations versus heating time.....	72
Figure 4.17: Main effects plot of undulations vs heating time and Shape.....	74
Figure 4.18: Interaction plot of undulations vs heating time and shape .....	74
Figure 4.19: Plastics contact with the pins.....	80
Figure 5.1: Contact points on the pin tool.....	86
Figure B.1: Aligner.....	96
Figure B.2: Aligner and the surface mounted on to the pin tool.....	97
Figure B.3: Horizontal surface modeled with alignment features.....	98
Figure D.1: User interface of CloudCompare®.....	102
Figure D.2: Pop-up window to complete importing point clouds.....	103
Figure D.3: Move/orient and 3-point registration icons.....	104
Figure D.4: Pop-up to swap the reference and to-be-aligned clouds.....	105
Figure D.5: 3 point registration for coarse alignment.....	106
Figure D.6: Sequence of operations for trimming.....	107
Figure D.7: Procedure to determine the number of points in the reference cloud.....	108
Figure D.8: Sequence of operations for trimming.....	109

List of Figures (Continued)

<u>Figure</u>	<u>Page</u>
Figure D.9: Sequence of operations for fine registration.....	110
Figure D.10: Sequence of operations for fine registration.....	111
Figure D.11: Octree level and splitting the X, Y, and Z components.....	112
Figure D.12: Sequence of operations to extract cloud to cloud z distances.....	113
Figure D.13: Sequence of operations for frequency distribution of z distances.....	113



## CHAPTER 1: INTRODUCTION

*The purpose of this chapter is:*

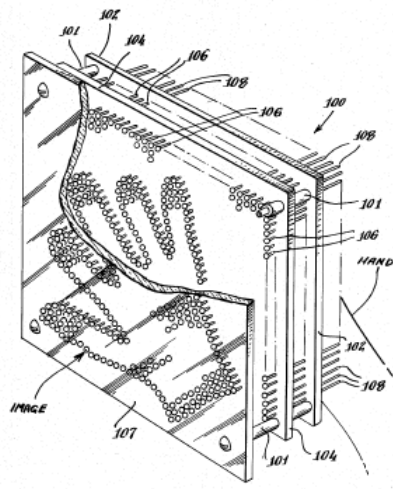
- *To give an overview of the concept of pin actuation and thereby, introduce the reconfigurable pin tooling.*
- *To explain the motivation behind the work presented in the thesis.*
- *To state the research objectives and approach to accomplish the same.*

### **1.1 Flexibility and Reconfigurability**

Manufacturing environments are subject to changes with respect to global competition or rapidly evolving technology [1]. Often times, engineering changes result in evolution of products during their life cycle and the manufacturers have to adapt to these ever changing situations quickly. Flexibility will enable the manufacturer to adapt and implement the changes efficiently. For example, assembling different bodies on a single frame has proved to be advantageous and has added flexibility and reconfigurability enabling the assembly of different models on a single assembly line (Product-platforming) [2].

### **1.2 Motivation**

Reconfigurability of a system may be defined as its ability to rearrange and change its constituents economically [3]. An example of a reconfigurable system is the pin-art [4]. The pin art system comprises of pins that take the shape of any object actuating them from underneath (see Figure 1.1).



(a) Patent [4]



(b) Commercially available [5]

**Figure 1.1: Pin-art toy**

A similar system in the reconfigurable pin tool would add adaptability to a certain manufacturing setting. Considering an example where a car manufacturer decides to redesign the hood, a new stamping tool would be required to implement the new design. The engineering change timeline would depend on the time taken to design and develop the tool, which may be a deterring factor to successful change implementation. Whereas, a reconfigurable tool will alter the timeline significantly.

Different shapes could be produced using the reconfigurable tool and the shapes could be changed in real time. Conventional tools on the other hand, are shape-specific and cannot be easily modified to cater to the needs of a new part and manufacturing a new forming die is a time consuming process.

The computational simulation tool developed in [6] predicts the time taken to manufacture a 2176×230 mm<sup>2</sup> piercing and trimming die producing a 0.8mm thick part to be about 3200 hours(~4.5 months). The system tool also predicts the cost for the die to be around \$20000. This paper was published in 2003 and the current cost accounting for an average inflation rate of 2.33% yields a cost of approximately \$26000 [7].

Rapid prototyping has been used to decrease mold manufacturing times [8], but a reconfigurable tool would better address the above mentioned drawbacks of a conventional forming/molding tool.

### **1.3 Research objectives**

A reconfigurable tool has potential to replace conventional tooling, but has a few limitations. The major limitations are: (i) the undulations caused by the pins need to be smoothed to match the quality from a conventional tool, and (ii) the cross-sectional size of the pins and their arrangement significantly impacts the parts that could be manufactured.

Figure 1.2 shows the limitations of the pin tool. Figure 1.2 (a) shows the surface produced on a pin tool in comparison with the desired surface. The surface produced on the pin tool will have bumps and valleys (called as undulations) which are undesirable. Figure 1.2 (b) shows the cross-sectional size of the pins restricting the part dimensions. If the cross-sectional dimension of the pin in the view shown is “x”, then the projection of the desired part must be divisible by “x” to be manufactured on the pin tool.

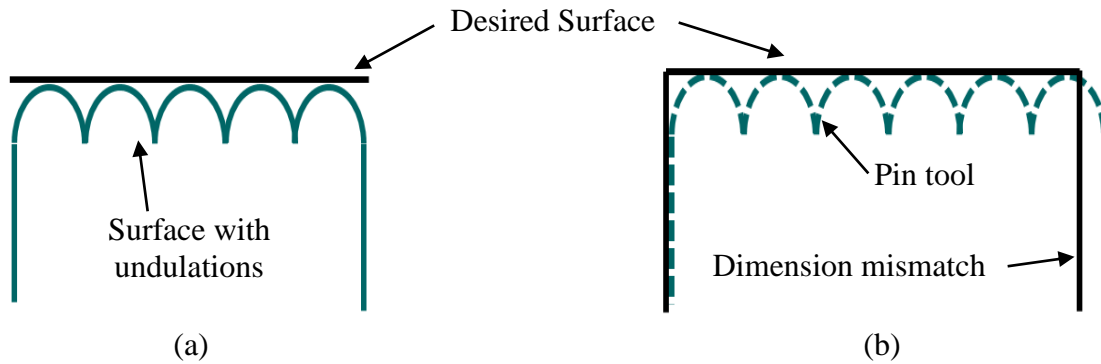


**Figure 1.2: Limitations of the pin tool**

The pins could be made smaller to address the first drawback. This would increase the cost investment and may not be beneficial in comparison to the conventional tooling. The second drawback can be addressed by adding a membrane or machining the pins to the desired shape. These approaches will result in a hindrance either in terms of cost or in terms of an additional process to the reconfigurability of the tool.

Based on this preliminary understanding, the research objectives are listed below. The reason for choosing thermoforming is discussed in the following chapter.

**Research objective 1:** Understand the advantages and limitations of using the pin tool in thermoforming.

**Research objective 2:** Increase surface-quality by reducing the intensity of undulations without (a) reducing the pin size and (b) the smoothening membrane.

**Research objective 3:** Understand the effect of the process parameters on the quality of the surfaces produced and identify the significant parameters.

#### **1.4 Outline of the thesis:**

The work presented in this thesis is divided into five chapters. The current chapter introduces the concept of pin actuation in accordance with flexibility and reconfigurability and gives an overview of the research. The second chapter discusses the various applications of the pin actuator concept by surveying the literature available and identifies possible research opportunities. The third chapter discusses the application of reconfigurable pin tool to thermoforming. Experiments are conducted to understand the capabilities of the pin tool. The fourth chapter describes the shape specific experimentations carried out, their comparisons with the desired surface, and the quantitative analyses that follow. The fifth chapter discusses the results, conclusions from the qualitative and quantitative analyses and lays foundation towards the future research directions.

The ability to change shape in real time has led to inventors and researchers implementing the concept of pin-actuation in various domains, which will be discussed in the next chapter.

## CHAPTER 2: LITERATURE REVIEW

*The purpose of this chapter is:*

- *To conduct a literature review to understand the various applications of the pin tool.*
- *To identify possible guidelines for using the reconfigurable pin tool.*
- *To review the current state-of-the-art and identify research opportunities.*

Researchers have used pin actuator matrices as user interfaces in the Human Computer Interaction (HCI) domain [9–12]. In the manufacturing domain, the pin-actuator matrices have been used as forming tools [14–16, 18, 23, 29, 30], fixtures [20–22], and molding tools [24, 25, 27, 32]. The following sections discuss the research work pertaining to these two domains.

### **2.1 Pin actuators in the HCI domain**

HCI researchers have developed user interfaces with pin matrices to form specific shapes and thereby, interacting with the users. FEELEX [9], Digital Clay [10], [11], and inFORM [12] are a few notable works. The key take away from reviewing the literature pertaining to the user interfaces is the actuation techniques that have been developed for the rapid response requirement, which can be implemented to the pin tool to automate the actuation mechanism. Table 2.1 summarizes the pin actuators used in these papers.

**Table 2.1: Summary of pin actuator user interfaces in HCI**

<b>Paper</b>	<b>Matrix</b>	<b>Overall size</b>	<b>Pin shape and size</b>	<b>Max actuation height</b>	<b>Pin tip</b>	<b>Spacing between pins</b>	<b>Actuation mechanism</b>
Feelex [7]	6 by 6	240 mm by 240 mm	Not available	80 mm	Flat	8 mm	DC motor
Digital clay [9]	10 by 10	Not available	< 3 mm in diameter	> 50 mm (exact value is not given)	Flat	< 3mm between the pin centres	Micro fluidic actuators and high pressure control valves
inFORM [10]	30 by 30	381 mm by 381 mm	Square with area of c/s 9.525 mm <sup>2</sup>	100 mm	Flat	3.175 mm	Slide potentiometer

FEELEX [9] was one of the first pin-based user interfaces (see Figure 2.1(a)). It was developed to create haptic sensation aligned to images by actuating the pins. An image is projected over a thin membrane laid on top of an equally spaced pin matrix. The pins are actuated based on the actual subject of interest in the image. The actuated pins give a three dimensional impression to the image. The users interact with the system by touching the image projected onto the membrane. Each actuator is actuated by its own DC motor.

Digital Clay [10] was intended to be an interface to interact with *Computer Aided Design* (CAD) models (see Figure 2.1(b)). Inspired by FEELEX, one of the concepts of Digital Clay looked at using a set pin actuators instead of a computer mouse as the user interface. The idea was that the user's interaction with the pin actuators would result in the modification of a solid model displayed on the computer screen.

In continuation, the control techniques for the pin actuators of Digital Clay is discussed by Zhu and Book in [11]. Authors discuss a 10 by 10 prototype matrix comprising of pins less than 3 mm in diameter. Micro fluidic actuators and high pressure control valves displace the pins and non-contact resistance position sensors sense the user's interaction with the pin matrix.

inFORM [12], a shape display similar to FEELEX which incorporated dynamic shape change was developed by Follmer and colleagues (see Figure 2.1(c)). It comprises of a 30 by 30 matrix of polystyrene pins having a square cross-sectional area of 9.525 mm<sup>2</sup>. The pins are actuated based on the user's hand gestures, which are tracked by a motion sensor. The actuation mechanism comprised of individual motors for the pins driven by slide potentiometers.

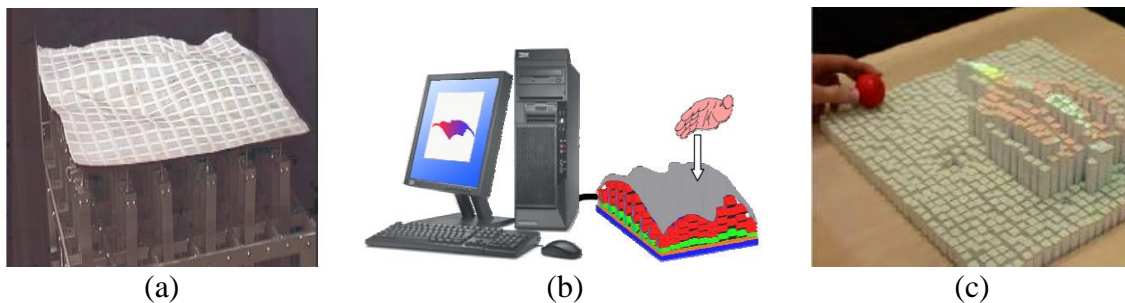


**Figure 2.1: Pin actuators as user interfaces: (a) FEELEX [9], (b) Digital Clay [11], and (c) inFORM [12]**

The following section discusses prior work pertaining to the implementation of pin matrices as manufacturing tools.



## 2.2 Pin actuators in the manufacturing domain

Sheet metal forming and plastic molding are possibly two of the most explored areas as far as implementation of a pin-tool in a manufacturing process is concerned. The idea of using an array or matrices of pins as a manufacturing tool is not new. In the patent dated 1892 [13], Anstead describes a leaf spring forming machine using a reconfigurable pin tool. Two opposite rows of compactly arranged pins constitute the forming tool (see Figure 2.2). Different sized spacers actuate the pins to form the desired shape.

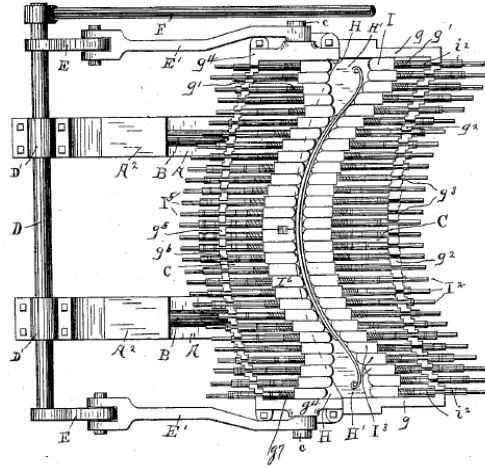


**Figure 2.2: Anstead's leaf-spring forming tool [13]**

Pinson [14], discusses a sheet metal forming tool similar to that of Anstead's. The tool's punch and die are made of equally spaced pin-actuator rams actuated by stepper motors setting them to the desired shape. Each ram is fitted with a round ram-head to improve the surface finish.

Nakajima [15] describes a sheet metal forming tool inspired by the pin-actuation concept. The forming die is made of densely packed thin wires which are actuated to the desired shape by a numerically controlled milling machine.

Nakajima's concept was explored further by Walczyk and Hardt [16]. They discuss a generalized procedure for designing the pin-tool with respect to the pin dimensions, clamping forces, and increasing the pin matrix's ability to withstand the forming forces. They determine the factors influencing the load path during operation to be the pin-to-pin and pin-to-frame friction. They recommend the best pin-shape to ensure load path isolation to be a square cross-section as the pin matrix provides a plane surface for the clamping fixture.

On similar lines, Kirby and Stauffer [17] determine the most appropriate pin type for a variable geometry mold. They study the load paths for pin matrices comprising of different pin shapes, and conclude as Walczyk and Hardt in [16] that the close packed square pins are best suited to withstand the forming loads. They also state that flat tops mitigate the dimpling effect depending on the geometry desired.

Walczyk and colleagues [18], to form aircraft body panels, have developed a pin based tooling system. Their primary focus is the hydraulic actuation system. Numerically controlled solenoid valves control individual pins by either of the two methods- (a) Open loop computer control: Individual pin heights are obtained using the time taken by each pin to move a certain distance. (b) Closed loop computer control: Individual pin heights are obtained by a setting platen that moved upward.

Cook and colleagues [19] discuss an actuation mechanism that can actuate a large group of pins of 1 mm by 1mm cross-section at an accuracy of  $+0.09$  mm  $-0.05$ mm. They use Shape Memory Alloy actuators to actuate the pins and state that a matrix of 15000 pins can be actuated in 50 minutes and could be improved to approximately 3 minutes. A 50 by 50 matrix of pins is shown in Figure 2.3.

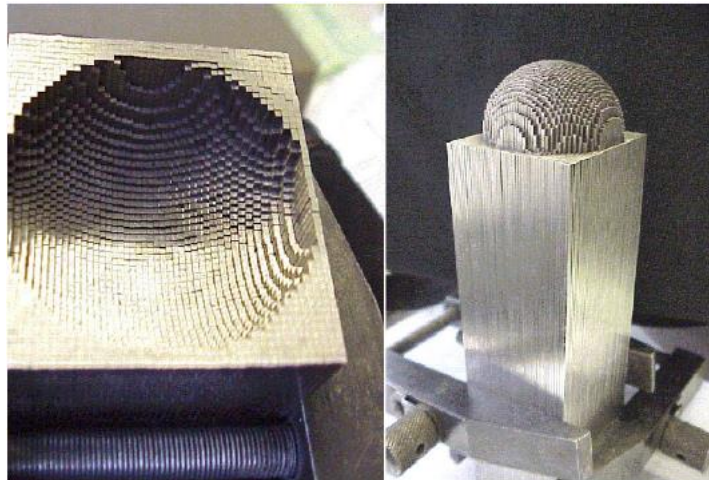


**Figure 2.3: 50 by 50 pin matrix comprising of 1mm pins [19]**

Soderberg and colleagues [20] describe an idea for a flexible tooling system similar to the pin tool. They describe the invention of a fixture for supporting work pieces/components to be assembled. The fixture comprises of cylindrical actuator actuated to complement the workpiece/component geometry using computers. The workpiece/component are constrained using vacuum pressure applied through the holes of the cylindrical actuators.

Walczyk and Longtin [21] describe a computer controlled *Reconfigurable Fixturing Device (RFD)* concept as a low cost alternative for complaint parts. The fixture is made of

a matrix of pins. A rigid platen lowers the pins, which can be stopped individually. Two stopping mechanisms: (a) pneumatic clamp and (b) a toggle mechanism compressing a combination of gas springs and electromagnet assist are tested. They conclude that the RFD is a feasible alternative to conventional fixturing devices.

Al-Habaibeh and colleagues [22] compare a universal pin-type clamping system with a customized and dedicated clamping system. The authors through their experiments conclude that the pin type clamping system's performance is comparable to that of the dedicated clamping system.

Walczyk and Hardt [23] compare three fabrication methods for sheet metal forming dies. The methods compared by the authors are (a) *Computer Numerical Control (CNC)* milling of a solid billet, (b) An array of profiled-edge laminations (PEL) clamped together, and (c) A matrix of closely packed pins clamped together (called as the discrete die by the authors). Dies of the same shape are manufactured using each fabrication method to stamp a benchmarked part. Through the stamping experiments conducted, the authors conclude that the discrete die performed better than the other two dies with respect to fabrication costs and production time.

The pin actuator concept has been used to build molds by a few inventors. Hong [24] proposes to build gypsum molds using pin actuators. The object to be molded sits inside a cube formed by six sets of pin matrices. The object actuates the pins, the pin sets are clamped in the actuated position, removed, and assembled back to form the mold cavity.

Hoffman [25] also describes developing mold cavities for injection molding applications using pin tooling. The tooling system comprises of hexagonal pins with square heads mounted on top via ball joints. The mold is produced by initially housing the pins in an elastomeric block, actuating the pins individually and locking their positions by giving them a 30° rotation. The input for individual positions of the pins are obtained by from a *Computer Aided Design (CAD)* software. The shape is confirmed by a flexible face-sheet placed on top of the pin matrix. Once all the pins are actuated and locked, the block is separated and used as a mold surface. Figure 2.4 shows the pin and the pin head from Hoffman’s patent.

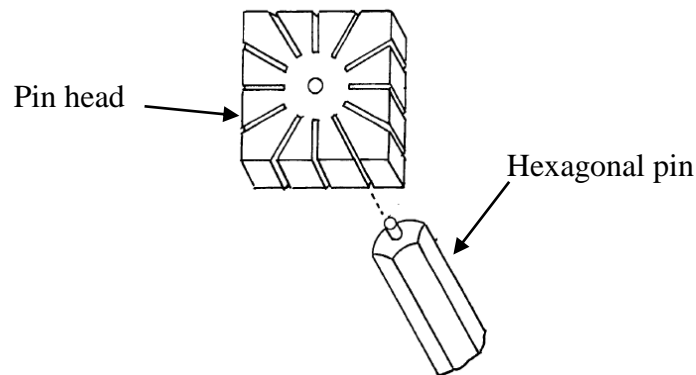


**Figure 2.4: Hexagonal pin with square pinhead [25]**

Munro and Walczyk [26] describe the evolution of the pin-tooling from 1863 to 2003. They define a set of 9 characteristics of an ideal reconfigurable tool. A weightage between 0 and 1 is assigned to each of those characteristics. The authors justify the selection of the 9 characteristics and the weights associated with them, by attributing it to their prior

research experience pertaining to the pin tool. The authors state the significant factors that limit the pin tool to be the ideal tool to be:

- (i) Density of the pins.
- (ii) Actuation method employed.
- (iii) Method of obtaining pin heights.
- (iv) Method used to smoothen the surface of the forming die.
- (v) Tooling weight and its portability.

Pedersen and Lenau [27] discuss the use of a variable geometry mold comprising of pins with hemispherical tops. They describe the application of pin tooling to cast concrete elements. They use a 0.3 mm stretchable interpolating layer to reduce the dimpling effect on horizontal surfaces. They opine that in cases of artistic elements, the dimpling might be desirable.

Though a variety of shapes can be actuated on the pin tool, one of the major limitations of the reconfigurable tool is the undulations (bumps and valleys) formed due to the discrete nature of the pins. Walczyk and colleagues [28] focus on addressing this issue by using a diaphragm and a smoothening membrane (interpolator) on top of the tool. They describe the application of pin-tooling to thermoform composite parts of aircrafts. The composite is heated and formed onto the pin tool by the application of vacuum between the tool and the composite. The tooling comprised of an 8 by 12 matrix of 28.6mm by 28.6 mm cross-section pins. The authors determine that Polyurethane and Polyethylene foam with a

thickness of 36 mm to be the most suitable interpolator material, and Silicone with a thickness of 1.6 mm to be the most suitable diaphragm material.

Eigen [29] also attempts to address the dimpling (undulations) effect by using an interpolator on top of the pins. Figure 2.5 shows the intended function of the interpolator. Eigen proposed to pre-form the pin tool with the interpolator. Experiments were conducted with the following variables:

- (i) Pin size is 0.25 inch by 0.25 inch.
- (ii) Interpolator thickness between 0.125 inch and 0.25 inch.
- (iii) Interpolator materials are Neoprene, Polyurethane and Elvax (ethylene vinyl acetate).

Eigen determined that Elvax with a thickness of 0.25 inch gave the best results in comparison with the other interpolators experimented.

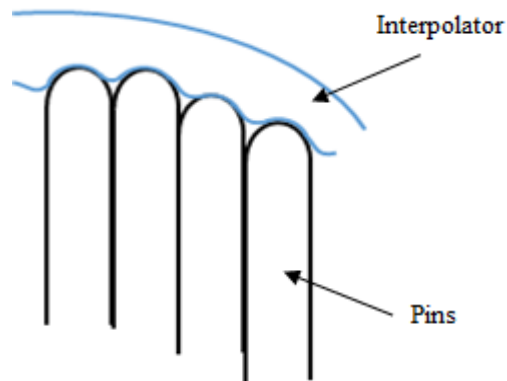


**Figure 2.5: Pin-tool with the interpolator**

Rao and Dhande [30] simulate interpolating membranes for reconfigurable pin tool for sheet metal forming applications. They propose a verification of the computational results through experiments. Kleespies III and Crawford [31] did similar computational simulations for interpolators for thermoforming applications. They are one of the first to study the application of pin tooling to thermoforming and use classical plate theory to model the interpolating layer and compare the finite element analysis results with those of the experiments. They conclude that the reconfigurable tool though having limitations with respect to surface quality, can be used for prototyping purposes.

Zäh and colleagues [32] discuss the development of a pin type flexible tooling system for injection molding of small parts. The pins are of 0.4 mm by 0.4 mm square cross-section and the bounding box for the biggest part that could be produced via their setup is 100 mm by 100 mm by 50 mm. They also identify the dimpling effect to be one of the limitations of the pin tool and suggest the use of membranes to smoothen the dimples.

Simon and colleagues [33] discuss thermoforming using reconfigurable pin tool comprising of equally spaced pins with round heads. They also use an interpolating layer to smoothen the undulations. They compare the quality of surfaces produced pins with rounded and square heads by simulating the process. They conclude that pins with square heads produce better quality surfaces than round headed pins. The round and the square pin-heads are shown in Figure 2.6(a) and Figure 2.6(b) respectively.





**Figure 2.6: (a) Round pin heads, and (b) Square pin heads [33]**

Kelkar and colleagues [34] describe geometric algorithms for freeform objects to be manufactured using the pin tool. They develop a surface error calculation method to control the accuracy. They conclude by stating that a tradeoff needs to be struck between accuracy required and the size of the pins to be used.

Wang [35] addresses the surface quality issue using machinable screw-pin tooling in their hybrid vacuum forming machine system. The tool comprises of identical pins engaging with each other by virtue of the threads present on their surfaces (see Figure 2.7). A tool controlled by a CNC machine actuates every screw to form the desired shape and then used a subsequent machining operation produces the forming surface. A similar idea is patented by Halford [36]. He describes a flexible tooling system with a matrix of machinable pin elements. The pins are actuated and machined to form the desired molding surface.

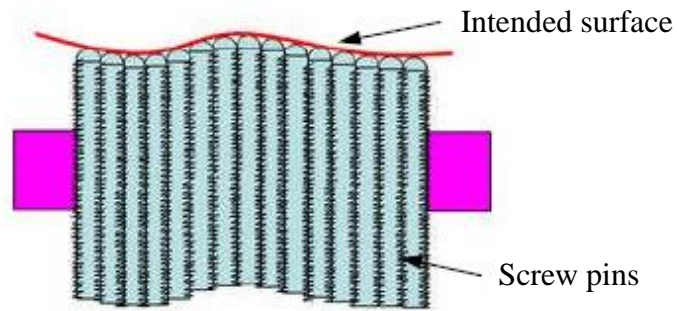


**Figure 2.7: Machinable screw pin tooling [35]**

A table summarizing the different types of pin actuators used in the literature pertaining to manufacturing is shown in Appendix A.

In the literature reviewed, it has been determined that the reconfigurable pin tool is a viable option, but like any other process, it is not perfect and has its own limitations. Advantages of a pin tool are:

- (a) Different shapes can be actuated on a single tool.
- (b) The time consumed in reconfiguring the tool is less.

Therefore, the time taken in manufacturing a part, including tool design and development, through reconfigurable pin tool will be much faster than the conventional tooling. However, the pin tool has the following limitations:

- (a) The surfaces produced will have undulations due to the pins.
- (b) The dimensions of the projection of the intended surface should be in accordance with the pin dimensions.

The research work and the patented ideas reviewed in this chapter are focused on different ways in which the produced surface could be smoothed. The most popular approaches have been:

- (a) Using an interpolating layer,
- (b) Reducing the pin's cross-sectional dimensions, and
- (c) Machining the pin heads to form a smooth molding surface.

These approaches add an additional process and are a hindrance to flexibility. Other approaches to achieve undulation-free surfaces have not been pursued in the literature reviewed in this chapter. One possible approach with respect to polymer and composite processing methods could be- experimenting with the process parameters to try and manufacture dimple-free, higher quality surfaces.

### **2.3 Key conclusions from this chapter**

The application of the pin tool to various manufacturing processes has been discussed and a review of the state of the art pertaining to the reconfigurable pin tool is presented in this chapter. The table below summarizes the key learnings from the literature review.

**Table 2.2: Key learnings from the literature review**

Sl. No.	Attribute	Key learning
1	Pin shape	- Pins with square cross-section and hemispherical tips are best suited for forming
2	Pin matrix	- Square and rectangular matrix of pins aid easier clamping. - Densely packed pins (no spacing between the pins) aids in withstanding high forming loads.
3	Processes	- Sheet metal forming - Injection molding - Concrete casting - Polymer and composite forming - Fixturing
4	Advantages	- Different shapes can be actuated on a single tool. - The time consumed in reconfiguring the tool is less.
5	Limitations	- The surfaces produced will have undulations. - Possibility of dimension mismatch between the pins and the projection of the intended surface.
6	Smoothing techniques pursued	- Interpolating layer - Reducing the pin's cross-sectional dimensions. - Machining the pin heads. - Equally spaced pins with pin-head interpolators.

The undulations caused by the pin tool seems to be the main focus of most of the literature reviewed. The undulations, however, could be a requirement of the part design or may not affect the part's performance, or may not be a negation to the aesthetic requirement. For example, the inner panels of a car which are hidden from the user's plain sight, could be manufactured using the pin tool. Also, the reconfigurable pin tooling has the potential to be a rapid prototyping technique and with further research it can potentially replace the conventional tooling owing to its low costs and lesser fabrication times.

Based on the conclusions from the literature review, the next step is to conduct experiments using the pin tool. Thermoforming using the pin tool has not been pursued

with as much fervor as the other processes have been. Other than four researchers [28, 31, 33, 36], few people have pursued thermoforming. Thermoforming also presents the opportunity to produce higher quality surfaces by controlling the process parameters instead of using an interpolator. Hence, the manufacturing process chosen for the experimentation is thermoforming. The next chapter discusses the application of the pin tool to thermoforming and the preliminary experiments that were conducted to explore the capabilities of the pin tool.

## CHAPTER 3: EXPERIMENTAL SETUP

*The purpose of this chapter is:*

- *To discuss the capabilities of the pin tooling.*
- *To study the effect of several parameters that influence the quality of the surfaces produced.*
- *To determine the factors that have a greater influence the surface quality.*
- *To determine whether it is possible to arrive at an optimal set of parameters resulting in higher quality surfaces.*

### **3.1 Thermoforming Process**

Thermoforming is a manufacturing process where a thermoplastic sheet is heated to a temperature just above its glass transition temperature and formed on to a mold using vacuum [37]. The vacuum is applied from underneath the sheet as soon as the mold comes in contact with the sheet. The application of vacuum is accomplished through small holes in the mold. A stage by stage representation of the manufacturing process is shown in Figure 3.1.

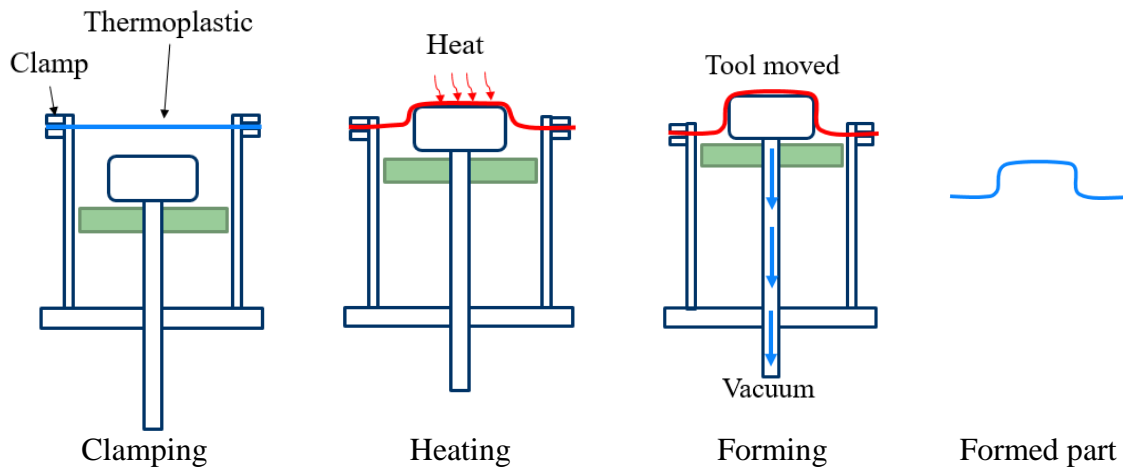


**Figure 3.1: Stage by stage representation of the thermoforming process**

Thermoforming is also carried out by heating the thermoplastic sheet to its formable temperature, applying a vacuum above the sheet, positioning the tool, and finally applying vacuum underneath the sheet. The target temperature and the heating times are dependent on the thermoplastic material and the parameters that affect the quality of the parts produced through thermoforming are:

- (i) Thermoplastic material
- (ii) Plastic sheet thickness
- (iii) Heating temperature
- (iv) Heating time
- (v) Vacuum pressure

### **3.2 Application of the pin-tool to thermoforming and experimentation**

The pin-tool (Figure 3.2) is made of a 10 by 10 matrix of square pins (total of 100). The pins are 2.5 inches long, made of aluminum and have a square cross-section with the sides measuring 0.25 inch by 0.25 inch. The pins have rounded tops, have 6-32 threads tapped at the bottom, and matching screws to accomplish their actuation. The pins are actuated manually. A housing fixture clamps the pins in a dense matrix.

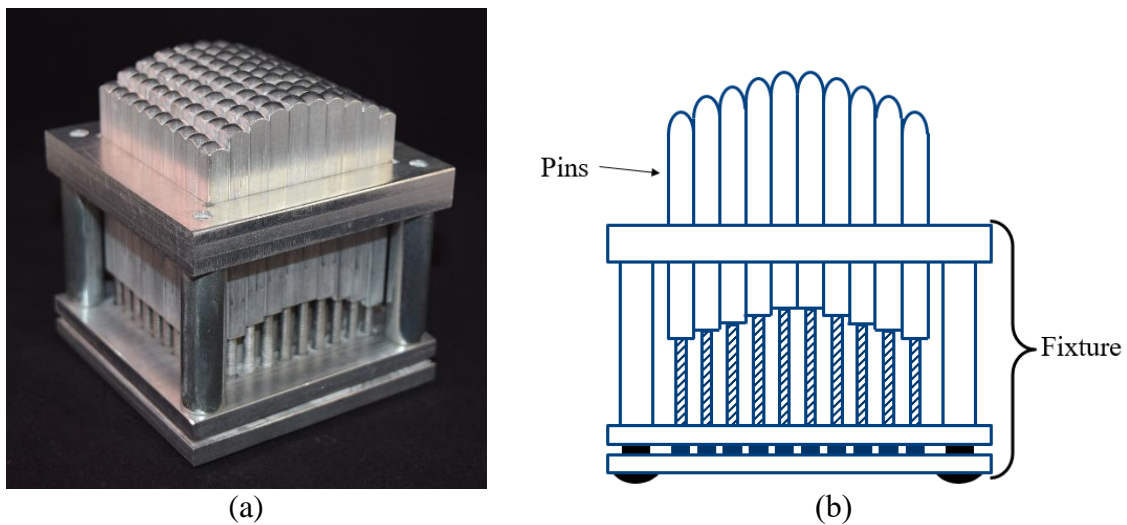


**Figure 3.2: Reconfigurable pin tool**

Experiments were carried out to explore and understand the influence of different process variables on the surfaces produced. The experimental setup, which is a desktop thermoformer (see Figure 3.3) comprises of the following four subsystems:

1. Heating element
2. Frame to clamp the thermoplastic
3. Pin-tool location
4. The vacuum chamber



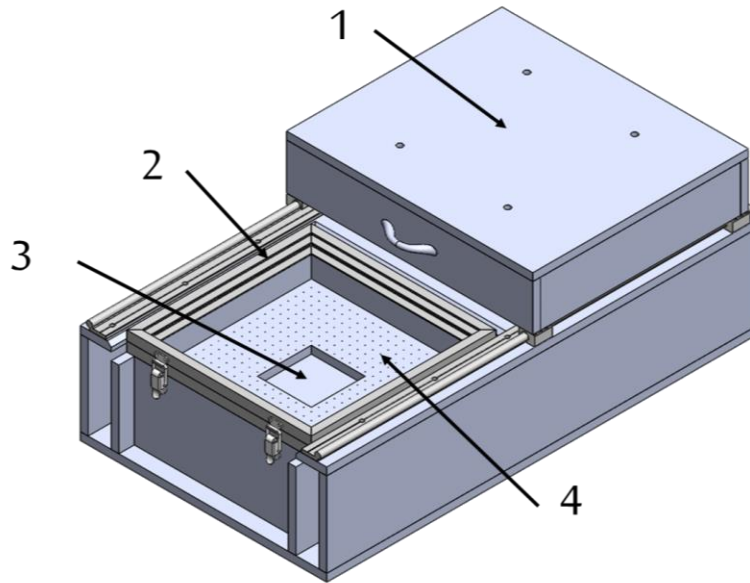


**Figure 3.3: Experimental Setup; 1. Heating element, 2. Frame, 3. Pin-tool location, 4. Vacuum chamber**

The pin tool sits in location labelled (Item 3) in Figure 3.3 and a thermoplastic sheet measuring 12 inch by 12 inch is clamped in the frame above the tool. Buckles are used to secure the plastic sheet in the frame. Heating of the plastic is accomplished through the heating element located in Item 1 of Figure 3.3 by sliding it over the sheet. The plastic is formed onto the tool as soon as it reaches the formable temperature by applying a vacuum from underneath. The key difference from the conventional process is that the tool remains stationary. Figure 3.4 shows a step by step representation of the experimentation process.

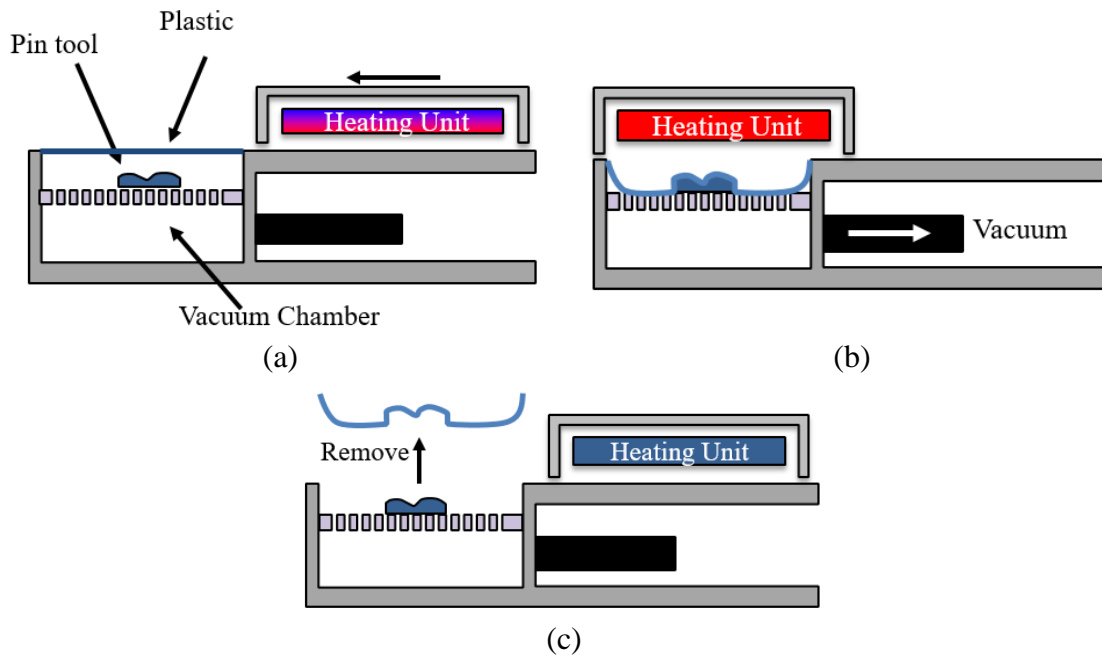


**Figure 3.4: Schematic representation of the experimental process**

A *Design of Experiments* (DOE) was setup to check the feasibility of producing accurate surfaces by varying the process parameters. Each experiment depending on the heating time, takes approximately 10 minutes and an additional 25 minutes for allowing the heating element to cool down to room temperature.

In setting up the DOE, each variable/parameter was associated with at least two settings (a higher and a lower setting). To reduce the total number of experiments, a half factorial DOE was chosen, the material of the thermoplastic (Polystyrene) and the shape (parabolic) to be produced were kept constant. The process variables chosen for experimentation were:

- (i) Material thickness
- (ii) Heating time
- (iii) Vacuum pressure

The interpolator, produced by forming the polystyrene sheets repeatedly above each other, was added to the list of DOE parameters. The thickness of the interpolator was comparable to the cross-sectional dimension of an individual pin.

An opening was made in the vacuum hose to attain a reduction in the vacuum pressure. The vacuum pressure was not quantified as the intention behind conducting the experiments was to understand the influence of various parameters on the quality of the surfaces and the vacuum pressure would be quantified for future experimentation if deemed necessary. The preliminary results from the experiments are discussed in the following section.

### **3.3 Qualitative Analysis of the initial experiments**

Prior researchers have focused on changing the shape of the pins, changing the shape of the pin tips, reducing the cross-sectional area and spacing between them to address the surface quality. These aspects of the pin tool do address the quality of surfaces produced, but the number of pins, their manufacturing, the size of the actuating mechanisms and the costs involved become limitations to use the pin tooling. Thus, the DOE was conducted without changing the pin dimensions, with the main intension of exploring the effect of process parameters on the surface quality. The shape chosen to conduct the experiments was a simple parabola. Four variables (Table 3.1) were chosen for the experimentation with the shape and the material held constant. The thermoplastic material chosen was Polystyrene due to its glass transition temperature of 100°C and its nonhazardous nature.

**Table 3.1: Design variables in experiments**

<b>Design Variable</b>	<b>Set of Values</b>
1. Material thickness (inch)	{0.03125, 0.0625}
2. Heating time (minutes)	{4, 5, 6}
3. Interpolator	{Yes, No}
4. Vacuum pressure	{Partial, Full}





The half factorial DOE resulted in sixteen experiments and the variables associated with each of them are shown in Table 3.2.

**Table 3.2: Summary of experiment conditions**

<b>Experiment Number</b>	<b>Material Thickness (inch)</b>	<b>Heating Time (minutes)</b>	<b>Interpolator</b>	<b>Vacuum</b>
1	0.03125	4	No	Partial
2	0.0625	4	No	Full
3	0.03125	5	No	Full
4	0.0625	4	Yes	Partial
5	0.03125	6	No	Full
6	0.03125	6	Yes	Partial
7	0.0625	5	Yes	Partial
8	0.03125	5	Yes	Full
9	0.03125	5	No	Partial
10	0.03125	4	Yes	Full
11	0.0625	6	No	Partial
12	0.03125	5	Yes	Partial
13	0.0625	5	No	Partial
14	0.0625	5	Yes	Full
15	0.0625	6	Yes	Full
16	0.0625	5	No	Full

The next step after conducting the experiments was to evaluate the surfaces produced. The surfaces were visually inspected and evaluated by six raters using the rubric (shown in Table 3.3).

**Table 3.3: Qualitative evaluation rubric for surface quality**

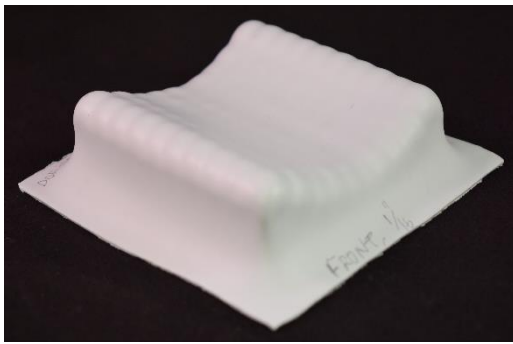
Rating	Description	Shape
4	Exact surface	
3	Limited undulations	
2	Noticeable undulations	
1	No interpolation	

Evaluations from the six raters with the average ratings are shown in Table 3.4. Figure 3.5 and Figure 3.6 show four examples of the surfaces that were produced through the experiments.

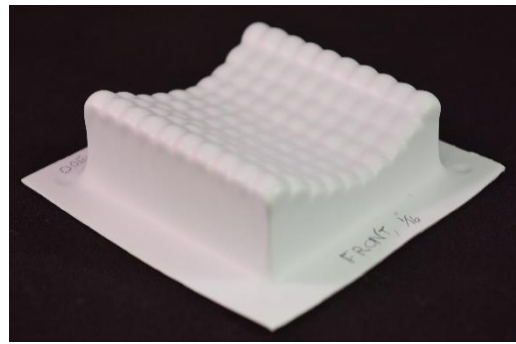
**Table 3.4: Surface quality rating for each experiment**

Experiment Number	Raters						Average rating
	R1	R2	R3	R4	R5	R6	
1	2	2	2	2	3	2	2.1667
2	2	3	3	2	3	2	2.5
3	1	1	1	1	1	1	1
4	1	1	1	1	1	1	1
5	1	1	1	1	1	1	1
6	3	3	3	3	3	3	3
7	2	3	3	1	1	3	2.1667
8	3	3	3	3	3	3	3
9	1	1	1	1	1	1	1
10	3	3	3	3	3	3	3
11	1	1	2	1	1	1	1
12	2	3	3	3	3	3	2.8333
13	1	2	3	2	2	2	2
14	3	3	3	3	3	3	3
15	3	3	3	3	2	2	2.6667
16	1	1	2	1	1	1	1.1667

The process variables used to produce surfaces in Figure 3.5(a) and Figure 3.5(b) were that of experiment 14 and experiment 16 respectively. The corresponding average quality ratings for the surfaces are 3 and 1.1667 respectively (from Table 3.4).



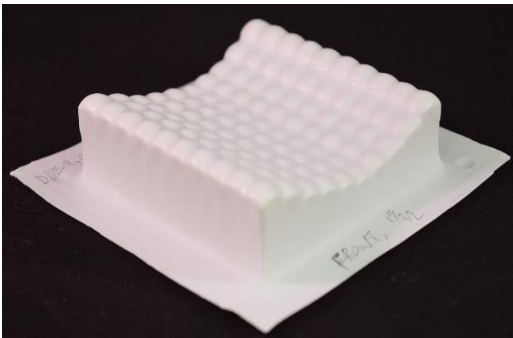
(a)



(b)

**Figure 3.5: Parabolic shape produced (a) with the interpolator and (b) without the interpolator**

Similarly the surfaces in Figure 3.6(a) and Figure 3.6(b) were produced from experiments 9 and 1 respectively; and the average ratings are 1 and 2.1667 respectively.



(a)



(b)

**Figure 3.6: Parabolic shape produced (a) Heating time of 5 minutes, (b) Heating time of 4 minutes.**

Due to the pictorial nature of the rubric, the evaluations could be highly subjective and the ratings between two different raters might not match. Hence, it is critical to determine the inter rater agreement

### **3.3.1 Inter rater reliability**

Evaluating the surface-quality based on the rubric shown in Table 3.3 is a subjective process. A convenient method to analyze this subjective data collected from the ratings is to determine the agreement between individual raters. The inter rater agreement can be statistically determined using inter rater reliability. When a work is reviewed by more than two raters and the evaluations are ordinal in nature, the method used to determine inter rater reliability is the Krippendorff's alpha method [38]. The alpha was determined to be 0.798 using ReCal OIR [39]. An alpha value in the interval  $0.67 < \alpha < 0.8$  indicates acceptable agreement to draw tentative conclusions in exploratory experiments [40]. Therefore, tentatively, the surface evaluation was higher when:

- (i) The interpolator was used over molding directly on pins.
- (ii) The thickness of the molded sheet was greater.
- (iii) The heating time was minimized.
- (iv) The vacuum pressure was reduced.

Three ordinal logistic regressions [41] were carried out to in Minitab® (with  $\alpha = 0.05$ ) to determine the most significant variables (ratings 1, 2, and 3 were named severe, medium and almost respectively). The tests were:



- a) Rating (dependent variable) versus heating time, material thickness, and vacuum (independent variables)- Figure 3.7
- b) Rating (dependent variable) versus heating time, and material thickness, (independent variables) – Figure 3.8
- c) Rating (dependent variable) versus heating time, and vacuum (independent variables)-see

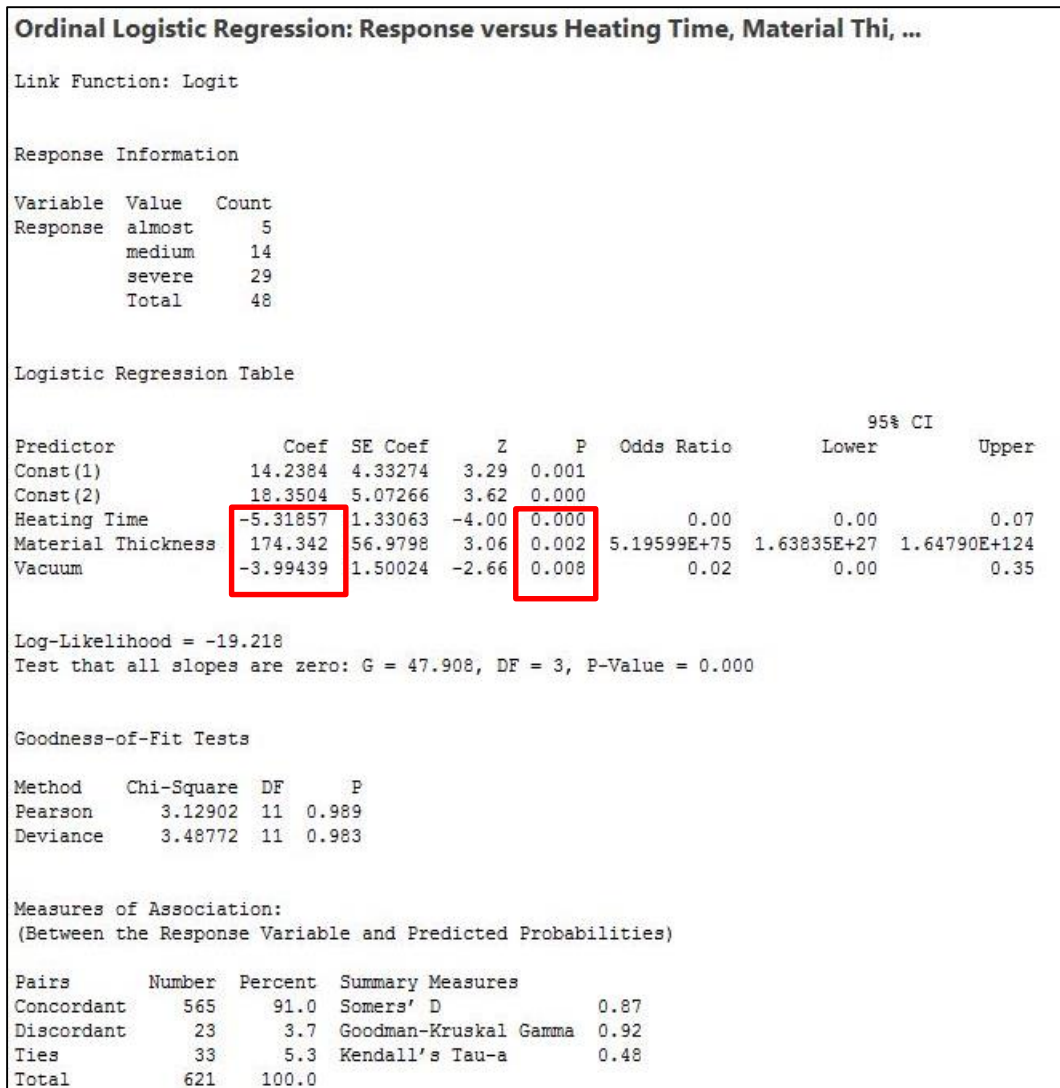


**Figure 3.7: Ordinal Logistic regression: Rating vs Heating time, material thickness, and vacuum**

In Figure 3.7, the highlighted regions are of the coefficients and the P-value. The sign of the coefficients indicate the nature of relationship between the input variable (example: Heating time) and the response (Rating). The P-values for all the three variables are less than  $\alpha$  and hence, all the three variables are significant in combination.

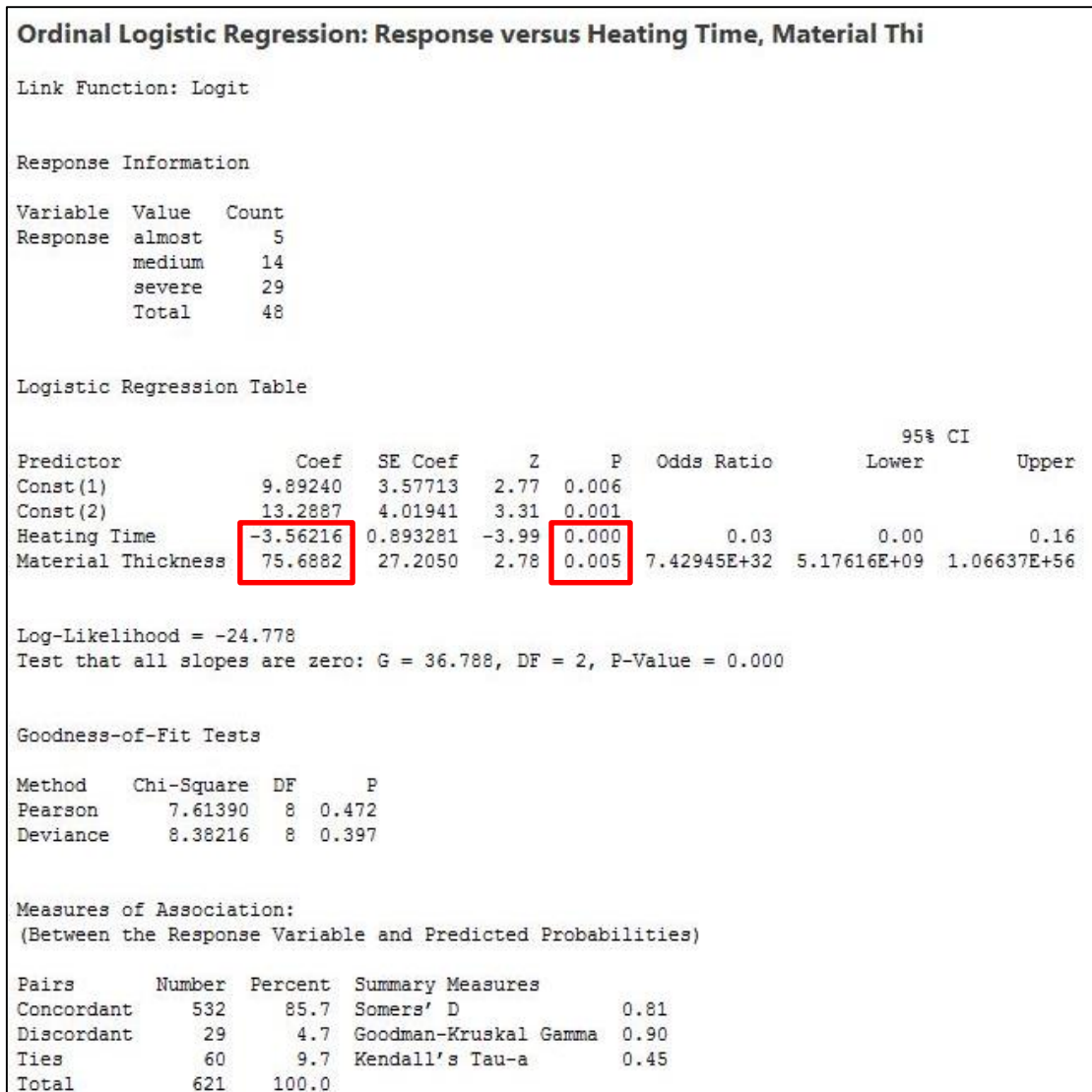


**Figure 3.8: Ordinal Logistic regression: Rating vs Heating time, and material thickness**

Similar to Figure 3.7, in Figure 3.8 the coefficients and the P-values are highlighted. Both the P-values are less than 0.05, therefore, between heating time and material thickness, neither variable is insignificant.

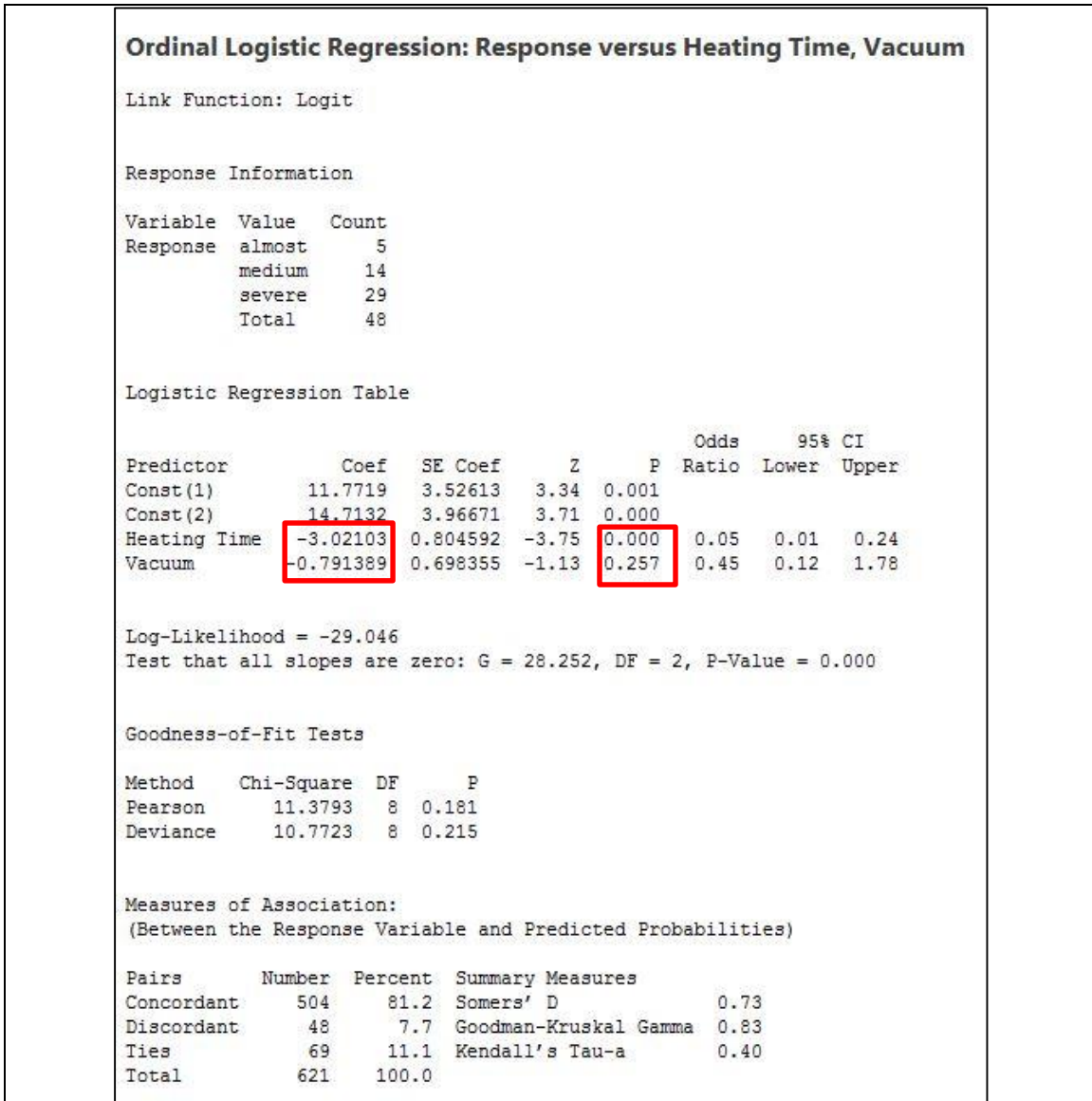


**Figure 3.9: Ordinal Logistic regression: Rating vs Heating time, and vacuum**

In Figure 3.9 the coefficients and the P-values are highlighted similar to the previous figures. The P-value pertaining to heating time is less than 0.05, whereas the P-value pertaining to vacuum is more than 0.05. Therefore, statistically, heating time has a greater influence on the response in comparison with the vacuum pressure.

The interpolator was not considered in the regression as model as one of the objectives of the work presented here is to not use the interpolator (Research objective 2). From the regression models discussed above, heating time and material thickness are the significant factors influencing the quality of the surfaces produced.

To explore the quality of surfaces produced without the interpolator, experiments were conducted with decreased heating times, reduced vacuum pressure and plastic sheet of 0.0625 inch thickness. Figure 3.10(a) and Figure 3.10(b) show preliminary results for a parabolic shape and a parabolic bowl respectively.

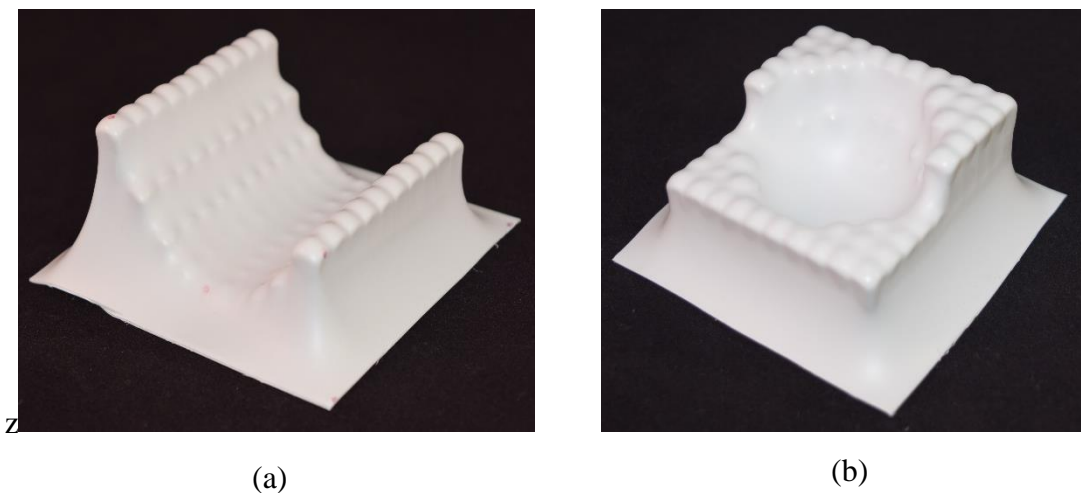


**Figure 3.10: (a) A parabolic shape and (b) a parabolic bowl**

The intensity of the undulations on surface shown in Figure 3.10(a) is less than that of the surface show in Figure 3.6(b). The process parameters for both these experiments were different and the interpolator was not used in either of the two experiments. Figure 3.10(b) shows another surface produced without the interpolator. The surface quality in the bowl area is higher as there are only a few undulations. Thus, by controlling the process

parameters, higher quality surfaces can be produced on the pin tool without using the interpolator. Therefore, it can be hypothesized that an optimal set of parameters that results in higher quality surface can be determined, but those optimal parameters are going to be shape exclusive.

To further explore the capability of the pin tool without the interpolator, exploratory experiments were conducted and their examples are shown in Figure 3.11. Figure 3.11(a) shows an inclined surface with a square hole in the middle. The intended shape was reproduced, but the thickness of the sheet at the far corner of the hole labelled on Figure 3.11(a) was significantly lesser than the other regions of the surface.

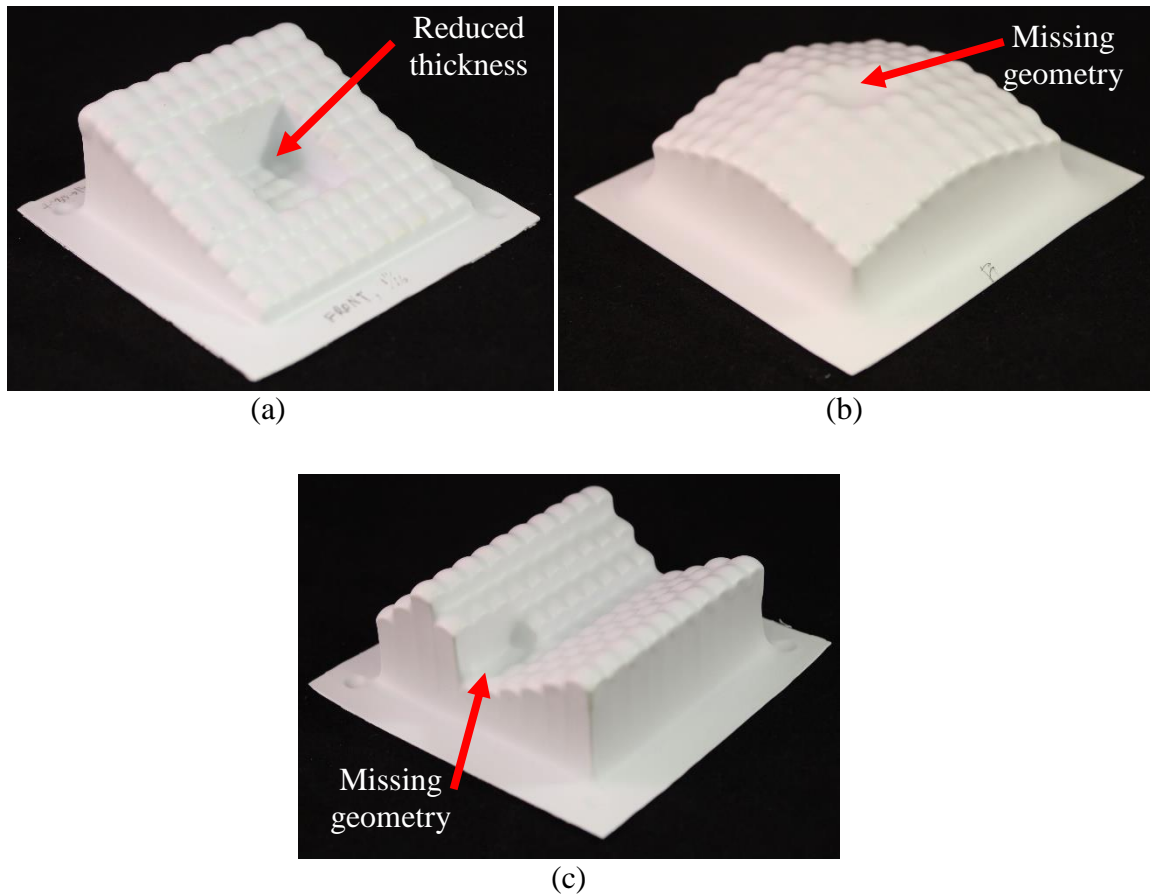


**Figure 3.11: Different shapes produced to understand the capabilities of the pin tool**

Figure 3.11(b) shows a dome shape with a depression in the center. The intended shape at the center of the dome was that of a square-hole (with four pins not actuated at all), instead a depression was formed. The reason for this missing geometry is that the sheet was not at the required temperature for the hole to be formed, but the temperature was sufficient to produce the dome shape.

Figure 3.11(c) shows a combination of an inclined surface with another random shape. The plastic did not make contact with the pins at the labelled regions of the figure. These

pictures indicate that there is a relation between conformance with respect to the tool and conformance with respect to the intended/desired shape, i.e. the distance between the pins representing a particular feature of the intended shape and the plastic sheet before heating significantly influences the outcome of the process.

It is clear from Figure 3.11 that the pin tool is capable of producing a variety of shapes. However, the pin tool poses a few challenges such as non-uniform sheet thickness and missing geometry in case of complex shapes. Producing higher quality surfaces for shapes containing sharp changes in geometry will be a limitation of the pin tool.

### **3.4 Key conclusions from this chapter**

The reconfigurable pin tool is a viable method to be applied to the thermoforming process. The size of the experimental setup and the size of tool constrain the sheet's size (length, breadth, and thickness). Without considering the size of the tool and the experimental setup; from the exploratory experiments, the following conclusions can be made:

- A variety of shapes can be produced using the reconfigurable pin tool.
- The distance from the tool to the sheet has a significant impact on the quality of the surfaces.
- The variables that influence surface-quality are sheet thickness, heating time, vacuum pressure, and most importantly desired shape to be produced.



- Assuming the material and the thickness of the thermoplastic to be constant, the variables that greatly influence the surface quality are: (i) the heating time, (ii) the distance between the tool and the sheet, and (iii) the intended shape
- Conformance with respect to tool gives a measure of quality of the surfaces produced using the pin tool as there is a possibility of missing/unintentional geometry.
- An optimal set of parameters resulting in controlled conformance and less undulations is possible, but they are going to be shape exclusive.

The next step is to determine the process parameters that result in higher quality surfaces for specific shapes. To find an optimal set of process parameters, shape specific experiments have to be conducted by setting up individual DOEs with smaller range between the higher and the lower bounds. New DOE variables could be added and current variables could be deleted if deemed necessary. The next chapter discusses the experimentation with full factorial DOE for flat, inclined, convex and concave shapes.

## CHAPTER 4: SHAPE SPECIFIC EXPERIMENTATION

*The purpose of this chapter is:*

- *To determine the reproducibility of the experimental setup.*
- *To conduct shape specific experiments.*
- *To determine quality of the surfaces produced by comparing them to the desired surface quantitatively.*
- *To prove the optimal set of parameters are shape exclusive.*
- *To compare the quality of surfaces on the basis of shapes.*

### **4.1 Quantifying quality of the surfaces**

As discussed and presented in Chapter 3, the surface quality is impacted by process parameters. Further, high quality surfaces can be produced using pin tools without the use of an interpolating layer. In this chapter, the surfaces are evaluated using a quantitative measurement using laser scanning technology and comparing the “as manufactured” to the “ideal” *Computer Aided Design (CAD)* surface. The idea of *shape conformance* is introduced in this chapter as a measure of how closely the manufactured surface matches the CAD surface.

If the produced surface has complete conformance to the tool, it will result in highly undulated shapes – thereby a low quality. A surface that is not conformed to the tool may result in an undulation free surface, but a low quality surface because it is not conformed to the CAD shape. A controlled conformance of the plastic with respect to the tool will ensure the surface produced is closer to the desired surface. Ideally, it is desired that a

controlled conformance with respect the tool produces an undulation free surface. The intensity of these undulations gives a measure of quality of the surface (see Figure 4.1)

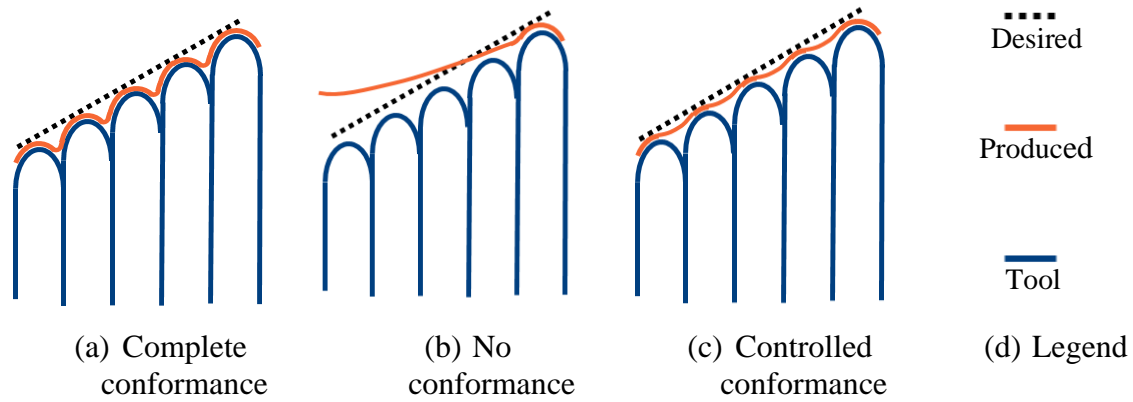


**Figure 4.1: Conformance of the produced surface with respect to the tool**

The quality of the surface produced using the reconfigurable pin tool is influenced by four factors explored in this research. The intended shape of the surface to be produced is one of the critical factors and the optimal set of parameters will be different for different shapes. To determine the optimal set of process parameters, shape specific experiments have to be conducted. The shapes that are chosen to conduct the experiments are a horizontal flat shape, an inclined flat shape, a convex parabolic shape, and a concave parabolic shape. These shapes are chosen as they are simple and would serve as a starting point to analyze the effect of the parameters on shapes of higher complexity in the future.

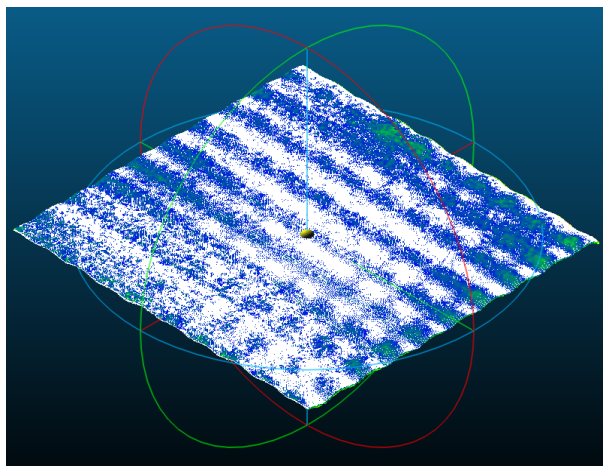
#### **4.2 Surface Reproducibility of the thermoformer**

Surface reproducibility was determined by producing ten horizontal surfaces using the same set of process parameters and comparing them with each other. The surfaces were

scanned using a NextEngine® desktop 3D scanner, saved as point clouds and then compared using the CloudCompare® software application. The parameters studied are:

- (i) Sheet thickness of 0.0625 inches.
- (ii) Heating time of 4 minutes.
- (iii) Full vacuum pressure.

The surfaces scanned using the 3D scanner were saved as a point cloud, imported into CloudCompare® and then compared with each other. CloudCompare® measures distances between two point clouds and calculates the mean and standard deviation of all the distance values between the clouds. The surfaces are compared by first aligning and registering the cloud data (see Figure 4.2). The surface in white is the reference and the compared surface is colored based on its distance with respect to the reference. (A detailed explanation of alignment and registration is given in Appendix D)



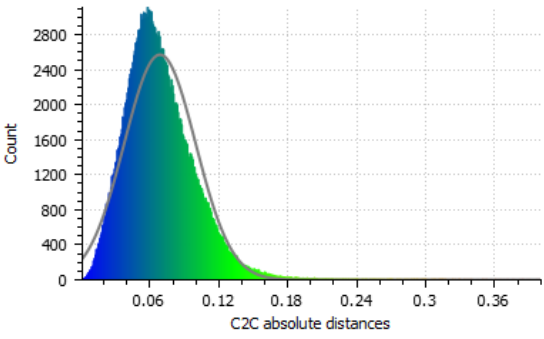
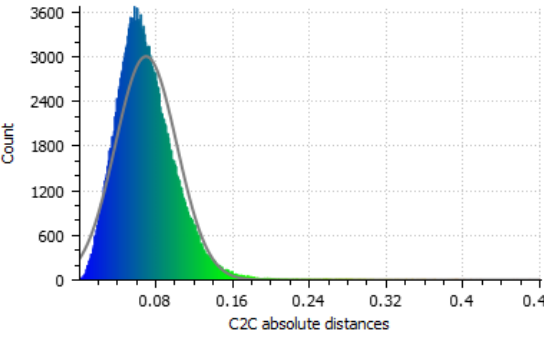
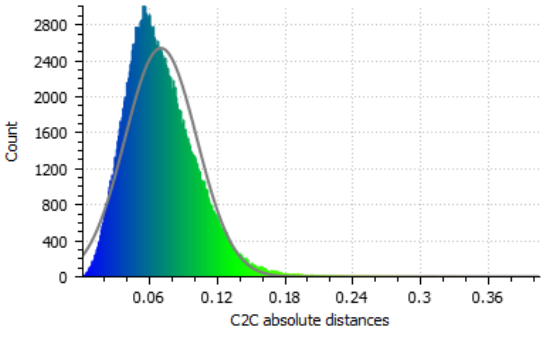
**Figure 4.2: Registered surfaces in CloudCompare®**

Table 4.1 below shows the means and standard deviations of the point cloud to point cloud distances of all the surfaces with respect to the first surface. The reason for producing ten surfaces was to get more than 30 data points (the difference between the means would yield 36 data points) for statistical significance.

**Table 4.1: Cloud to cloud distances for reproducibility**

Experiments	Cloud to cloud distances		Normal distribution
	Mean (mm)	Std. Dev (mm)	
1 and 2	0.0709	0.035704	<p>Gauss: mean = 0.070900 / std.dev. = 0.035704 [500 classes]</p>
1 and 3	0.07327	0.032976	<p>Gauss: mean = 0.073270 / std.dev. = 0.032976 [500 classes]</p>

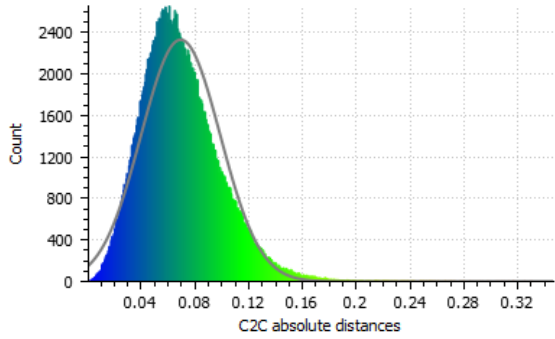
**Table 4.1(continued...): Cloud to cloud distances for reproducibility**

Experiments	Cloud to cloud distances		Normal distribution
	Mean (mm)	Std. Dev. (mm)	
1 and 4	0.068979	0.030971	<p>Gauss: mean = 0.068979 / std.dev. = 0.030971 [500 classes]</p> 
1 and 5	0.070478	0.031886	<p>Gauss: mean = 0.070478 / std.dev. = 0.031886 [500 classes]</p> 
1 and 6	0.070623	0.031614	<p>Gauss: mean = 0.070623 / std.dev. = 0.031614 [500 classes]</p> 

**Table 4.1(continued...): Cloud to cloud distances for reproducibility**

Experiments	Cloud to cloud distances		Normal distribution
	Mean (mm)	Std. Dev. (mm)	
1 and 7	0.074868	0.04151	<p>Gauss: mean = 0.074868 / std.dev. = 0.041510 [500 classes]</p>
1 and 8	0.079085	0.047362	<p>Gauss: mean = 0.079085 / std.dev. = 0.047362 [500 classes]</p>
1 and 9	0.070569	0.031355	<p>Gauss: mean = 0.070569 / std.dev. = 0.031355 [500 classes]</p>

**Table 4.1(continued...): Cloud to cloud distances for reproducibility**

Experiments	Cloud to cloud distances		Normal distribution
	Mean (mm)	Std. Dev. (mm)	
1 and 10	0.069643	0.029324	<p>Gauss: mean = 0.069643 / std.dev. = 0.029324 [496 classes]</p> 

A hypotheses test [42] was completed to determine the cumulative probability of the difference between mean distances of individual surfaces. The significance level of  $\alpha = 0.05$  was chosen for the hypotheses test with the hypotheses being:

Null hypothesis,  $H_o$ : The difference between the means,  $\Delta\mu \geq 0.0045$  mm.

Alternate hypothesis,  $H_a$ : The difference between the means,  $\Delta\mu < 0.0045$  mm.

The reason for choosing the 0.0045 mm to be the hypotheses-testing mean is explained in Appendix E.1. A t-distribution test was conducted to determine the cumulative probability. The t-value is calculated using the formula,

$$t = \frac{\mu_t - \mu}{\sigma / \sqrt{n}} \quad (4.1)$$



where,  $\mu_t$  is the hypotheses-test mean (in this case it is  $\Delta\mu_t = 0.0045$  mm),  $\mu$  is the mean of the population (in this case it is  $\Delta\mu = 0.00344$  mm, refer Appendix E.1),  $\sigma$  is the standard deviation of the population (in this case it is 0.002945 mm, refer Appendix E.1), and  $n$  is the population size ( $n = 36$ ). The  $t$  value was calculated to be 2.1490, which results in a  $p_{critical}$  value of 0.019315 and the null hypothesis was rejected as  $p_{critical} < \alpha$ .

The cumulative probability ( $p_{cumulative}$ ) is given by

$$P_{cumulative} = 1 - P_{critical} \quad (4.2)$$

Thus, the cumulative is 0.9807 which means that there is a 98% probability that the difference between the mean distances of the clouds will be  $< 0.0045$  mm. Therefore, the reproducibility of the device will vary by  $\pm 0.0045$  mm.

The cloud to cloud distance is desired to be zero, but the average of the mean distances from Table 4.1 of 0.072 mm can be accounted for the human error involved in synchronizing the stop watch and the elements of the thermoformer.

### **4.3 Shape specific experimentation**

Shape specific experiments were conducted by setting up individual *Design of Experiments (DOE)* with smaller range between the higher and the lower bounds. The experimental parameters are (a) heating time, and (b) distance between the polymer sheet and the tool- D (see Figure 4.3). The second parameter was not a part of the initial experimentation, but was determined to be a critical factor in the exploratory experiments conducted later.

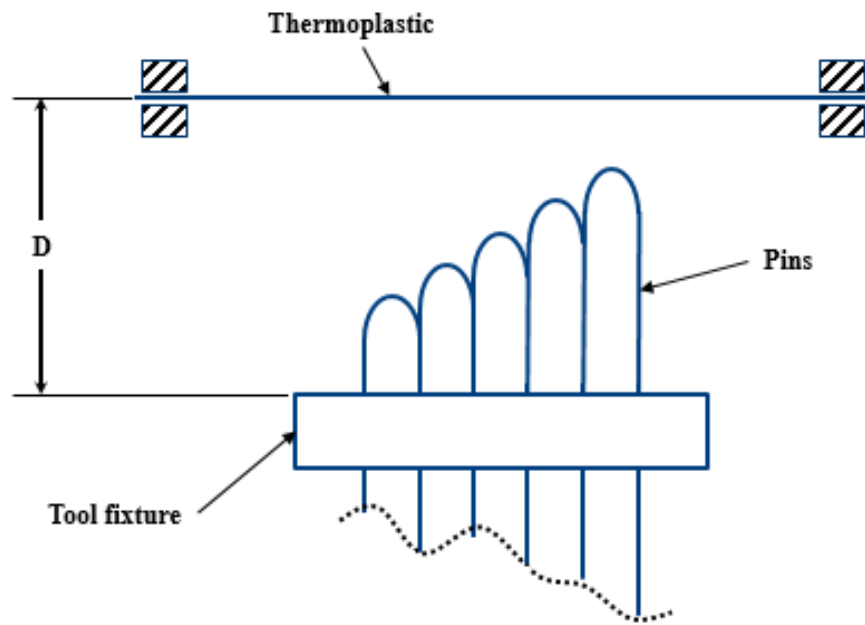


**Figure 4.3: Distance between plastic sheet and the pin tool**

The variables in the experiments are shown in the table below.

**Table 4.2: Design variables for shape specific experiments**

<b>Design Variable</b>	<b>Set of Values</b>
1. Heating time in minutes.	{3:30, 3:45, 4:00, 4:15}
2. Distance between tool and the plastic sheet (D) in inches.	{2.125, 2.625}

A full factorial DOE for each shape was setup and the table below shows all the variables associated with the experiments.

**Table 4.3: DOE variables for each shape**

<b>Experiment number</b>	<b>Heating time (minutes)</b>	<b>Tool to sheet distance (inches)</b>
1	3:45	2.625
2	3:30	2.125
3	3:30	2.625
4	4:15	2.125
5	3:45	2.125
6	4:15	2.625
7	4:00	2.125
8	4:00	2.625

#### **4.4 Comparison of produced surfaces with the desired surface**

Surfaces produced from the experiments are scanned using the scanner and then imported to CloudCompare® to quantify the error between the produced surface and the desired surface. The desired surface is modelled in SolidWorks®, converted to a point cloud using Osada’s random points generator [43], and imported to CloudCompare®. Only the surfaces that conformed to the tool are considered for analysis as point to point alignment in a point cloud alignment software application is difficult to achieve and is not repeatable.

The point cloud of the surface is coarsely aligned it with the point cloud of the CAD surface to aid the removal of the curvature of the outermost pins (Details are be given in Appendix D). Once the produced surface is segmented, the surfaces are registered with

each other to limit the *Root Mean Square (RMS)* difference between them to be  $10^{-10}$  mm. The distance between the two surfaces is then computed in terms of mean and standard deviation in the software. The mean distance and the standard deviation of the distance between the two surfaces are desired to be zero. Figure 4.4 shows an exaggerated representation of the distance between the produced surface and the desired surface.

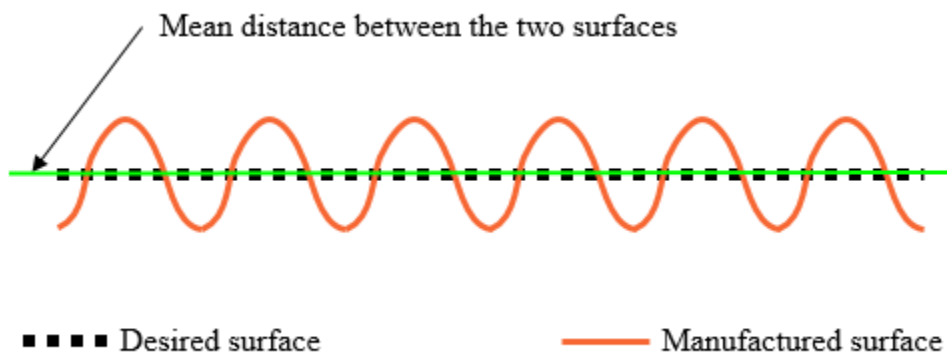


**Figure 4.4: Schematic representation of registered surfaces**

The standard deviation of the distance between the surfaces gives the measure of the intensity of undulations- with higher quality surfaces having smaller standard deviation. However, before inferring about the quality of the surfaces, repeatability of registration method needs to be determined.

#### **4.4.1 Repeatability of the registration method**

The repeatability of registration was determined by conducting a hypotheses test similar to the one described in Section 4.1. The process was repeated nine times and the difference between the individual standard deviations was calculated to determine the

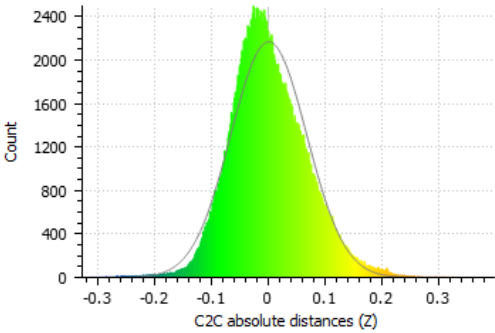
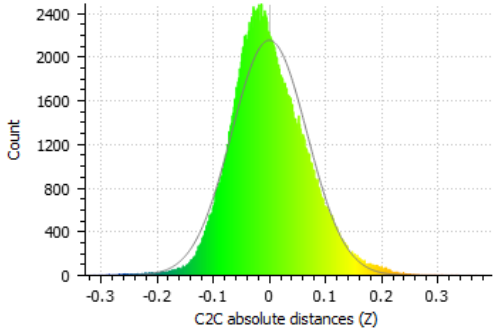
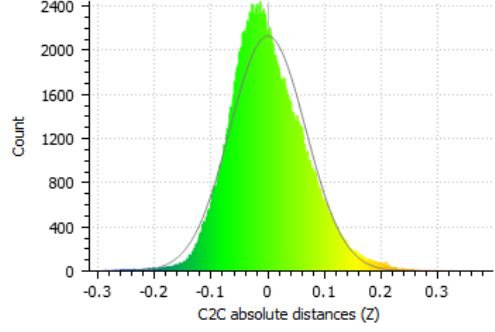
cumulative probability of the difference being close to zero. The reason behind choosing nine repetitions was to have enough data points for statistical significance. A horizontal flat surface, produced using the parameters pertaining to experiment-1 (Table 4.3), was chosen to carry out the hypotheses test with the significance level  $\alpha = 0.05$ .

Null hypothesis,  $H_0$ : The difference between the standard deviations,  $\Delta\sigma \geq 0.00027$  mm.

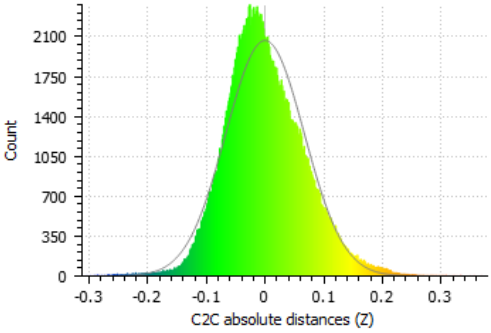
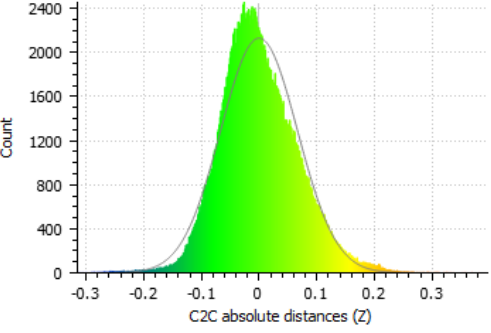
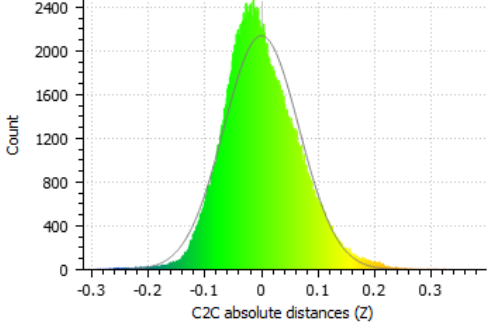
Alternate hypothesis,  $H_a$ : The difference between the means,  $\Delta\sigma < 0.00027$  mm.

Table 4.4 shows the standard deviations for the nine repetitions of registering the two surfaces and measuring the distance between the surface and the plane.

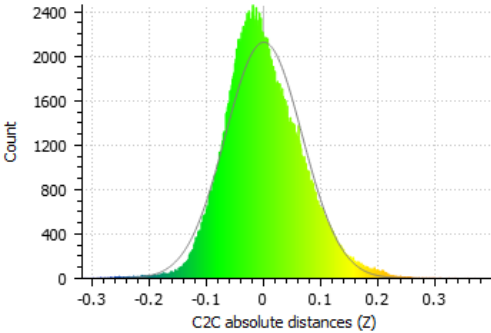
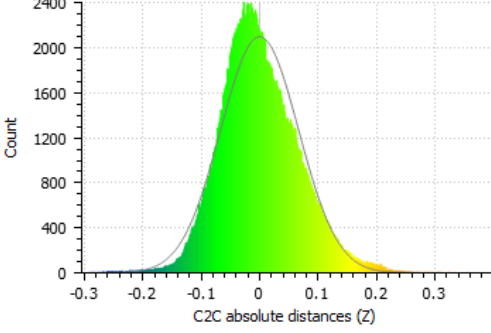
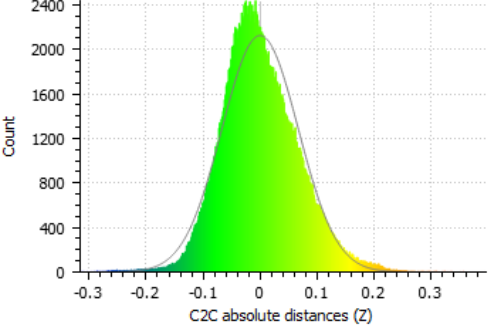
**Table 4.4: Repeatability of registration**

Sl. No.	Mean (mm)	Standard Deviation (mm)	Normal distribution
1	-0.00001	0.066598	<p>Gauss: mean = -0.000010 / std.dev. = 0.066598 [501 classes]</p> 
2	0.00000	0.06688	<p>Gauss: mean = 0.000000 / std.dev. = 0.066880 [501 classes]</p> 
3	0.000034	0.066571	<p>Gauss: mean = 0.000034 / std.dev. = 0.066571 [501 classes]</p> 

**Table 4.4(continued...): Repeatability of registration**

Sl. No.	Mean (mm)	Standard Deviation (mm)	Normal distribution
4	0.000032	0.06666	<p>Gauss: mean = 0.000032 / std.dev. = 0.066660 [501 classes]</p> 
5	-0.000012	0.066478	<p>Gauss: mean = -0.000012 / std.dev. = 0.066478 [501 classes]</p> 
6	0.000002	0.066333	<p>Gauss: mean = 0.000002 / std.dev. = 0.066333 [501 classes]</p> 

**Table 4.4(continued...): Repeatability of registration**

Sl. No.	Mean (mm)	Standard Deviation (mm)	Normal distribution
7	0.000064	0.066847	<p>Gauss: mean = 0.000064 / std.dev. = 0.066847 [501 classes]</p> 
8	-0.000072	0.066459	<p>Gauss: mean = -0.000072 / std.dev. = 0.066459 [501 classes]</p> 
9	0.000032	0.066674	<p>Gauss: mean = 0.000032 / std.dev. = 0.066674 [501 classes]</p> 



The standard deviations for each of the comparisons are of the same order and the means are ignored as they are either zero or of the order of  $10^{-5}$  and  $10^{-6}$ . The absolute difference between each standard deviation was computed and a t-distribution test was conducted to determine the cumulative probability of the difference being less than 0.00027 mm. (Details of the hypotheses test are given in Appendix E.2)

The t value was calculated to be 2.5359, which results in a  $p_{\text{critical}}$  value of 0.007917 and as  $p_{\text{critical}} < \alpha$ , the null hypothesis was rejected. The cumulative probability ( $1 - p_{\text{critical}}$ ) for  $\Delta\sigma < 0.00027$  mm was determined to be 0.9921 which means there is 99% chance that the difference between standard deviations is  $< 0.00027$  mm. Thus, the method of registration of the surfaces is repeatable with an error less than  $\pm 0.00027$  mm.

The next step is to determine the best set of process parameters for the four different shapes. The intention is to determine whether the parameters resulting in the best quality surface for one shape would result in a best quality surface for a different shape.

#### **4.4.2 Quality of the individual shapes**

The shapes chosen for the shape specific experimentation were horizontal, inclined, concave, and convex shapes.

##### **(a) Horizontal surface**

The pins tool was actuated to a distance of 1 inch above the fixturing (see Figure 4.5) to form a horizontal flat shape and the surfaces were produced based on Table 4.3.

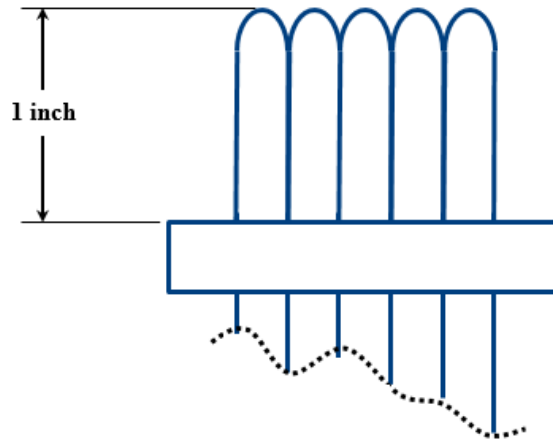
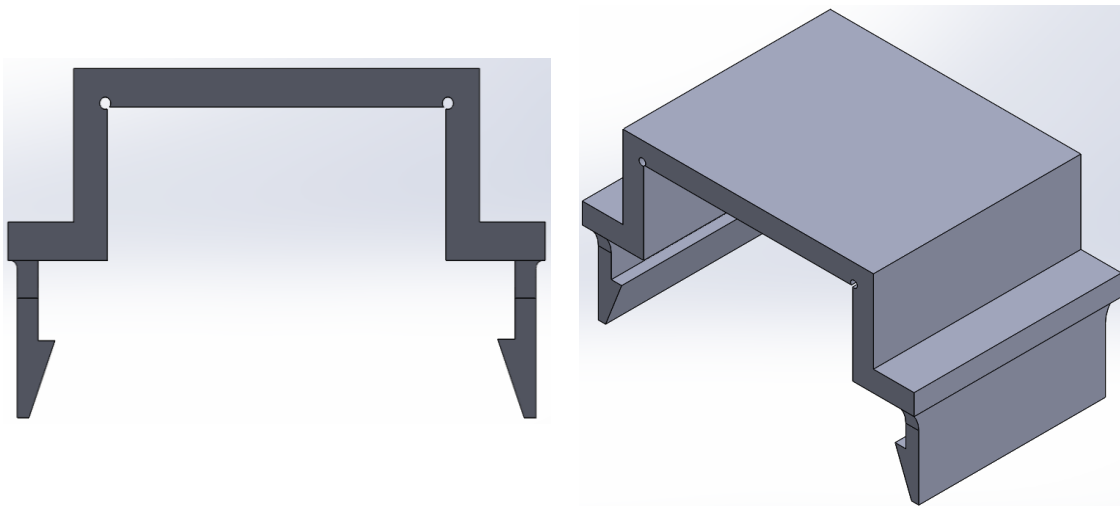


**Figure 4.5: Actuated shape for the horizontal surface**

The shape was actuated manually using the template shown in Figure 4.6. The template was produced by additive manufacturing. The template was slid on to the pin tool and the pins were actuated till their tops made contact with the template.



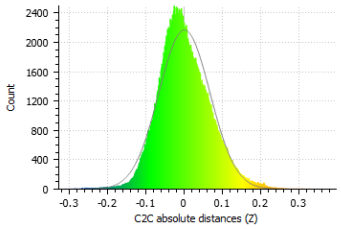
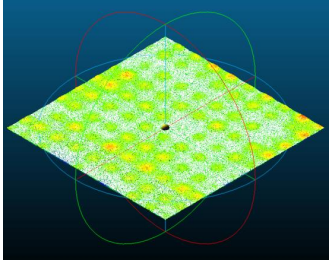
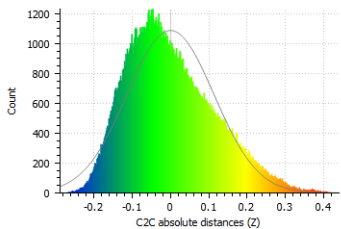
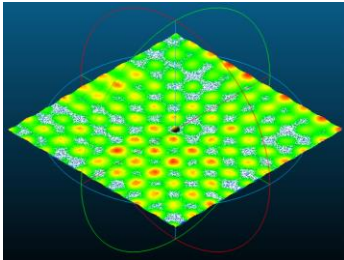
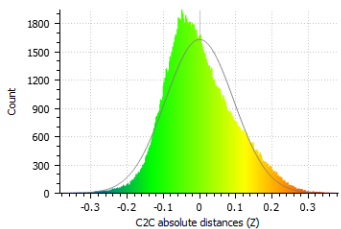
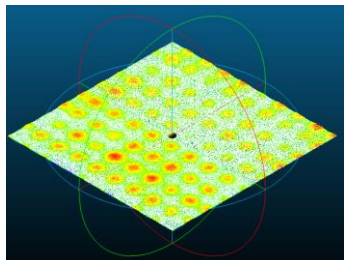
(a) Front view

(b) Isometric view

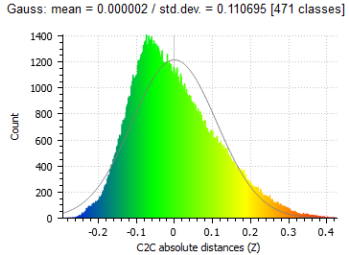
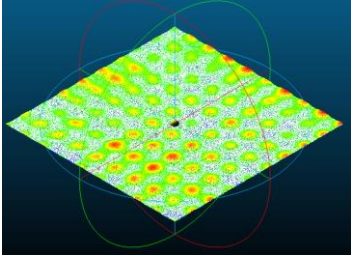
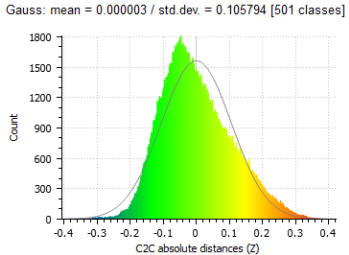
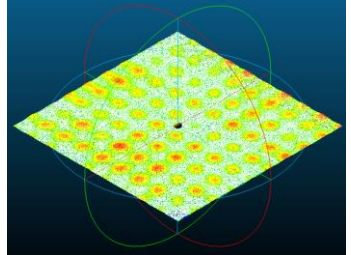
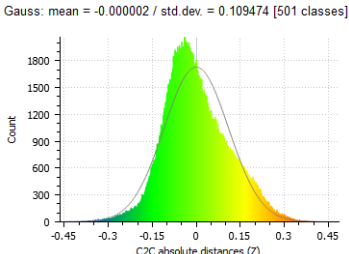
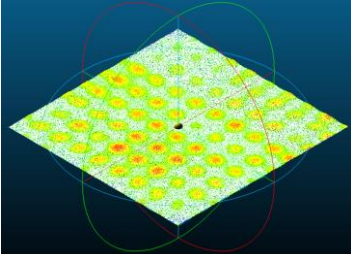
**Figure 4.6: Template for horizontal shape**

The variables pertaining to experiments 2 and 3 resulted in non-conforming surfaces with experiment 2 not conforming to only a few pins in the last row. Thus, experiments 2 and 3 were not considered for analysis. Table 4.5 shows the comparison of the horizontal flat surface with respect to the desired surface for each of the experiments that produced conforming surfaces. The means can be ignored as they are of the order of  $10^{-5}$  mm and  $10^{-6}$  mm.

**Table 4.5: Horizontal surface point cloud to point cloud distance comparison**

Exp.	Mean (mm)	Std. Dev (mm)	Normal distribution	Plot of surface
1	-0.00001	0.066598	<p>Gauss: mean = -0.000010 / std.dev. = 0.066598 [501 classes]</p> 	
4	-0.000001	0.113216	<p>Gauss: mean = -0.000001 / std.dev. = 0.113216 [425 classes]</p> 	
5	-0.000009	0.093855	<p>Gauss: mean = -0.000009 / std.dev. = 0.093855 [501 classes]</p> 	

**Table 4.5(continued...): Horizontal surface point cloud to point cloud distance comparison**

Exp.	Mean (mm)	Std. Dev (mm)	Normal distribution	Plot of surface
6	0.000002	0.110695		
7	0.000003	0.105794		
8	-0.000002	0.109474		

The least difference between the standard deviations ( $\Delta\sigma = |\sigma_4 - \sigma_6|$ , between experiment 6 and experiment 4) is 0.002521 mm, which is significantly greater than the  $\Delta\sigma$  of 0.00027 mm chosen for repeatability in Section 4.3.1.

The graph in Figure 4.7 shows the variation of intensity of undulations with respect to heating time. The graph is plotted with blue bars for a sheet-to-fixture distance of 2.125

inches and red for 2.625 inches. Heating time of 3 min. 30 seconds did not yield conforming surfaces and hence, does not have bars representing them.

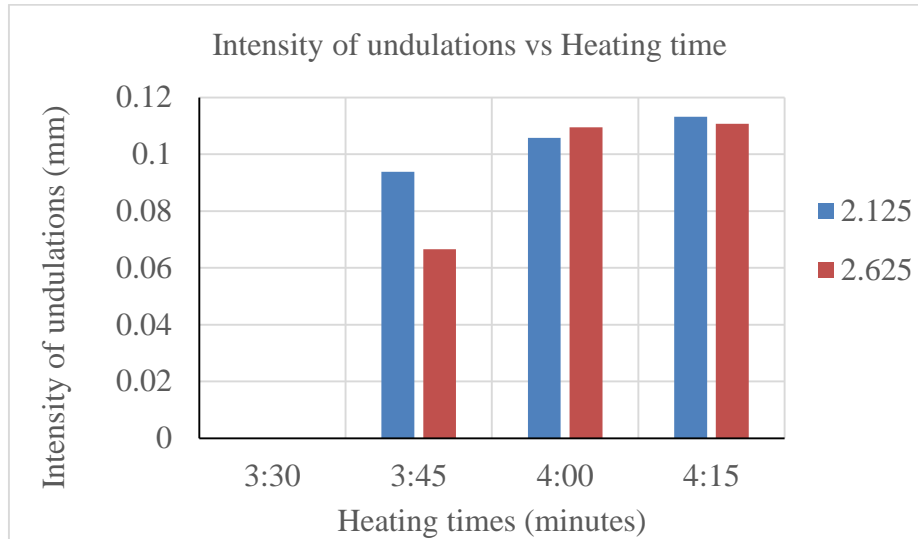


**Figure 4.7: Horizontal surface: Intensity of undulations versus heating time**

The intensity of undulations is less when heating times are less (see graph in Figure 4.7), however the distance between the thermoplastic sheet and the tool also contributes to the surface quality. The intensity of undulations is least for the surface produced in experiment 1, which corresponds to a heating time of 3 min. 45 seconds and the distance between the tool and the sheet of 2.625 inches.

**(b) Inclined surface:**

The pins were actuated to a 30 degree inclination to constitute the inclined surface and the DOE from Table 4.3 was conducted. Figure 4.8 shows the actuated shape of the pins.

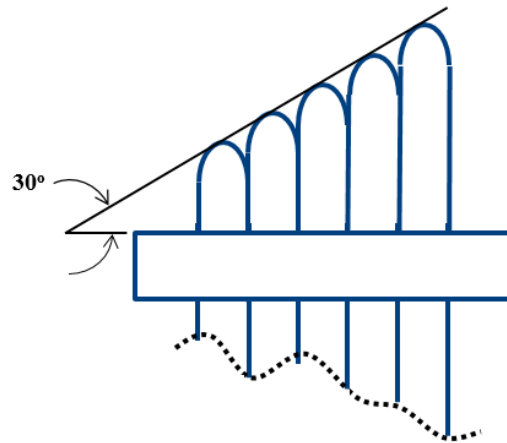
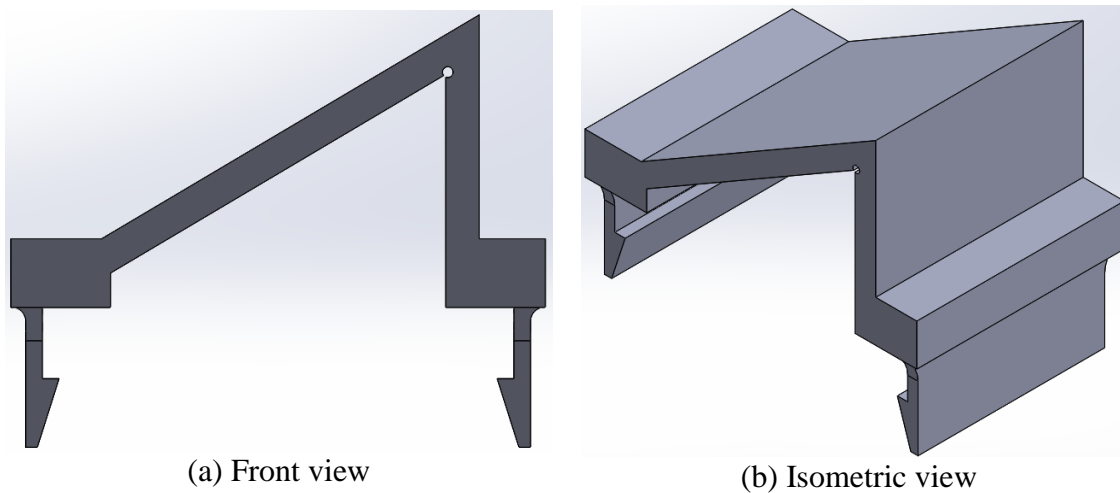


**Figure 4.8: Actuated shape for the inclined surface**

The inclined shape was actuated manually using the template shown below. The template was slid on to the pin tool and the pins were actuated till their tops made contact with the template. The template was manufactured by 3D printing.



(a) Front view

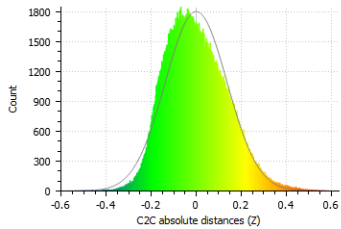
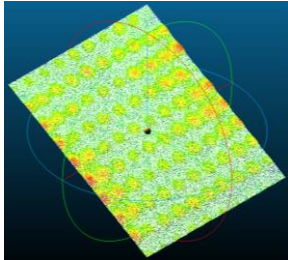
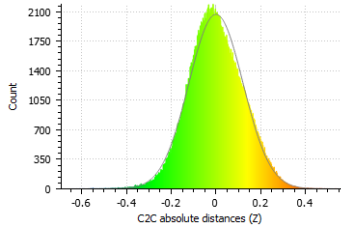
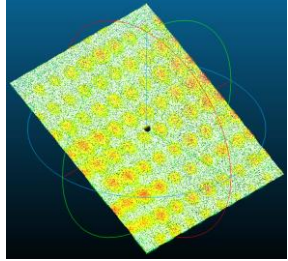
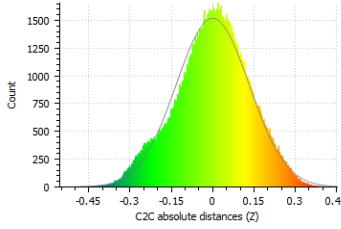
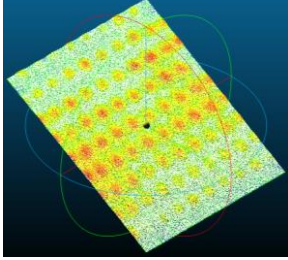
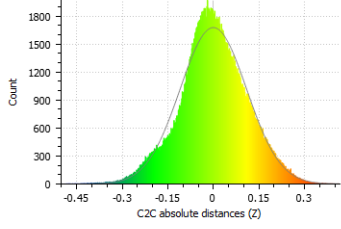
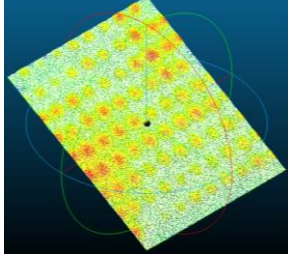
(b) Isometric view

**Figure 4.9: Template for inclined shape**

The variables pertaining to experiments 1, 2, 3, and 5 resulted in non-conforming surfaces and hence were left out of further analysis. The least difference between the

standard deviations for this shape is 0.004578 mm ( $|\sigma_4 - \sigma_7|$ ), which again is significantly greater than  $\Delta\sigma$  of 0.00027 mm.

**Table 4.6: Inclined surface point cloud to point cloud distance comparison**

Exp. No.	Mean (mm)	Std. Dev (mm)	Normal distribution	Plot of surface
4	0.000032	0.137055	<p>Gauss: mean = -0.000032 / std.dev. = 0.137055 [500 classes]</p> 	
6	-0.000039	0.120582	<p>Gauss: mean = -0.000039 / std.dev. = 0.120582 [500 classes]</p> 	
7	0.000049	0.132477	<p>Gauss: mean = -0.000049 / std.dev. = 0.132477 [500 classes]</p> 	
8	0.000021	0.109267	<p>Gauss: mean = -0.000021 / std.dev. = 0.109267 [500 classes]</p> 	

The graph in Figure 4.10 shows that the intensity of undulations is less when heating time is less and sheet-to-fixture distance is more. The fields for heating times of 3 minutes and 3 min. 30 seconds are empty as those experiments did not yield conforming surfaces. The blue and red bars are the surface quality values for 2.125 inch and 2.625 inch sheet-to-fixture distances respectively. The experiment corresponding to the least intensity of undulations is experiment 8 which is different from that of the horizontal surface.

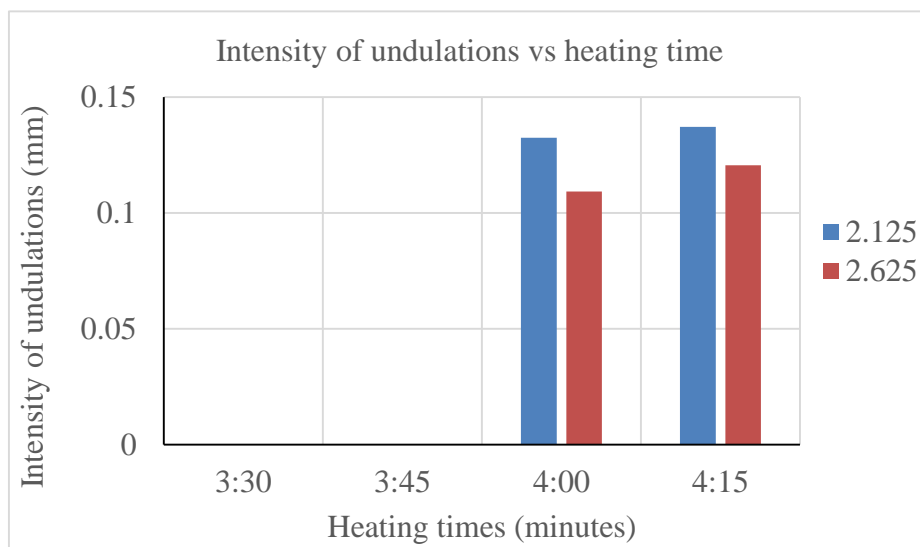


**Figure 4.10: Inclined surface: Intensity of undulations versus heating time**

**(c) Concave parabolic surface**

The pins were actuated to form a concave parabolic shape. The parabolic shape follows the equation  $y = 0.25 \cdot x^2 + 0.6$ . The reason for choosing the equation was to have the top most pin at a distance of 1 inch from the fixturing as shown in Figure 4.11.



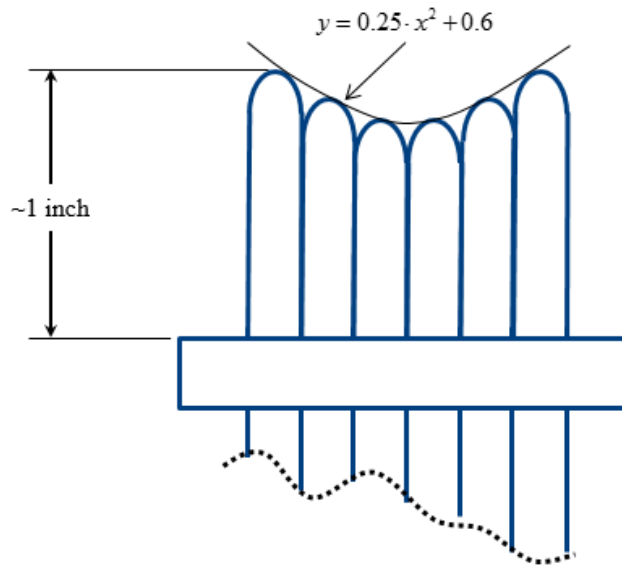


**Figure 4.11: Actuated shape for the concave parabolic surface**

The concave shape was actuated manually using the template shown in Figure 4.12. The template was manufactured by laser cutting a plywood sheet. The shape was actuated by sliding the template on each row of pins and actuating them.

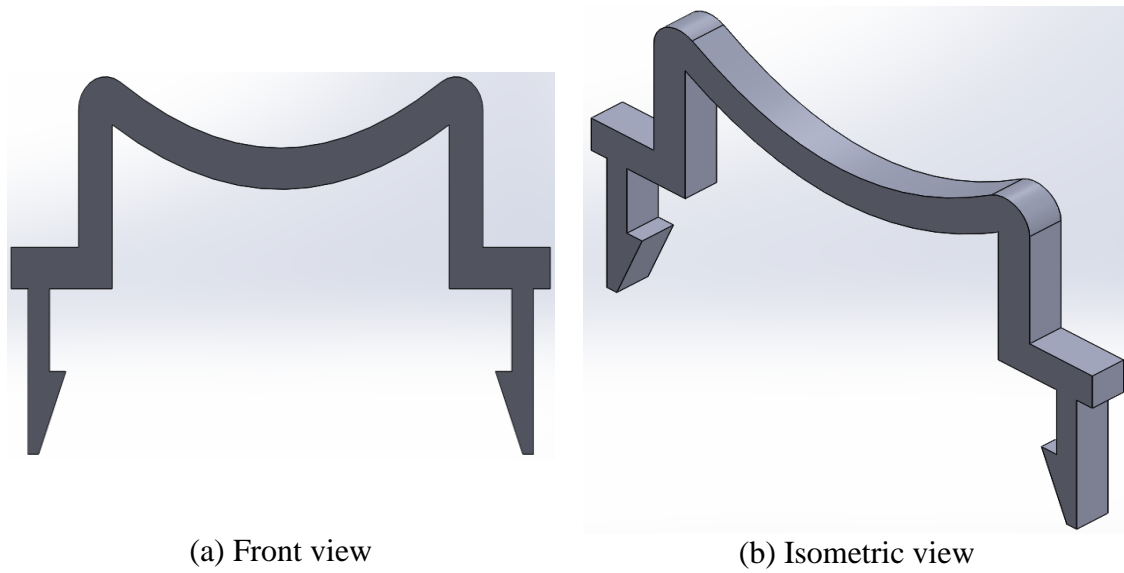


**Figure 4.12: Template for concave shape**

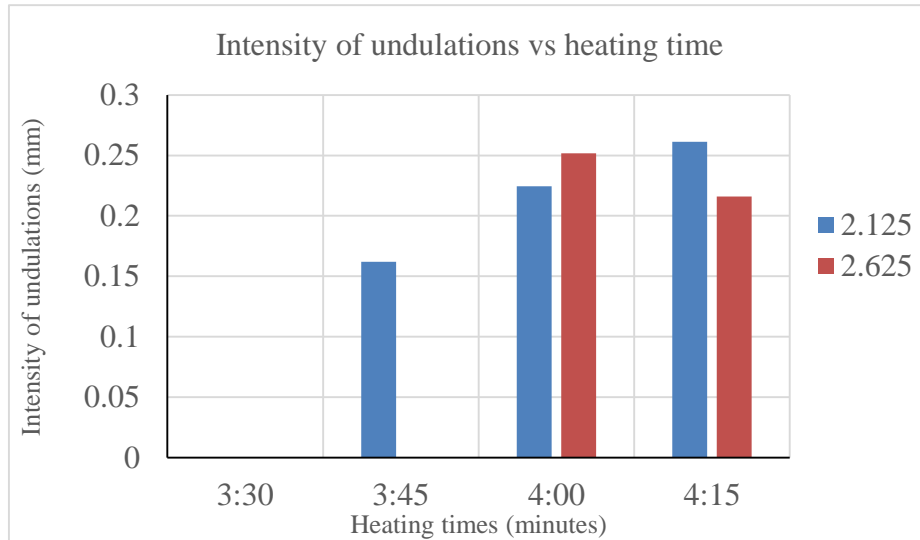
The experiments were conducted as per the setup in Table 4.3. The surfaces produced using the variables pertaining to experiments 1, 2, and 3 produced non-conforming surfaces and were not compared with the desired surface. The surfaces from the other experiments were scanned and their point clouds were compared with that of the desired surface.

Table 4.7 below shows the point cloud comparisons, their means and standard deviations. The least difference between the standard deviations ( $|\sigma_4 - \sigma_8|$ ) is 0.009506 mm which is greater than 0.00027 mm chosen for repeatability in Section 4.3.1.

**Table 4.7: Concave surface point cloud to point cloud distance comparison**

Exp. No.	Mean (mm)	Std. Dev (mm)	Normal distribution	Plot of surface
4	0.000117	0.261332	<p>Gauss: mean = 0.000117 / std.dev. = 0.261332 [633 classes]</p>	
5	0.000124	0.162049	<p>Gauss: mean = 0.000124 / std.dev. = 0.162049 [548 classes]</p>	
6	0.000005	0.21608	<p>Gauss: mean = 0.000005 / std.dev. = 0.216080 [548 classes]</p>	
7	0.000064	0.224352	<p>Gauss: mean = 0.000064 / std.dev. = 0.224352 [548 classes]</p>	
8	0.000105	0.251826	<p>Gauss: mean = 0.000105 / std.dev. = 0.251826 [633 classes]</p>	

The graph in Figure 4.13 shows a plot of intensity of undulations is less and heating times. The empty fields belong to the experiments which resulted in non-conforming surfaces. The blue and red bars are for 2.125 inch and 2.625 inch sheet-to-fixture distances respectively.



**Figure 4.13: Concave surface: Intensity of undulations versus heating time**

The intensity of undulations and heating times have an inverse relationship, and the same is true for the sheet to fixture distance in this case. The intensity of undulations is least for surface produced from experiment 5. The variables associated with experiment 5 were a heating time of 3 minutes 45 seconds and a distance D of 2.125 inches. Again, these variables are different from that of the first two shapes.

**(d) Convex parabolic surface**

A convex parabolic shape is actuated on the pin tool. The parabolic shape is similar to the previous shape, but follows the equation  $y = -0.25 \cdot x^2 + 1$  (see Figure 4.14). The reason for choosing the equation was to have the top most pin at a distance of 1 inch from the fixturing.

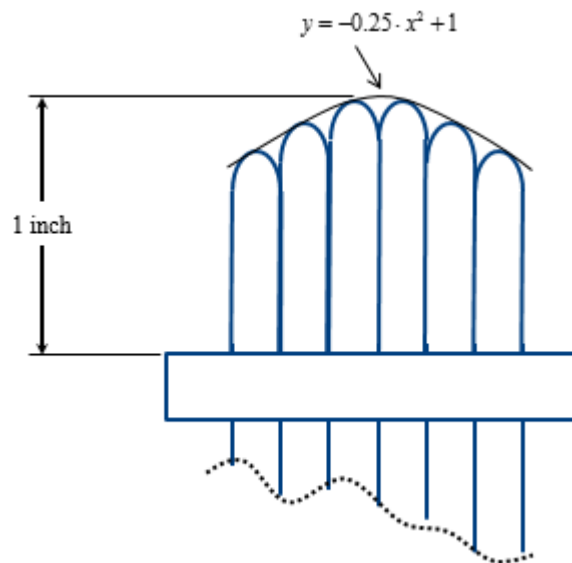


**Figure 4.14: Actuated shape for the parabolic convex surface**

The concave shape was actuated manually using the template shown in Figure 4.12. The template was manufactured by laser cutting a plywood sheet. The shape was actuated by sliding the template on each row of pins and actuating them.

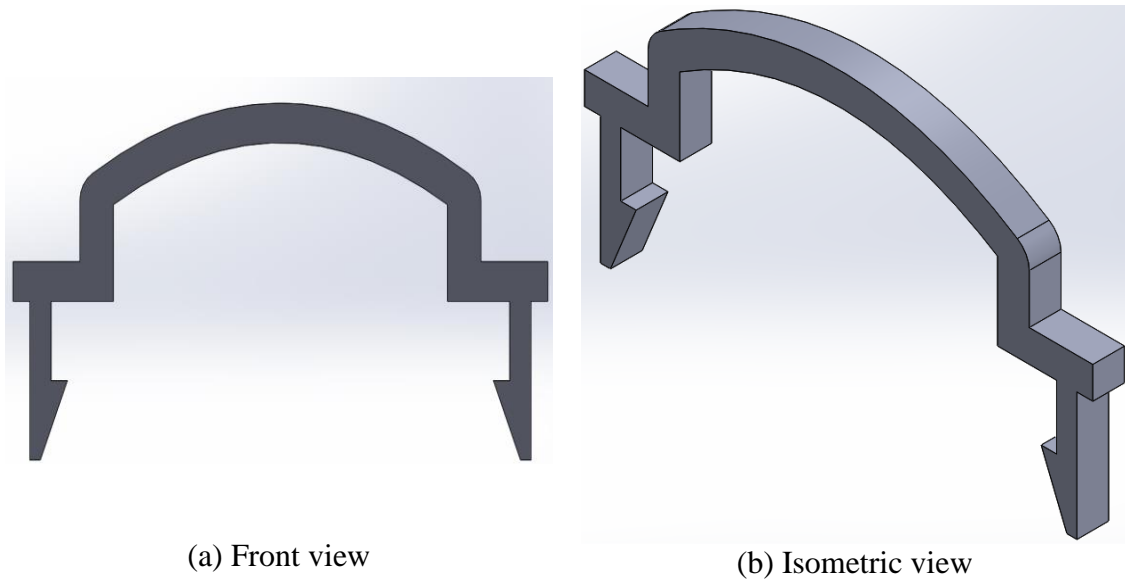


**Figure 4.15: Template for convex shape**

The experiments were conducted for the convex shape according to the DOE setup shown in Table 4.2. Similar to the concave shape, non-conforming surfaces were produced from the variables pertaining to experiments 1, 2, and 3. The surfaces produced from the other experiments were compared to the desired surface in CloudCompare®. The means and the standard deviations of the distances between the two surfaces are shown in Table 4.8.

**Table 4.8: Convex surface point cloud to point cloud distance comparison**

Exp. No.	Mean (mm)	Std. Dev (mm)	Normal distribution	Plot of surface
4	0.000001	0.192952	<p>Gauss: mean = 0.000001 / std.dev. = 0.192952 [548 classes]</p>	
5	0.00001	0.122611	<p>Gauss: mean = 0.000010 / std.dev. = 0.122611 [633 classes]</p>	
6	0.00001	0.191647	<p>Gauss: mean = 0.000010 / std.dev. = 0.191647 [633 classes]</p>	
7	0.000003	0.181716	<p>Gauss: mean = 0.000003 / std.dev. = 0.181716 [633 classes]</p>	
8	0.000003	0.166783	<p>Gauss: mean = 0.000003 / std.dev. = 0.166783 [633 classes]</p>	

A plot of variation of intensity of undulations with respect to heating time is shown in Figure 4.16. Blue and red bars represent surface quality for the 2.125 inch and 2.625 inch sheet-to-fixture distances respectively. The empty entries represent non-conforming surfaces.

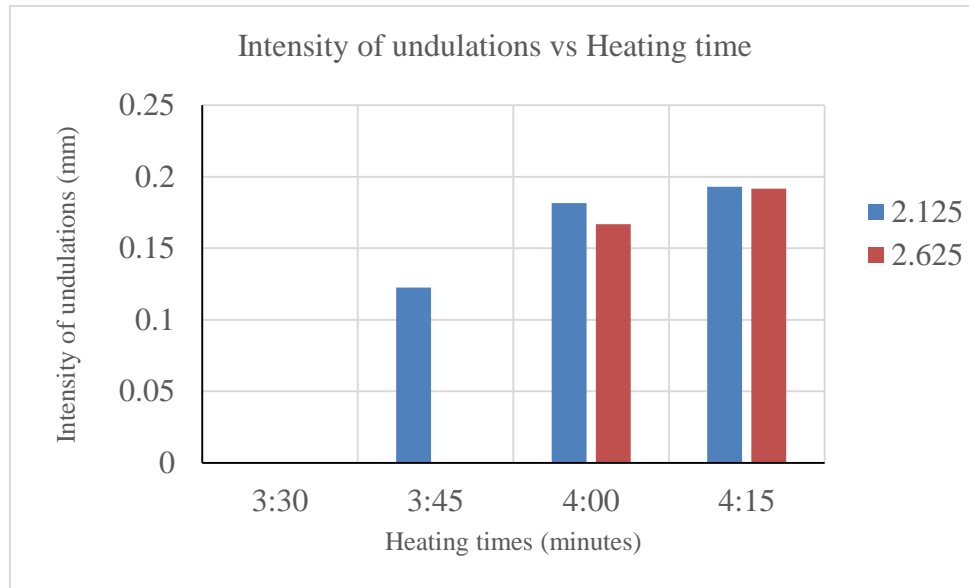


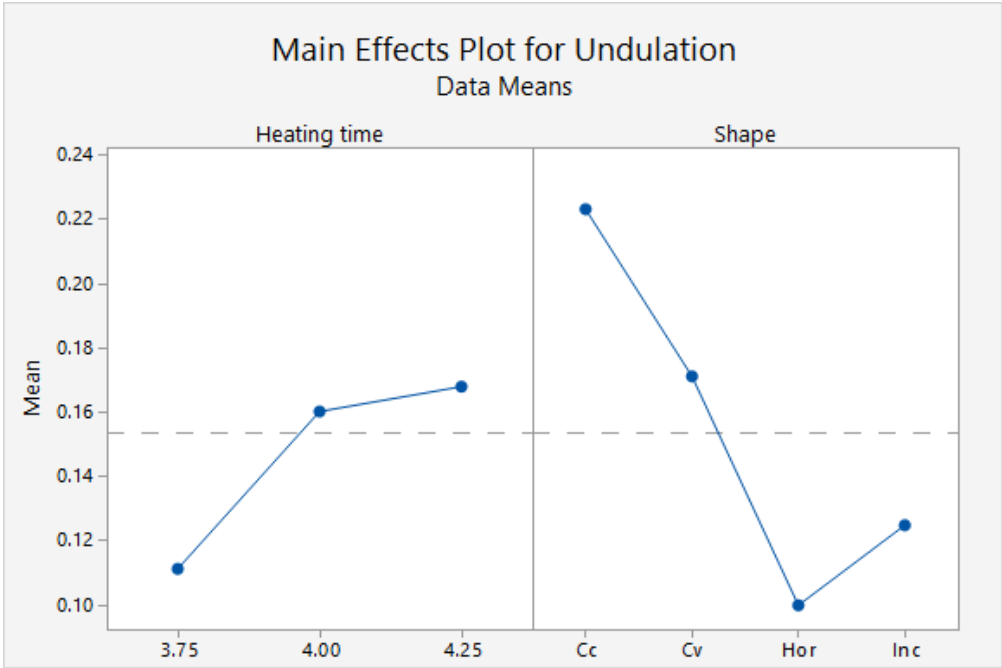
**Figure 4.16: Convex surface: Intensity of undulations versus heating time**

An inverse relationship is exhibited by intensity of undulations and heating times, but the sheet to fixture distance influences the surface quality as well. The experiment that resulted in the best quality of the convex surface was experiment 5, which is the same set of parameters contributing to the best quality of the concave surface.

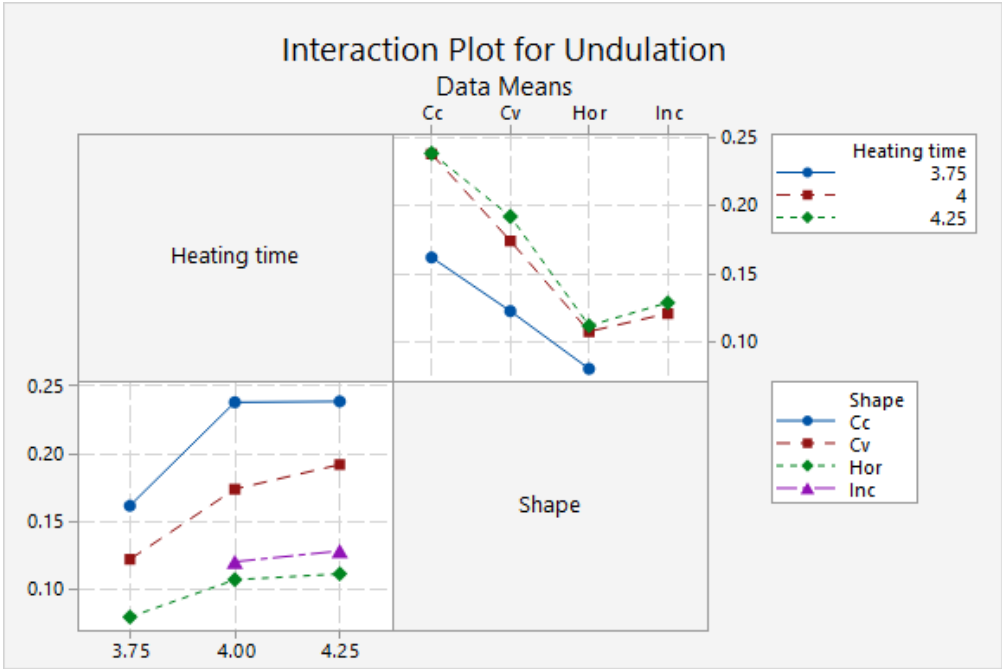
A main effects plot and an interaction plot of intensity of undulations versus heating time and intended shape was generated using Minitab Express®. These plots are shown in



Figure 4.17 and Figure 4.18 respectively, where  $C_c$  is concave,  $C_v$  is convex,  $Inc$  is inclined, and  $Hor$  is horizontal.



**Figure 4.17: Main effects plot of undulations vs heating time and Shape**



**Figure 4.18: Interaction plot of undulations vs heating time and shape**

The shape specific experiments resulted in different set of parameters contributing towards the best quality surface for different shapes. As seen in Figure 4.17 and Figure 4.18, lower heating times resulted in better quality surfaces with the flat shape resulting in the best average quality. The next step, however, is to determine if there is any statistical significance to the hypothesis – optimal process parameters are shape specific. An *Analysis of Variance (ANOVA)* test [42] and Fisher's *Least Significance Difference (LSD)* test [42] were completed to determine the same and will be discussed in detail in the following section.

#### **4.4.3 Analysis of Variance and Least Significant Difference**

It can be intuitively stated that the desired shape is a critical contributor to the quality of the surfaces. It is important to understand the relationship between the shape and the surface quality. The LSD follows the ANOVA and helps to statistically understand the influence of shape on the surface quality.

As quality is indicated by the standard deviations, the means and variances of these standard deviations (observations) was used in the analysis. A hypothesis test using the one way ANOVA and LSD was completed with the hypotheses being:

Null hypothesis,  $H_0$ : The means of the observations of different shapes are equal to each other, i.e.  $\mu_{s1} = \mu_{s2} = \mu_{s3} = \mu_{s4}$ .

Alternate hypothesis,  $H_a$ : At least one of the means is different.

Table 4.9 shows the shapes and their standard deviations summarized.

**Table 4.9: Standard deviations for individual shapes**

Experiment number \ Shape	Horizontal (mm)	Inclined (mm)	Concave (mm)	Convex (mm)
1	0.066598			
2				
3				
4	0.113216	0.137055	0.261332	0.192952
5	0.093855		0.162049	0.122611
6	0.110695	0.120582	0.21608	0.191647
7	0.105794	0.132477	0.224352	0.181716
8	0.109474	0.109267	0.251826	0.166783
<b>Mean (<math>\mu</math>)</b>	0.099938667	0.12484525	0.2231278	0.1711418
<b>Variance (V)</b>	0.000260967	0.000117045	0.001212988	0.00067644
<b>Global Mean (<math>\mu_g</math>)</b>	<b>0.15351805</b>			

A one way ANOVA was conducted for the above standard deviations shown above and a significance level of 0.05 was chosen for the F statistic. Table 4.10 shows the calculations of the one-way ANOVA test, where the following formulae are used.

Total sum of squares (SST) is calculated using

$$SST = \sum_{i=1}^a \sum_{j=1}^{n_i} (\sigma_{ij} - \mu_g)^2 \quad (4.3)$$

Sum of squares within the groups (SSW) is calculated using:

$$SSW = \sum_{i=1}^a \sum_{j=1}^{n_i} (\sigma_{ij} - \mu_i)^2 \quad (4.4)$$

Sum of squares within the groups (SSW) is calculated using

$$SSB = \sum_{i=1}^a n_i (\mu_i - \mu_g)^2 \quad (4.5)$$

Variance between the shapes ( $V_b$ ) is calculated using

$$V_b = \frac{SSB}{n_s - 1} \quad (4.6)$$

Variance within the shape is calculated using

$$V_w = \sum_{i=1}^a \sum_{j=1}^{n_i} \frac{(\sigma_{ij} - \mu_i)^2}{n_i - 1} \quad (4.7)$$

F-statistic is calculated using

$$F - statistic = \frac{V_b}{V_w} \quad (4.8)$$

where; a = number of shapes,  $n_i$  = the number of observations for  $i^{\text{th}}$  shape (standard deviation in this case),  $\sigma_{ij}$  = the  $j^{\text{th}}$  observation for the  $i^{\text{th}}$  shape,  $\mu_g$  = the global mean,  $\mu_i$  = mean of the observations for  $i^{\text{th}}$  shape, and  $n_s$  = total number of observations.

**Table 4.10: One way ANOVA table**

		<b>DOF</b>	<b><math>V_b</math></b>	<b><math>V_w</math></b>	<b>F-statistic</b>	<b><math>F_{\text{critical for } \alpha = 0.05}</math></b>
<b>SST</b>	0.05777471	19			6.80556	3.24
<b>SSW</b>	0.011481121	16		0.00226744		
<b>SSB</b>	0.046293589	3	0.015431196			

The F-statistic from the ANOVA test is significantly larger than the  $F_{\text{critical}}$  obtained from the F-distribution tables in [42]. Therefore, the Null Hypothesis can be rejected, which means the means are statistically not equal to each other. The same hypotheses can be tested pairwise between the shapes using the LSD test. Again, the significance level,  $\alpha$ , was chosen to be 0.05. Table shows the LSD calculations where the least significant difference (LSD) determined by the equation below.

$$LSD = t_{\alpha/2} \cdot \sqrt{V_w^2 \cdot \left( \frac{1}{n_{di}} + \frac{1}{n_{dj}} \right)} \quad (4.9)$$

where,  $\mu_i$  and  $\mu_k$  are the means for  $i^{\text{th}}$  and the  $k^{\text{th}}$  shape respectively,  $t_{\alpha/2}$  is obtained from t-distribution tables for  $\alpha = 0.05$ ,  $V_w$  is the variance within the groups (from ANOVA), and  $n_{di}$  and  $n_{dj}$  are the degrees of freedom for  $i^{\text{th}}$  and the  $j^{\text{th}}$  shape respectively.

The LSD value is then compared with the difference between the means of the concerned shapes. If  $|\mu_i - \mu_k| \geq LSD$ , then the null hypothesis can be rejected for the pairs being compared.

**Table 4.11: LSD calculations table**

<b>Shapes</b>	<b><math> \mu_i - \mu_k </math></b>	<b><math>t_{\alpha/2}</math></b>	<b><math>V_w</math></b>	<b><math>1/n_i</math></b>	<b><math>1/n_j</math></b>	<b>LSD</b>
H and In	0.024906583	2.12	0.00226744	0.166666667	0.25	0.065162561
H and Cc	0.123189133	2.12	0.00226744	0.166666667	0.2	0.0611279
H and Cv	0.071203133	2.12	0.00226744	0.166666667	0.2	0.0611279
In and Cc	0.09828255	2.12	0.00226744	0.25	0.2	0.067718919
In and Cv	0.04629655	2.12	0.00226744	0.25	0.2	0.067718919
Cc and Cv	0.051986	2.12	0.00226744	0.2	0.2	0.06384601

where, H is horizontal, In is inclined, Cc is concave and Cv is convex.

From

Table 4.11, the highlighted fields  $|\mu_1 - \mu_2|$ ,  $|\mu_2 - \mu_3|$ , and  $|\mu_2 - \mu_4|$  are all less than their corresponding LSD. The null hypothesis cannot be rejected while comparing the means of these pairs. For pairs of shapes where  $|\mu_i - \mu_k| < LSD$ , it can be said that the average quality between the compared pairs is not significantly different. These results from the LSD test, though seem contrary to the intuitive inferences made in the previous chapter, can be related back to the intended shape by looking at the means of the observations.

From Table 4.9, the means indicate that the best quality is exhibited by the horizontal shape, whereas the least quality is exhibited by the concave shape. The reason for this could be the type of contact made by the plastic sheet with the pins. An even contact with the pins results in a better quality surface (see Figure 4.19).

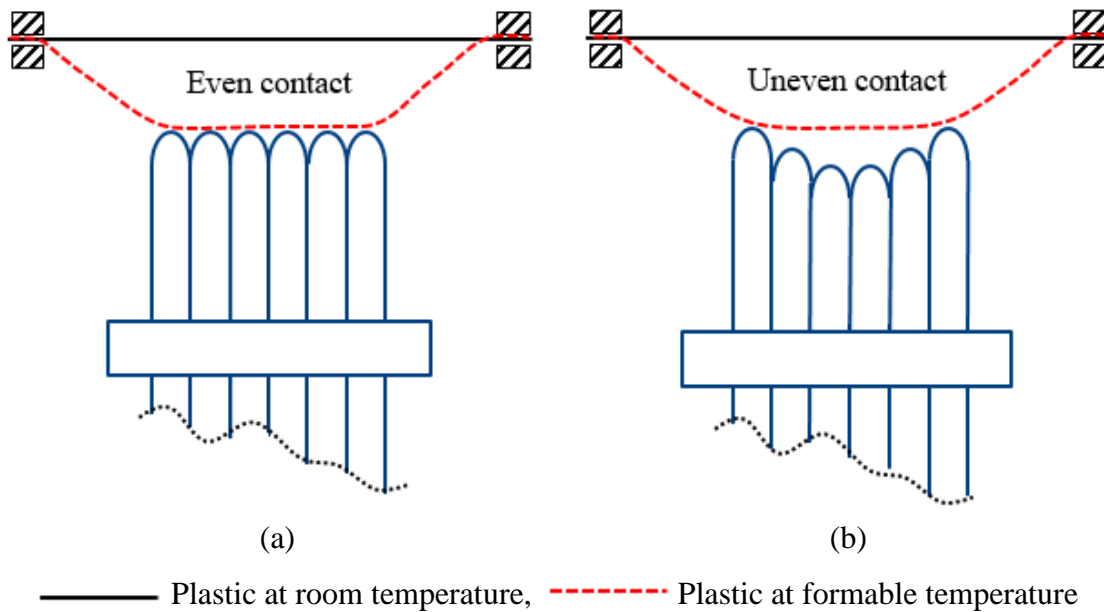


**Figure 4.19: Plastics contact with the pins**



The sheet makes contact with all the pins for horizontal shape, whereas it comes in contact with only two rows of pins. This causes the plastic to stretch in the valley between the two rows of pins due to the vacuum on the other side of the outer most row of pins. On the other hand the convex shape would not result in a valley and hence the pressure from the vacuum would be even underneath the plastic. Therefore, every shape that gives rise to valleys due to uneven contact with the pins will result in least quality surfaces. Thus, the intended shape has a significant influence on the quality of the surfaces produced. The key findings from all the statistically analysis completed in this chapter are summarized in the next section.

#### **4.5 Key conclusions from this chapter**

Experiments for four shapes (horizontal, inclined, concave, and convex surfaces) were conducted and the surfaces were scanned and compared quantitatively. The key findings from these experiments are summarized below:

- The parameters resulting in the best quality surface for each shape were determined and were observed to be different for different shapes.
- The reproducibility of the experimental setup was determined and the cumulative probability of reproducing the surfaces with an error of  $\pm 0.0045$  mm is 98%.
- The repeatability of registration and comparison of the point clouds was determined with a cumulative probability of 99% to repeat the process with an error of  $\pm 0.00027$  mm.
- It was shown quantitatively that higher quality surfaces can be produced by controlling the process parameters, but the optimal set of parameters were different for each shape.

- The results from the ANOVA and the LSD tests indicate that the desired shape significantly influences the quality with concave shapes resulting the least quality surfaces.

The next steps are to summarize the results from both the qualitative and the quantitative analyses, to conclude with key findings from each chapter of this thesis, and to comment on possible future research opportunities. All of the above are discussed in the next chapter.

## CHAPTER 5: CONCLUSIONS AND FUTURE WORK

*The purpose of this chapter is:*

- *To summarize the conclusions from previous chapters.*
- *To discuss these conclusions and key findings.*
- *To lay foundations for potential future research thrusts.*

### **5.1 Conclusions**

In the literature reviewed, different techniques have been developed to address the problem of undulations caused by the pin tool. The most popular among them being the interpolating layer as reducing the pin size has cost implications. Using the interpolating layer adds an additional process when a different shape is required to be formed and hence, is a hindrance to flexibility and reconfigurability.

The literature review led to the following research objectives:

**Research objective 1:** Understand the advantages and limitations of using the pin tool in thermoforming.

**Research objective 2:** Explore the possibility of reducing the intensity of undulations without (a) reducing the pin size and (b) the smoothening membrane.

**Research objective 3:** Understand the effect of the process parameters on the quality of the surfaces produced and identify the significant parameters.

Exploratory experiments were conducted to understand the capabilities of the pin tool as well as check the feasibility of manufacturing undulation-free surfaces without using the

interpolator. It was shown qualitatively that the intensity of undulations can be reduced by controlling the parameters. Through the exploratory experiments, it was also found that the distance between the sheet and the lowest pin (result of the intended shape) significantly influences surface quality. Therefore, it was hypothesized that an optimal set of parameters can be determined, but this set would be particular to the intended shape.

To prove the hypothesis, shape specific experiments were to be conducted. Before conducting shape specific experimentation, reproducibility of the device was determined. Point clouds of surfaces produced using the same set of process parameters were compared with each other. The error with which the device can reproduce a surface was determined by setting up hypotheses and completing a t-test. The error was  $\pm 0.0045$  mm with a cumulative probability of 98%.

The shapes chosen for shape specific experimentation were horizontal, inclined, concave and convex surfaces. The surfaces belonging to individual shapes were produced using the desktop thermoformer. The surfaces that exhibited conformance with respect to the tool were considered for further analysis. The repeatability of comparing point clouds of produced surfaces with that of the intended surface was determined similar to reproducibility. The repeatability error was  $\pm 0.00027$  mm with a cumulative probability of 99%.

The one way ANOVA and the LSD tests support the hypothesis that the desired shape significantly influences the quality of the surfaces produced with concave shapes resulting in least quality surfaces. Thus, the quality of surfaces produced using a pin tool (Q) is a

function of pin dimensions, thermoplastic material, thermoplastic sheet size, and the intended shape.

$$Q = f(T_h, S_i) \quad (5.1)$$

where,  $T_h$  is the heating time, and  $S_i$  is the intended shape.

## **5.2 Future research directions**

The future research directions identified include:

- (a) Studying the influence of a combination of shapes on surface quality by continuing the experimentation. Thereby, determining the optimal distance between the sheet and the pin tips for a controlled conformance.
- (b) Simulating the process by varying the input variables and determining the quality of output surface. Simulation, if comparable to the experimental results, can be used for different pin sizes, different materials, different sheet sizes, and different intended shapes. Simulation will aid in reduction of the number of experiments required to arrive at the optimal set of parameters.
- (c) Extracting pin heights from the desired shape modelled in a Computer Aided Design software by creating an iterative algorithm. A major challenge is to determine the contact point on the hemispherical pin tips. The contact point on each pin would be same for a planar shape, whereas the contact point will be different in the case of a higher order shape (see Figure 5.1).

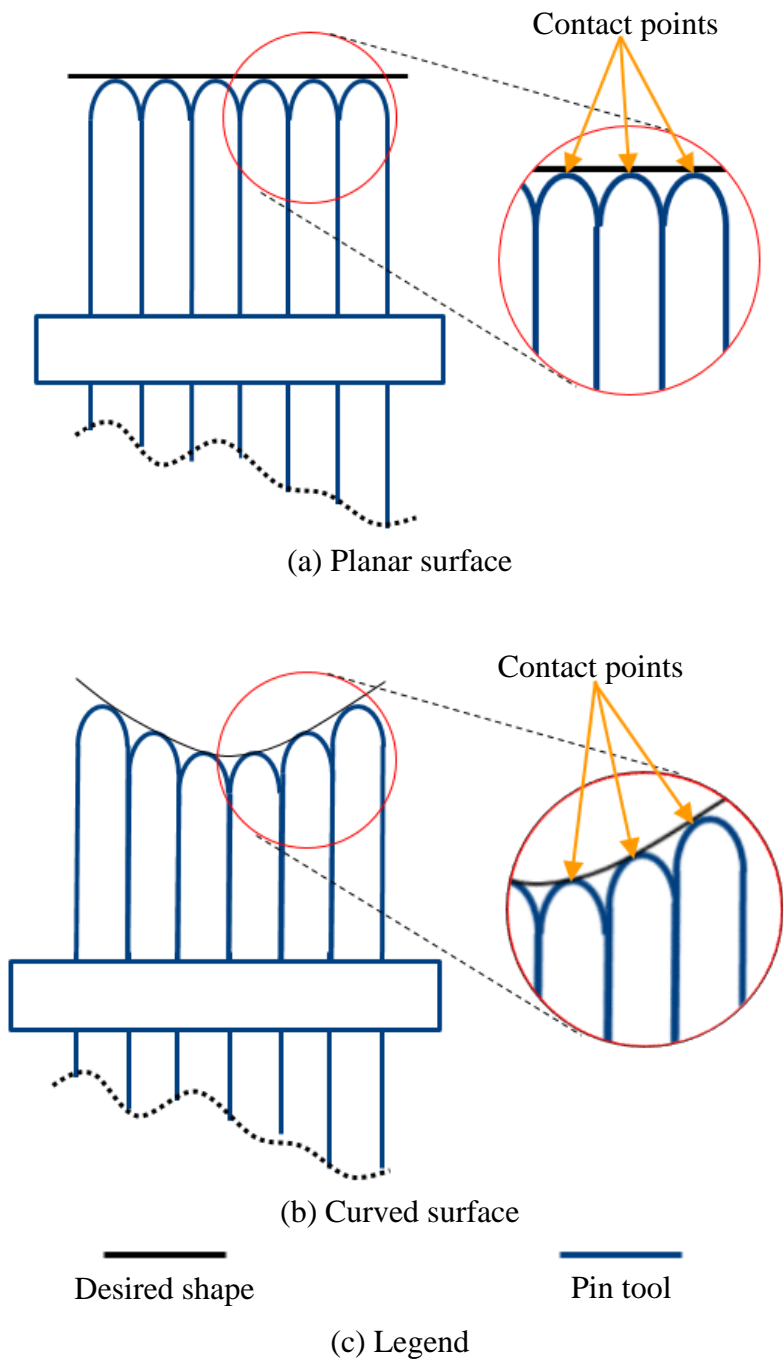


**Figure 5.1: Contact points on the pin tool**

- (d) Using pin heights to automate the actuation process.
- (e) Mathematically modeling the thermoplastic behavior with respect to surface quality based on all the dependent variables so that the learnings can be extended to an industrial thermoformer.
- (f) The possibility of forming polymer and composite sheets with the aid of localized heating and a single point tool (single pin) can be explored.

## CHAPTER 6: REFERENCES

- [1] H. A. ElMaraghy, “Flexible and reconfigurable manufacturing systems paradigms,” *Int. J. Flex. Manuf. Syst.*, vol. 17, no. 4, pp. 261–276, 2005.
- [2] F. Alizon, S. B. Shooter, and T. W. Simpson, “Henry Ford and the Model T: lessons for product platforming and mass customization,” *Des. Stud.*, vol. 30, no. 5, pp. 588–605, 2009.
- [3] R. M. Setchi and N. Lagos, “Reconfigurability and Reconfigurable Manufacturing Systems - State-of-the-art Review,” *Ind. Informatics, 2004. INDIN '04. 2004 2nd IEEE Int. Conf.*, pp. 529–535, 2004.
- [4] W. Fleming, “Vertical Three-Dimensional Image Screen,” U. S. Patent No. 4,654,989, 1987.
- [5] “<http://jopincushion.com/retro-corner-impressions3d-pin-art/> accessed on 11/28/2014 2:33 pm.” [Online]. Available: <http://jopincushion.com/retro-corner-impressions3d-pin-art/>. [Accessed: 01-Jan-2014].
- [6] D. . Tang, W. . Eversheim, G. . Schuh, and K.-S. . Chin, “Concurrent metal stamping part and die development system,” in *Proceedings of the Institution of Mechanical Engineers, Part B: Journal of Engineering Manufacture*, 2003, vol. 217, pp. 805–825.
- [7] “<http://www.in2013dollars.com/2003-dollars-in-2014?amount=20242> accessed on 12/29/2014 2:45 pm.” [Online]. Available: <http://www.in2013dollars.com/2003-dollars-in-2014?amount=20242>.
- [8] T. Altan, B. Lilly, Y. C. Yen, and T. Altan, “Manufacturing of Dies and Molds,” *CIRP Ann. - Manuf. Technol.*, vol. 50, no. 2, pp. 404–422, 2001.
- [9] Iwata, Yano, Nakaizumi, and Kawamura, “Project FEELEX: adding haptic surface to graphics,” in *Proceedings of SIGGRAPH 2001*, 2001, no. 1, pp. 469–475.
- [10] J. Rossignac, M. Allen, W. J. Book, A. Glezer, I. Ebert-Uphoff, C. Shaw, D. Rosen,



- S. Askins, J. Bai, P. Bosscher, J. Gargus, B. Kim, I. Llamas, A. Nguyen, G. Yuan, and H. Zhu, "Finger sculpting with digital clay: 3D shape input and output through a computer-controlled real surface," *Proc. - SMI 2003 Shape Model. Int. 2003*, pp. 229–231, 2003.
- [11] H. Zhu and W. J. Book, "IMECE2004-59743 Practical Structure Design and Control for Digital Clay," in *Proceedings of 2004 International Mechanical Engineering Congress and RD & D Expo, November 21, CA, 2004*, pp. 1–8.
- [12] S. Follmer, D. Leithinger, A. Olwal, A. Hogge, and H. Ishii, "inFORM: Dynamic Physical Affordances and Constraints through Shape and Object Actuation," in *Proceedings of the 26th annual ACM symposium on User interface software and technology - UIST '13, 2013*, pp. 417–426.
- [13] E. W. Anstead, "Machine for Bending and Forming Springs," United States Patent No. 483094, 1892.
- [14] G. T. Pinson, "Apparatus for Forming Sheet Metal," U.S. Patent No. 4,212,188, 1980.
- [15] N. Nakajima, "A newly developed technique to fabricate complicated dies and electrodes with wires, Bull. JSME 12 (54) (1969) 1546–1554."
- [16] D. F. Walczyk and D. E. Hardt, "Design and Analysis of Reconfigurable Discrete Dies for Sheet Metal Forming," *J. Manuf. Syst.*, vol. 17, no. 6, pp. 436–454, 1998.
- [17] A. Kirby and L. A. Stauffer, "Analysis of pin characteristics for a variable geometry mold," *Int. J. Adv. Manuf. Technol.*, vol. 32, no. 7–8, pp. 698–704, Mar. 2007.
- [18] D. F. Walczyk, J. Lakshmikanthan, and D. R. Kirk, "Development of a reconfigurable tool for forming aircraft body panels," *J. Manuf. Syst.*, vol. 17, no. 4, pp. 287–296, Jan. 1998.
- [19] N. J. Cook, G. F. Smith, and S. J. Maggs, "A Novel Multipin Positioning System for the Generation of High-Resolution 3-D Profiles by Pin-Arrays," *IEEE Trans. Autom. Sci. Eng.*, vol. 5, no. 2, pp. 216–222, Apr. 2008.

- [20] M. S. Soderberg, R. A. Starr, L. R. Cook, and R. J. Thomas, "Flexible Tooling Apparatus," United States Patent No. 5722646, 1998.
- [21] D. F. Walczyk and R. S. Longtin, "Fixturing of Compliant Parts Using a Matrix of Reconfigurable," *J. Manuf. Sci. Eng.*, vol. 122, no. 4, pp. 766–772, 2000.
- [22] A. Al-Habaibeh, N. Gindy, and R. M. Parkin, "Experimental design and investigation of a pin-type reconfigurable clamping system for manufacturing," *Proc. Inst. Mech. Eng. Part B J. Eng. Manuf. Vol. 217, No. 12, pp. 1771-1777.*, vol. 217, pp. 1771–1777.
- [23] D. F. Walczyk and D. E. Hardt, "A Comparison of Rapid Fabrication Methods for Sheet Metal Forming Dies," *J. Manuf. Sci. Eng.*, 1999.
- [24] K.-F. Hong, "Molding Mechanism," United States Patent No. 5,281,117, 1994.
- [25] P. L. Hoffman, "Method for Forming Composite Parts Using Reconfigurable Modular Tooling," United States Patent No. 5,846,464, 1998.
- [26] C. Munro and D. Walczyk, "Reconfigurable Pin-Type Tooling: A Survey of Prior Art and Reduction to Practice," *J. Manuf. Sci. Eng.*, vol. 129, no. 3, p. 551, 2007.
- [27] T. H. Pedersen and T. A. Lenau, "Variable Geometry Casting of Concrete Elements Using Pin-Type Tooling," *J. Manuf. Sci. Eng.*, vol. 132, no. 6, p. 061015, 2010.
- [28] D. F. Walczyk, J. F. Hosford, and J. M. Papazian, "Using Reconfigurable Tooling and Surface Heating for Incremental Forming of Composite Aircraft Parts," *J. Manuf. Sci. Eng.*, vol. 125, no. 2, p. 333, 2003.
- [29] G. F. Eigen, "Smoothing Methods for Discrete Die Forming," M.S Thesis, Department of Mechanical Engineering, Massachusetts Institute of Technology, 1992.
- [30] P. V. . Rao and S. G. Dhande, "A flexible surface tooling for sheet-forming processes: conceptual studies and numerical simulation," *J. Mater. Process. Technol.*, vol. 124, no. 1–2, pp. 133–143, Jun. 2002.

- [31] H. S. Kleespies and R. H. Crawford, "Vacuum Forming of Compound Curved Surfaces with a Variable Geometry Mold," *J. Manuf. Syst.*, vol. 17, no. 5, pp. 325–337, 1998.
- [32] M. F. Zäh, F. Hagemann, and S. Teufelhart, "Form-flexible tools for injection molding: Approach for the economic application of injection molding for small lot sizes," *Prod. Eng. Recent Dev. Ger. Acad. Soc. Prod. Eng.*, vol. 3, no. 3, pp. 281–285, 2009.
- [33] D. Simon, L. Kern, J. Wagner, and G. Reinhart, "A Reconfigurable Tooling System for Producing Plastic Shields," in *The 47th CIRP Conference on Manufacturing Systems*, 2014, vol. 17, pp. 853–858.
- [34] A. Kelkar, B. Koc, and R. Nagi, "Rapidly Re-Configurable Mold Manufacturing of Free-Form Objects," in *Proc 2003 ASME Design Engineering Technical Conferences, Chicago, IL, September 2–6, 2003*, 2003, pp. 355–362.
- [35] Z. Wang, "Rapid manufacturing of vacuum forming components utilising reconfigurable screw pin tooling," PhD Dissertation, University of Nottingham, 2010.
- [36] B. J. Halford and O. Gb, "(12) United States Patent," 2013.
- [37] S. Kalpakjian and S. Schmid, *Manufacturing Processes for Engineering Materials*, Fifth. Upper Sadle River, NJ: Pearson Prentice Hall, 2008.
- [38] *Krippendorff, K. (1980). Content analysis. An introduction to its methodology. Beverly Hills, CA: Sage. .*
- [39] D. Freelon, "ReCal OIR: Ordinal, Interval, and Ratio Intercoder Reliability as a Web Service.," *Int. J. Internet Sci.*, vol. 8, no. 1, pp. 10–16, 2013.
- [40] P. Wang and D. Soergel, "A cognitive model of document use during a research project. Study I. Document selection," *J. Am. Soc. Inf. Sci.*, vol. 49, no. 2, p. 120, 1998.
- [41] "Introduction to SAS. UCLA: Statistical Consulting Group. from

<http://www.ats.ucla.edu/stat/sas/notes2/> accessed on 12/3/2015 9.00 am.” [Online]. Available: [http://www.ats.ucla.edu/stat/mult\\_pkg/whatstat/](http://www.ats.ucla.edu/stat/mult_pkg/whatstat/).

[42] M. Longnecker and R. Ott, *An introduction to statistical methods and data analysis*. 2010.

[43] R. Osada, T. Funkhouser, B. Chazelle, and D. Dobkin, “Shape distributions,” *ACM Trans. Graph.*, vol. 21, no. 4, pp. 807–832, 2002.

## APPENDICES

APPENDIX A: SUMMARY OF THE PIN ACTUATION TECHNIQUES IN  
MANUFACTURING

**Table.A.1: Summary of the pin actuation techniques in manufacturing**

<b>Pap er</b>	<b>Applica tion</b>	<b>Matr ix</b>	<b>Over all size</b>	<b>Pin size</b>	<b>Max actuati on height</b>	<b>Pin tip</b>	<b>Actua tion mecha nism</b>	<b>Smoot hing techniq ue</b>	<b>Spacin g betwee n the pins</b>
[15]	Sheet metal forming and electrolytic machining	Not available	1600 wires bundled together	Diameters 1.81 mm and 5.4 mm	200 mm (length)	Flat	NC milling machine	Rubber interpolator	No space
[18]	Sheet metal forming	4 by 4	Not available	19mm bore diameter for hydraulic actuation	Not available	Hemispherical	Hydraulic	Not available	No space
[19]	NA	50 by 50	2500 mm <sup>2</sup>	Square 1 mm by 1mm	Not available	Flat	Shape memory alloy	Not available	No space
[21]	Fixturing	1	Not available	38 OD mm by 29 ID mm	58 mm	Hemispherical	Not available	Not available	No space
[22]	Fixturing	14 by 8	110 mm by 60 mm	5mm dia	Not available	Hemispherical	Not available	Not available	Not available
[23]	Sheet metal forming	64 by 64	Not available	1.59 mm square cross-section	Not available	Hemispherical	Manually placing a shape underneath	Deformable interpolator	No space
[27]	Concrete casting	10 by 6	260 X 433 mm <sup>2</sup>	43.3 mm by 43.3 mm	104.5 mm	Hemispherical	Manual	Polyether foam	No space

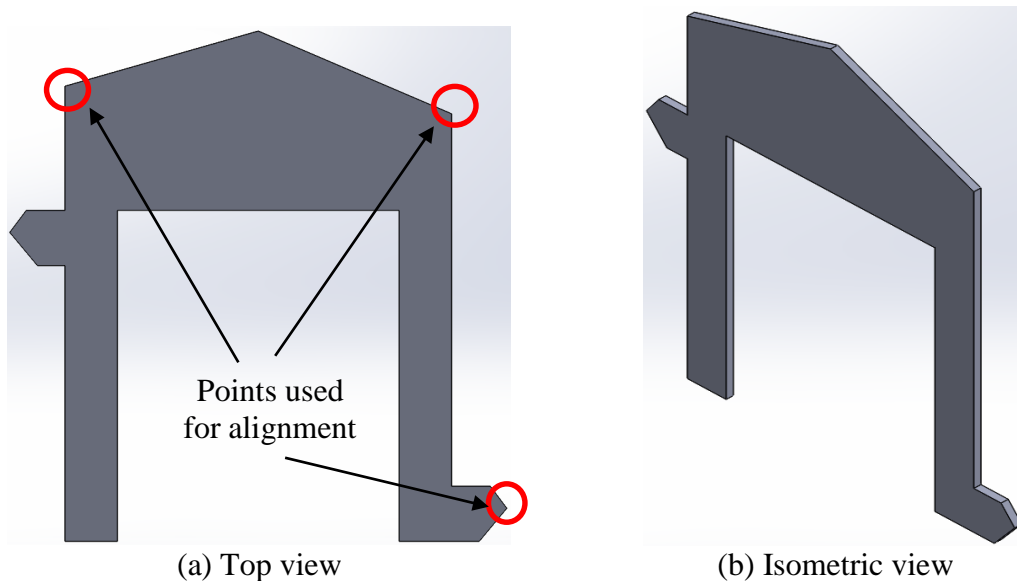
**Table A.1 (continued): Summary of the pin actuation techniques in manufacturing**

<b>Pap er</b>	<b>Applica tion</b>	<b>Matr ix</b>	<b>Over all size</b>	<b>Pin size</b>	<b>Max actuat ion height</b>	<b>Pin tip</b>	<b>Actua tion mecha nism</b>	<b>Smoot hing techniq ue</b>	<b>Spacin g betwee n the pins</b>
[28]	Vacuum forming	8 by 12	NA	26mm by 26 mm	30 cm	Hemispherical	NA	Polyurethane and Polyethylene foam + Silicone diaphragm	No space
[29]	Sheet metal forming	45 by 48	NA	0.25 inch by 0.25 inch	NA	Hemispherical	Hydraulic	Interpolating layer	No space
[32]	Injection molding	NA	100 mm by 100 mm	0.4 mm by 0.4 mm	50 mm	Flat	Using automating machines	Interpolating layer	No space
[35]	Vacuum forming	65 by 98	NA	M20X300 screw-pins	NA	Hemispherical	CNC milling machine	Machining	No space

## APPENDIX B: ALIGNER

A major challenge in comparing the point clouds of the surfaces produced with the intended surface was to align the two in CloudCompare®. To aid the alignment of point clouds, the aligner shown in figure was used. The surfaces were scanned along with the aligner and saved as point clouds. Similarly, the intended shape was modelled with the aligner and converted to point clouds. The aligner was used only to coarsely align the two point clouds, trim the outermost pins (using the point cloud of the intended shape as the reference as reference: further explained in Appendix D). Figure B.1 shows the aligner.

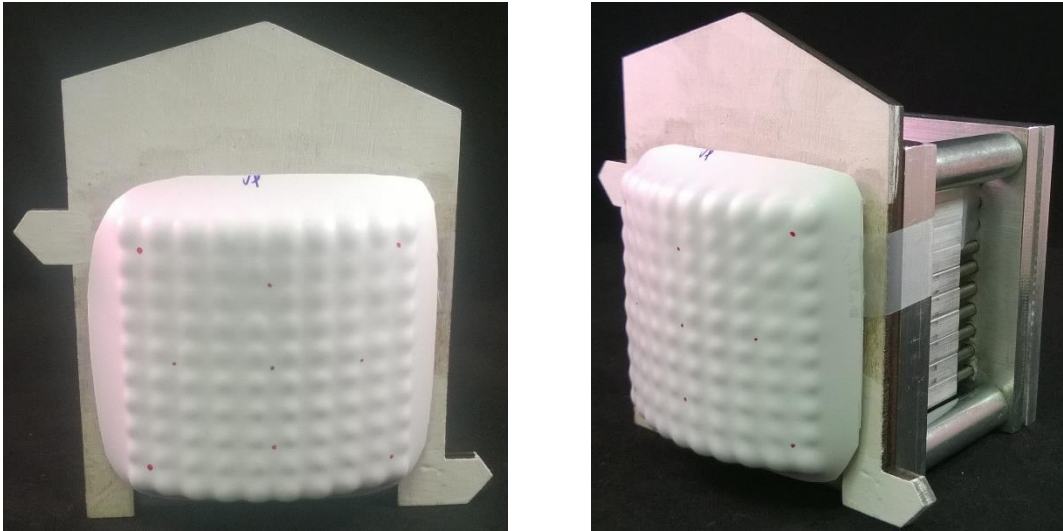
The aligner was manufactured by laser cutting a 5.5mm thick plywood sheet. Though the aligner has 5 points to align, only three were used to align the point clouds. The three points that resulted in the best alignment are highlighted in red circles in both the figures.



**Figure B.1: Aligner**

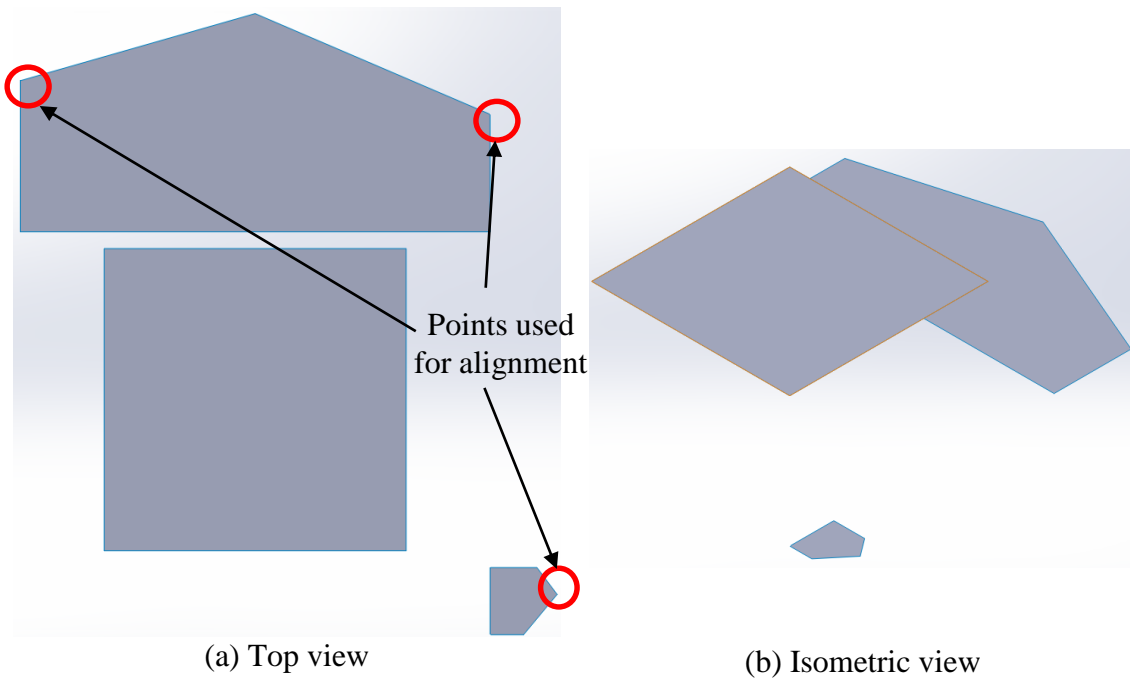


Figure B.2 shows the aligner and the surface mounted on to the pin tool. The surfaces were scanned in this condition.



**Figure B.2: Aligner and the surface mounted on to the pin tool**

Figure B.3 shows one of the intended shape modelled in SolidWorks® as surfaces with features to aid alignment.



**Figure B.3: Horizontal surface modeled with alignment features**

## APPENDIX C: OSADA'S RADOM POINT GENERATOR [43]: MATLAB CODE

The desired surface modelled in SolidWorks® was saved as a .stl file and converted to .xyz file using Osada's random point generator algorithm described in [43]. A MATLAB® code was written and is given below

```
%%Osada's random point generator to convert .stl files to .xyz file%%

clc
close all
clear all

reps = 500000; %number of random points required
histo21= zeros();
histo2= zeros();
histo3= zeros();

input_histo = zeros();

%open the stl file from the specified location
[file_name,input_file_path] = uigetfile('C:\Users\vsreedh\Google
Drive\research\DOE_2\3d scans\11_3_2015\*.stl');
input_file_path = strcat(input_file_path,file_name);

fid = fopen(input_file_path);

%get/read the first line from the .stl file
tline = fgetl(fid);

%'facet normal' indicates the line contains normal vector information
find_this = 'vertex';
rand_points = zeros();
iter = 1;
arr_counter = 1;
global_x = 0;
cumulative_area = 0;
pick_array = zeros();
%loop through all lines to get normal vector information
while ischar(tline)
    pq = zeros();
    pr = zeros();
    pqr = zeros();
    all_coords = zeros();
    %test to see if the line contains 'facet normal'
    test = strfind(tline,find_this);
    if isempty(test)
        %if the line being read does NOT have 'facet normal' then do
```

```

    %nothing
else
    %else explode the string to get its components; delimiter =
    %blankspace
    exploded_str = textscan(tline, '%s %f %f %f');

    %first element of the array is 'vector'
    p_x = exploded_str(1,2);
    p_y = exploded_str(1,3);
    p_z = exploded_str(1,4);

    %the next two rows are also vectors
    for i = 1:2
        tline = fgetl(fid);
        exploded_str = textscan(tline, '%s %f %f %f');
        if i == 1
            q_x = exploded_str(1,2);
            q_y = exploded_str(1,3);
            q_z = exploded_str(1,4);
        end
        if i == 2
            r_x = exploded_str(1,2);
            r_y = exploded_str(1,3);
            r_z = exploded_str(1,4);
        end
    end
end

rand_points(iter,1) = p_x{1};
rand_points(iter,2) = p_y{1};
rand_points(iter,3) = p_z{1};
iter = iter+1;
rand_points(iter,1) = q_x{1};
rand_points(iter,2) = q_y{1};
rand_points(iter,3) = q_z{1};
iter =iter+1;
rand_points(iter,1) = r_x{1};
rand_points(iter,2) = r_y{1};
rand_points(iter,3) = r_z{1};
iter = iter +1;

pick_array(arr_counter,1) = p_x{1};
pick_array(arr_counter,2) = p_y{1};
pick_array(arr_counter,3) = p_z{1};
pick_array(arr_counter,4) = q_x{1};
pick_array(arr_counter,5) = q_y{1};
pick_array(arr_counter,6) = q_z{1};
pick_array(arr_counter,7) = r_x{1};
pick_array(arr_counter,8) = r_y{1};
pick_array(arr_counter,9) = r_z{1};
arr_counter = arr_counter + 1;
end

```

```

    tline = fgetl(fid);
end

for i = 0 : reps
    rand_number = randi([1,arr_counter-1]);
    r1 = rand;
    r2 = rand;
    point_x = ((1-sqrt(r1))*pick_array(rand_number,1)) + (sqrt(r1)*(1-
r2)*pick_array(rand_number,4))+
((sqrt(r1)*r2)*pick_array(rand_number,7));
    point_y = ((1-sqrt(r1))*pick_array(rand_number,2)) + (sqrt(r1)*(1-
r2)*pick_array(rand_number,5))+
((sqrt(r1)*r2)*pick_array(rand_number,8));
    point_z = ((1-sqrt(r1))*pick_array(rand_number,3)) + (sqrt(r1)*(1-
r2)*pick_array(rand_number,6))+
((sqrt(r1)*r2)*pick_array(rand_number,9));
    rand_points(iter,1) = point_x;
    rand_points(iter,2) = point_y;
    rand_points(iter,3) = point_z;
    iter= iter + 1
end

%%storing the points generated as a .xyz file
dat_file_name = strcat(strrep(input_file_path, '.STL', ''), '.xyz');
csvwrite(dat_file_name,rand_points);

```

## APPENDIX D: COARSE ALIGNMENT AND REGISTRATION ON CLOUDCOMPARE®

A step by step procedure of aligning the point clouds and measuring the distance between them is given below.

### **D.1 Opening the point clouds**

The point clouds are opened by clicking on the open file icon and selecting the files from their location on the computer. Figure D.1 shows the user interface of CloudCompare® and the open file icon is labelled.

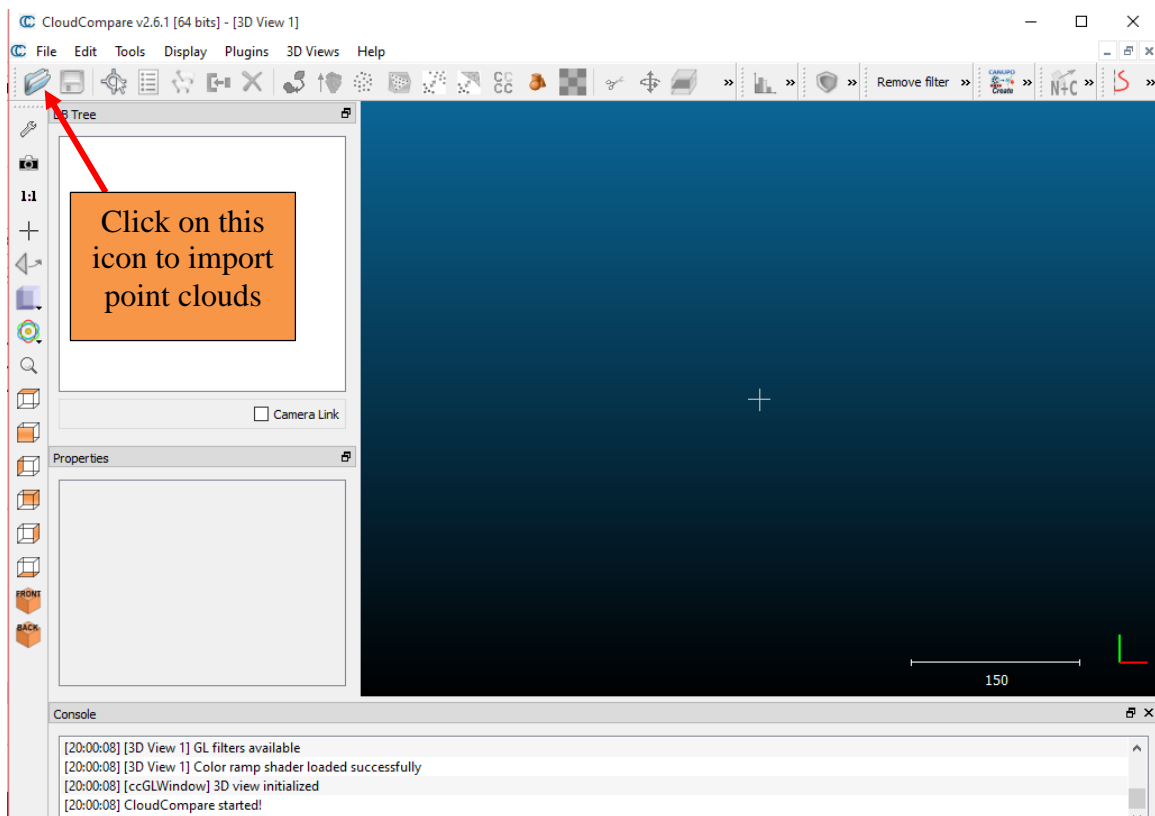


**Figure D.1: User interface of CloudCompare®**

Figure D.2 shows the pop-up window displayed before the point cloud is imported.

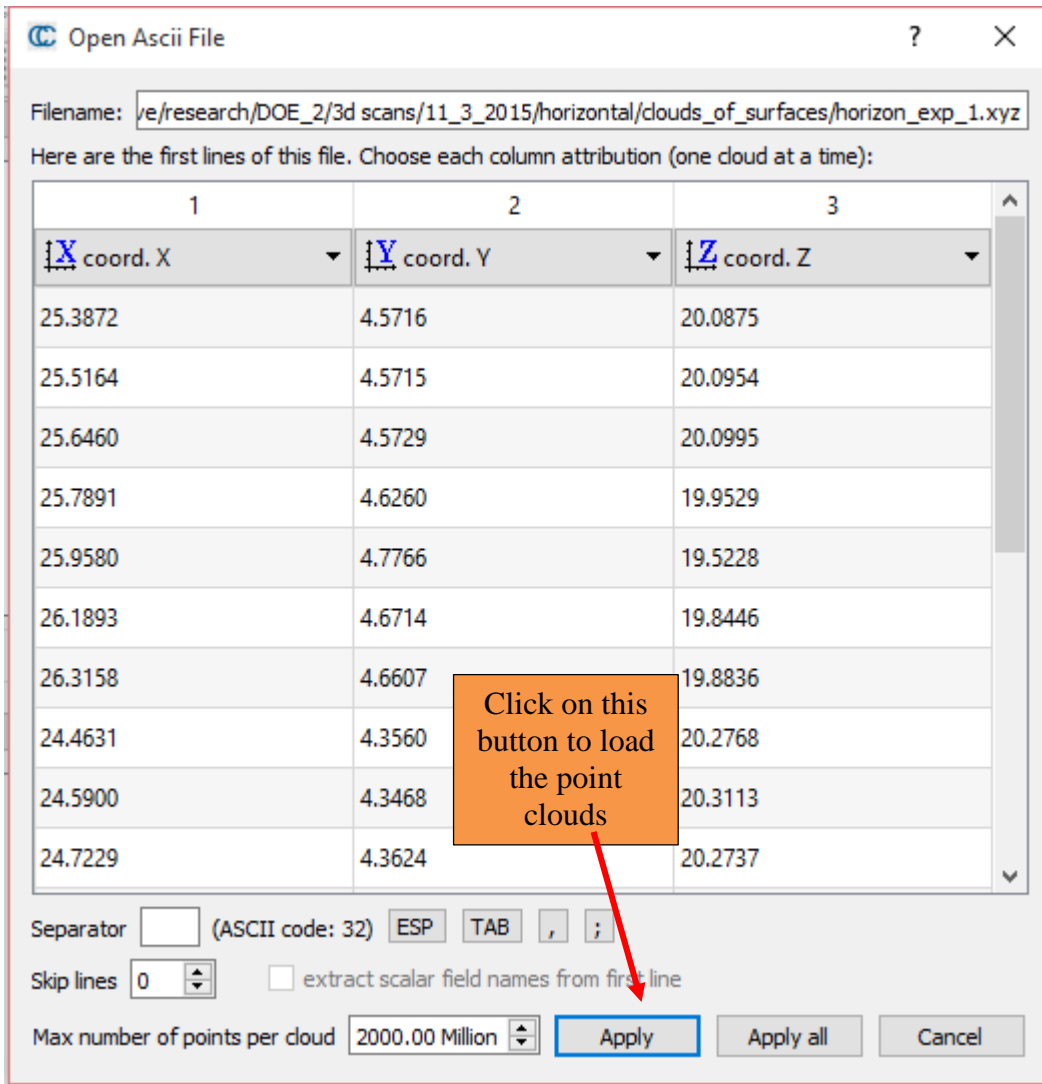


**Figure D.2: Pop-up window to complete importing point clouds**

## **D.2 Orientation and 3-point registration**

The next step after importing the point clouds is to orient them using the orient tool (labelled in Figure D.3) so that there is no overlap between the clouds and then align them

coarsely using the 3 point registration tool. Figure D.3 shows the orient tool and the 3-point registration tool icons labelled.

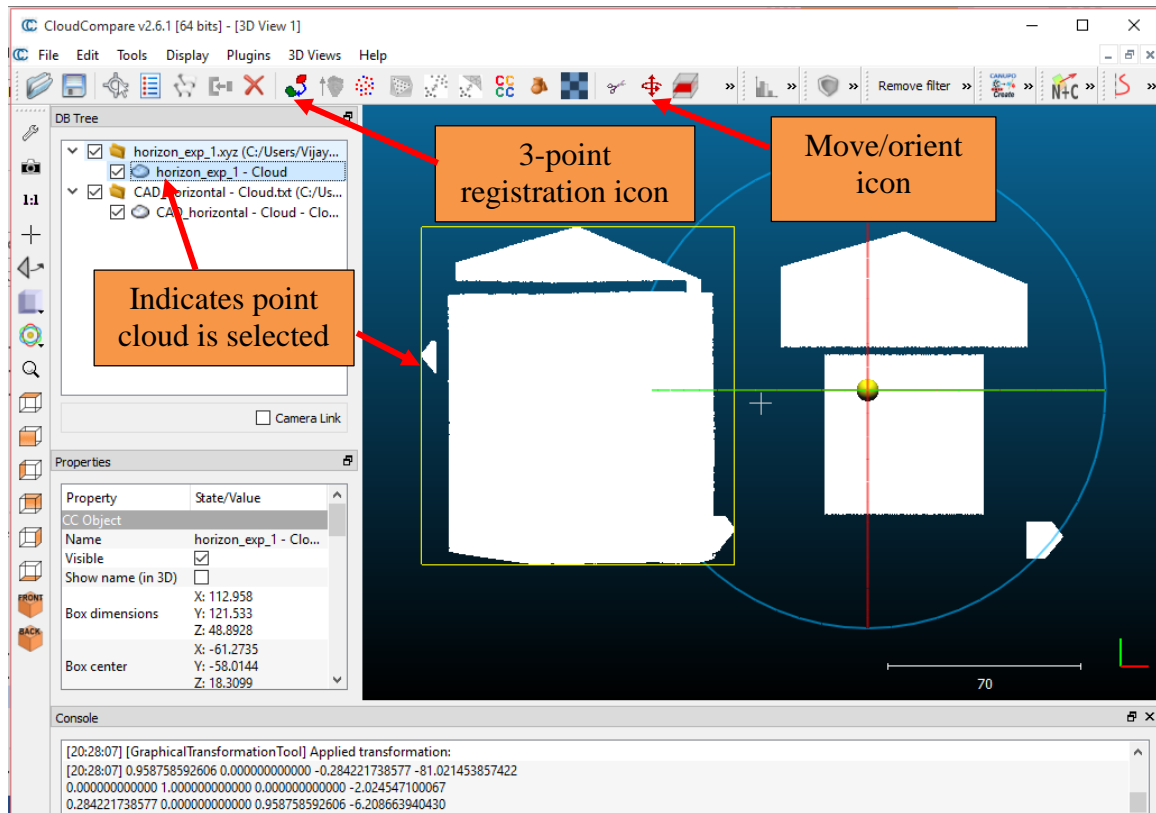


**Figure D.3: Move/orient and 3-point registration icons**

It is important to note that these icons are enabled only when at least one of the point clouds is selected (indicated by the yellow bounding box on the user interface in Figure D.3). Figure D.4 shows the pop-up window where the reference cloud and to be aligned cloud could be swapped. Both the point clouds are to be selected for 3-point registration. The reference cloud is highlighted in yellow and the to-be-aligned cloud is highlighted in red.



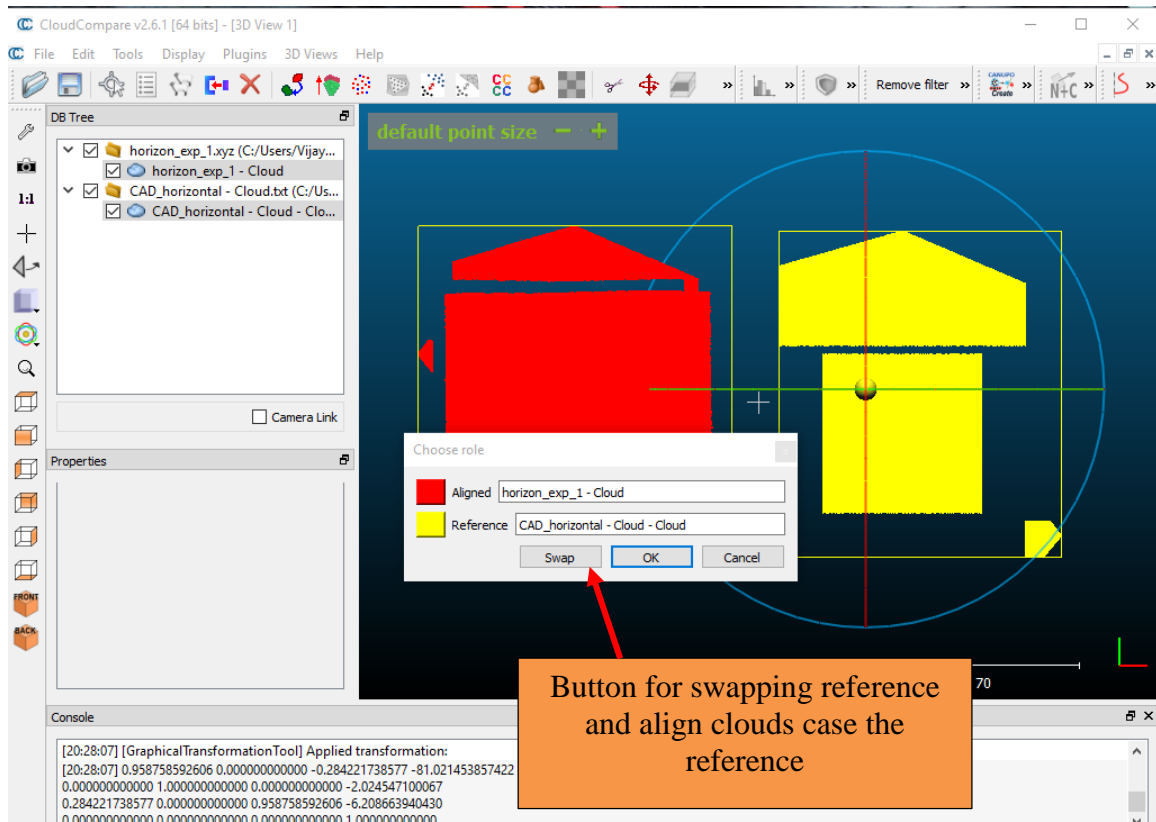


**Figure D.4: Pop-up to swap the reference and to-be-aligned clouds**

The next step is to align the clouds by selecting the alignments points on both the clouds. This is shown in Figure D.4. The alignment points are shown in pink at the three corners and the achievable root mean square error between the three points is shown at the top of the screen.

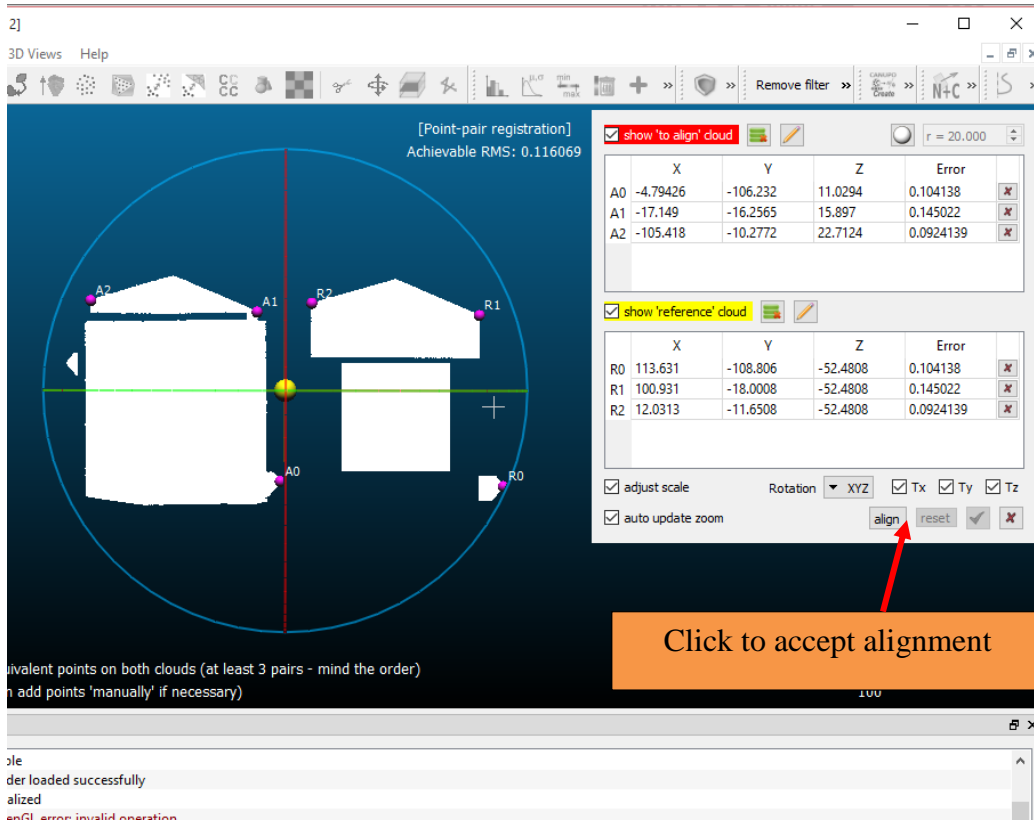


**Figure D.5: 3 point registration for coarse alignment**

The align button shown on Figure D.5 is clicked followed by the check mark which will be highlighted. This aligns the two clouds.

### **D.3 Trimming the aligned cloud**

The next step is to trim the aligned surface using the desired surface. Clicking the check mark beside the aligned surface's cloud on the model tree on the left side will hide its visibility. Thus the outline of the reference cloud can be used to trim the aligned cloud.

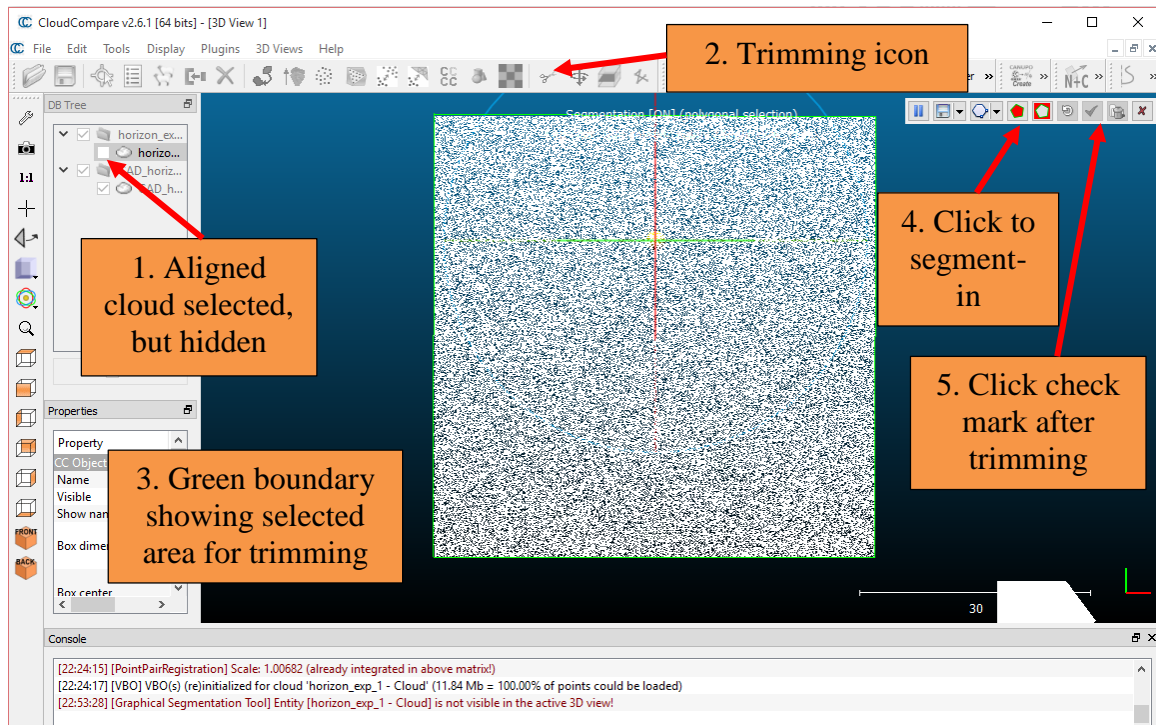
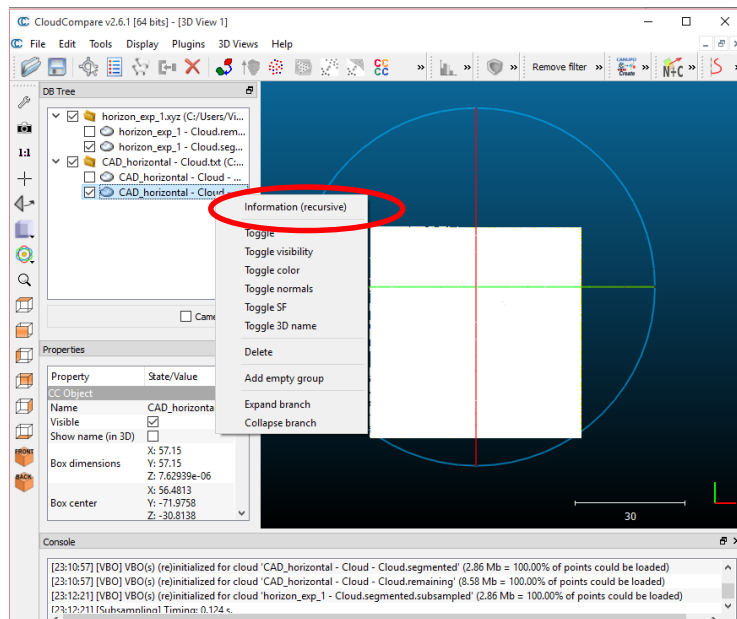


**Figure D.6: Sequence of operations for trimming**

The labels in Figure D.6 show the order in which trimming is carried out. The selection is done by drawing lines along the reference cloud's boundary and using the right click to complete the tracing. There are two buttons to trim: (a) segment in which retains the selection, and (b) segment out which removes the selection. The check mark highlighted once one of the two trim buttons are clicked. Upon clicking the check mark, trim operation will be completed. Similarly the aligner part of the reference cloud can be trimmed.

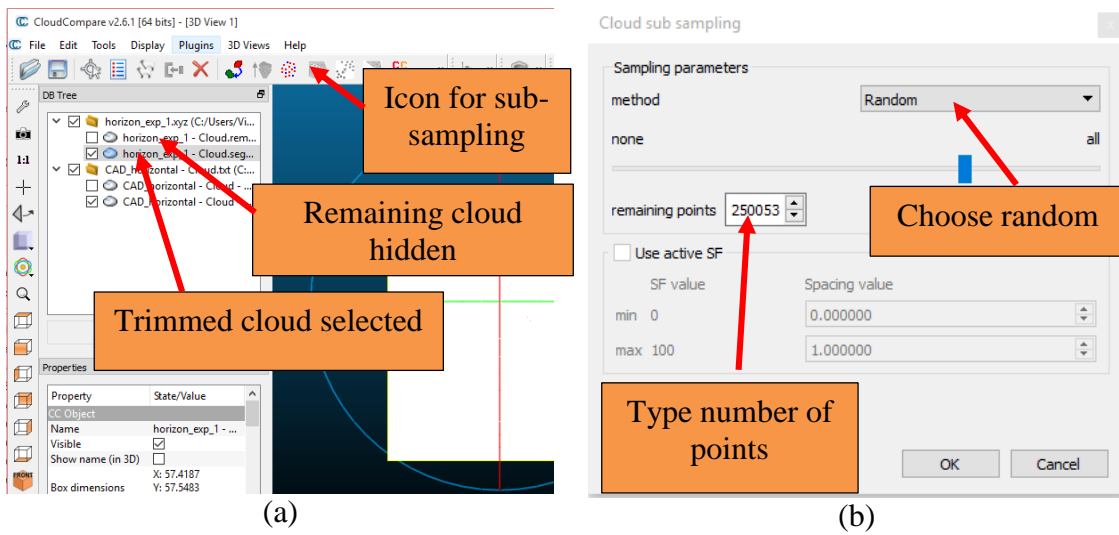
## D.4 Sub-sampling and registration

The next step is to sub-sample the trimmed cloud so that the reference cloud and the trimmed cloud have the same number of points. This will help registering the surfaces using the register tool. The number of points in the reference cloud can be determined by right clicking on the reference cloud in the model tree and then left-clicking on the Information field (see Figure D.7).



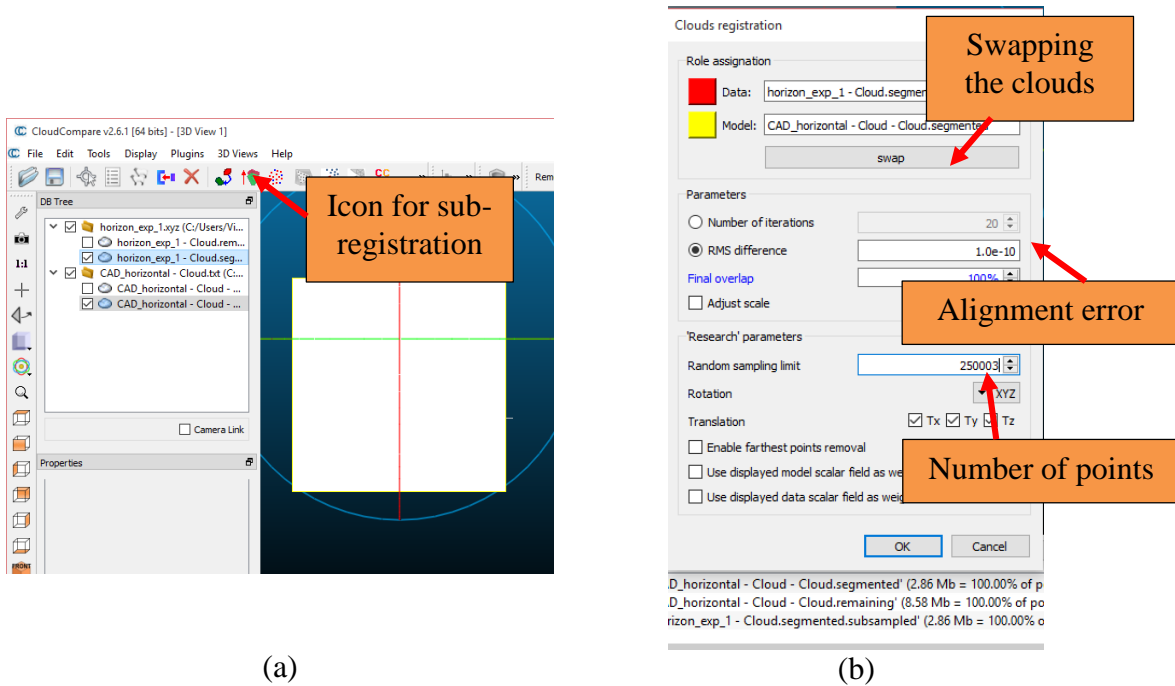
**Figure D.7: Procedure to determine the number of points in the reference cloud**

Figure D.8 shows the subsampling procedure. The subsampling will be complete as soon as the OK button is clicked on (Figure D.8(b)).



**Figure D.8: Sequence of operations for trimming**

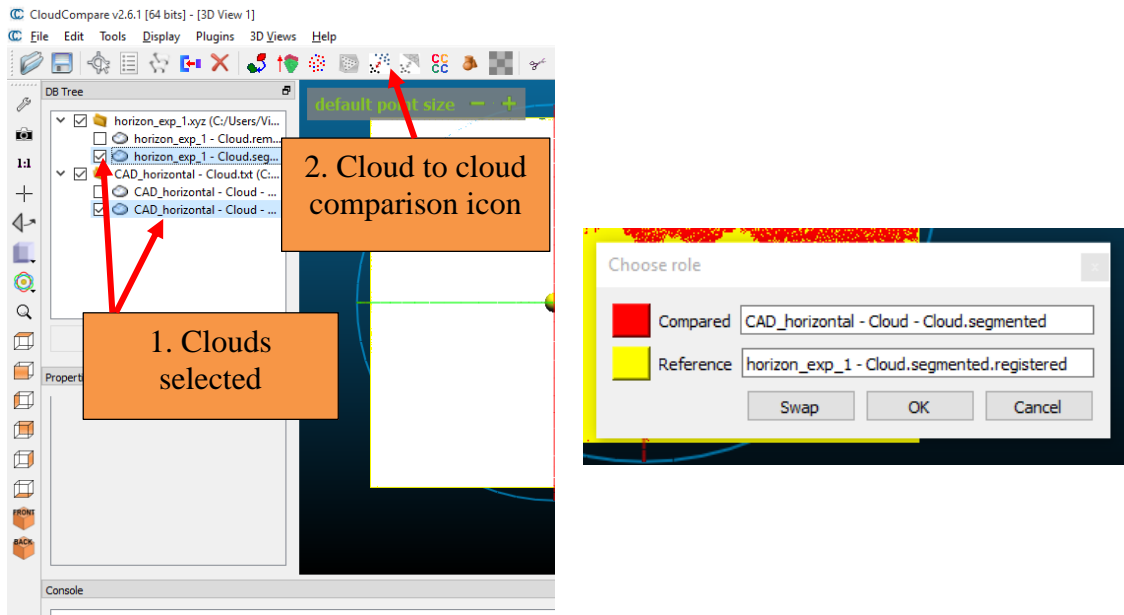
Figure D.9 shows the registration icon on the interface. As soon as the registration icon is clicked, a pop-up window is displayed which is shown in Figure D.9(b).



**Figure D.9: Sequence of operations for fine registration**

## **D.5 Comparing the clouds**

The next step is to compare the clouds. This is accomplished by clicking the cloud to cloud compare icon on the interface shown in Figure D.10. A pop-up window opens similar to the ones in 3 point registration and fine registration steps (Figure D.10 (b)). Again, both clouds have to be selected to be compared.



(a)

(b)

**Figure D.10: Sequence of operations for fine registration**

As soon as OK is clicked on Figure D.10(b), another pop-up window is displayed on the screen as shown in Figure D.11. An Octree level of 8 is chosen and the box beside split X, Y and Z components is checked to compute distances in all three directions.

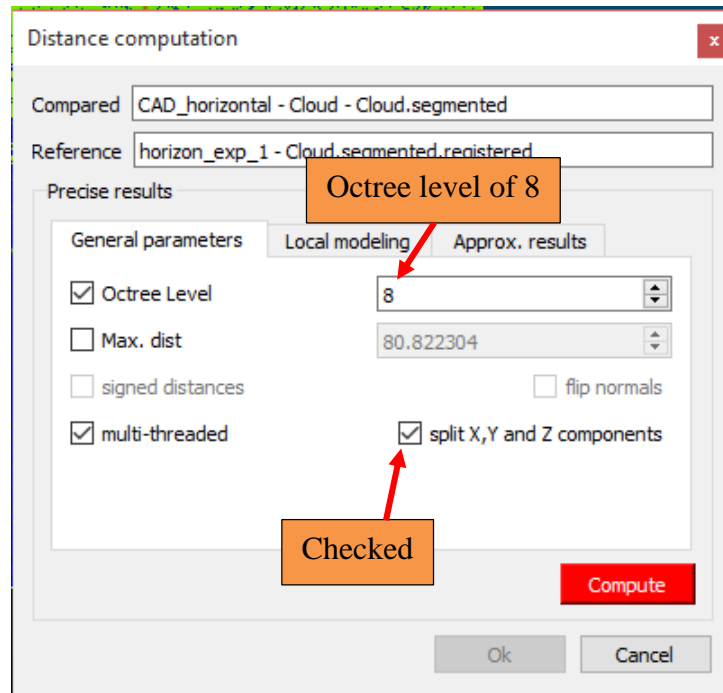


**Figure D.11: Octree level and splitting the X, Y, and Z components**

The distances computed appear as a contour plot on the point clouds. This is shown in Figure D.12. Figure D.12 (a) shows the location of selection to choose the z distances and Figure D.12 (b) shows the cloud to cloud distance in the z direction.



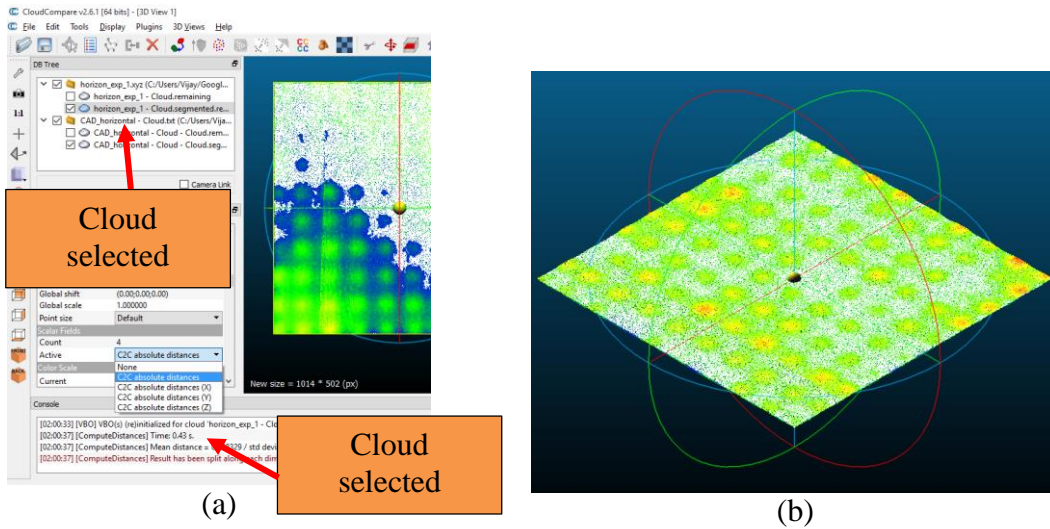


**Figure D.12: Sequence of operations to extract cloud to cloud z distances**

Figure D.13(a) shows the icon to plot the frequency distribution of cloud z distances. Figure D.13(b) shows the frequency distribution.

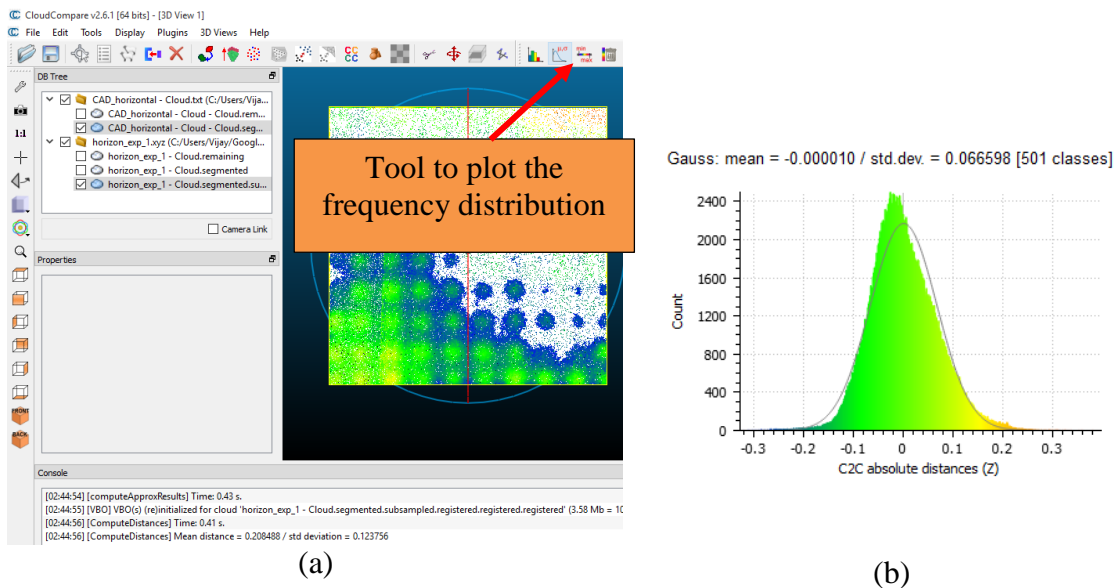


**Figure D.13: Sequence of operations for frequency distribution of z distances**

## APPENDIX E: HYPOTHESES TESTS

### **E.1 Hypotheses test for Reproducibility**

Ten surfaces were produced with the same input parameters. The point cloud of first surface was considered as a benchmark and the point clouds of the rest were compared to it. The Table E. below shows the comparison between the surfaces through mean and standard deviations.

**Table E.1: Comparison of surfaces with benchmark surface for reproducibility**

<b>Experiments</b>	<b>Mean (mm)</b>	<b>Standard deviation (mm)</b>
1 and 2	0.0709	0.035704
1 and 3	0.07327	0.032976
1 and 4	0.068979	0.030971
1 and 5	0.070478	0.031886
1 and 6	0.070623	0.031614
1 and 7	0.074868	0.04151
1 and 8	0.079085	0.047362
1 and 9	0.070569	0.031355
1 and 10	0.069643	0.029324

The absolute difference between the means was calculated pairwise resulting in thirty six differences. A hypotheses test was setup based on the mean of these differences. The pairwise mean differences are shown in Table E.

**Table E.2: Pairwise mean differences**

<b>Sl.no.</b>	<b>Pairs</b>	<b><math>\Delta\mu =  \mu_i - \mu_j </math> (mm)</b>
1	1-10 and 1-2	0.001257
2	1-10 and 1-3	0.003627
3	1-10 and 1-4	0.000664
4	1-10 and 1-5	0.000835
5	1-10 and 1-6	0.00098
6	1-10 and 1-7	0.005225
7	1-10 and 1-8	0.009442
8	1-10 and 1-9	0.000926
9	1-9 and 1-2	0.000331
10	1-9 and 1-3	0.002701
11	1-9 and 1-4	0.00159
12	1-9 and 1-5	0.000091
13	1-9 and 1-6	0.00054
14	1-9 and 1-7	0.004299
15	1-9 and 1-8	0.008516
16	1-8 and 1-2	0.008185
17	1-8 and 1-3	0.005815
18	1-8 and 1-4	0.010106
19	1-8 and 1-5	0.008607
20	1-8 and 1-6	0.008462
21	1-8 and 1-7	0.004217
22	1-7 and 1-2	0.003968
23	1-7 and 1-3	0.001598
24	1-7 and 1-4	0.005889
25	1-7 and 1-5	0.00439
26	1-7 and 1-6	0.004245
27	1-6 and 1-2	0.000277
28	1-6 and 1-3	0.002647
29	1-6 and 1-4	0.001644
30	1-6 and 1-5	0.000145
31	1-5 and 1-2	0.000422
32	1-5 and 1-3	0.002792
33	1-5 and 1-4	0.001499
34	1-4 and 1-2	0.001921
35	1-4 and 1-3	0.004291
36	1-3 and 1-2	0.00237
<b>Mean (mm)</b>		<b>0.003445222</b>
<b>SD (mm)</b>		<b>0.00294493</b>

The average of the pairwise mean differences is about 0.00344 mm and hence, a value of 0.0045 mm ( $\Delta\mu_t =$  hypotheses average mean difference) was chosen for the hypotheses test. The hypotheses are:

Null hypothesis,  $H_0$ : The difference between the means,  $\Delta\mu_t \geq 0.0045$  mm.

Alternate hypothesis,  $H_a$ : The difference between the means,  $\Delta\mu_t < 0.0045$  mm.

A t test was completed with a significance level  $\alpha = 0.05$ . The  $p_{\text{critical}}$  value was determined to be 0.019315 and the null hypothesis was rejected as  $p_{\text{critical}} < \alpha$ . The cumulative probability for the alternative hypothesis to be true is 98.07%.

## **E.2 Hypotheses test for repeatability of registration**

To determine the repeatability of the registration method, point cloud of a surface was compared nine times to the point cloud of its intended shape by following the method described in Appendix D. Table E. summarizes the mean distance and standard distributions for all repetitions.

**Table E.3: Comparison of surfaces for repeatability of registration**

<b>Sl. No.</b>	<b>Mean (mm)</b>	<b>Standard deviation (mm)</b>
1	-0.00001	0.066598
2	0.00000	0.06688
3	0.000034	0.066571
4	0.000032	0.06666
5	-0.000012	0.066478
6	0.000002	0.066333
7	0.000064	0.066847
8	-0.000072	0.066459
9	0.000032	0.066674

The absolute difference between the stand deviations was calculated pairwise resulting in thirty six differences. A hypotheses test was setup based on these differences. The pairwise standard deviation differences are shown in

**Table E.4: Pairwise standard deviation differences**

<b>Sl.no.</b>	<b>Pairs</b>	<b><math>\Delta\sigma =  \sigma_i - \sigma_j </math> (mm)</b>
1	9 and 1	0.000076
2	9 and 2	0.000206
3	9 and 3	0.000103
4	9 and 4	0.000014
5	9 and 5	0.000196
6	9 and 6	0.000341
7	9 and 7	0.000173
8	9 and 8	0.000215
9	8 and 1	0.000139
10	8 and 2	0.000421
11	8 and 3	0.000112
12	8 and 4	0.000201
13	8 and 5	0.000019
14	8 and 6	0.000126
15	8 and 7	0.000388
16	7 and 1	0.000249
17	7 and 2	0.000033
18	7 and 3	0.000276
19	7 and 4	0.000187
20	7 and 5	0.000369
21	7 and 6	0.000514
22	6 and 1	0.000265
23	6 and 2	0.000547
24	6 and 3	0.000238
25	6 and 4	0.000327
26	6 and 5	0.000145
27	5 and 1	0.00012
28	5 and 2	0.000402
29	5 and 3	0.000093
30	5 and 4	0.000182
31	4 and 1	0.000062
32	4 and 2	0.00022
33	4 and 3	0.000089
34	3 and 1	0.000027
35	3 and 2	0.000309
36	2 and 1	0.000282
<b>Mean (mm)</b>		<b>0.000212944</b>
<b>SD (mm)</b>		<b>0.000134992</b>

The average of the pairwise standard deviation differences is about 0.000213 mm and hence, a value of 0.00027 mm ( $\Delta\sigma_t =$  hypotheses average standard deviation difference) was chosen for the hypotheses test. The hypotheses are:

Null hypothesis,  $H_o$ : The difference between the standard deviations,  $\Delta\sigma \geq 0.00027$  mm.

Alternate hypothesis,  $H_a$ : The difference between the standard deviations,  $\Delta\sigma < 0.00027$  mm.

A t test was completed with a significance level  $\alpha = 0.05$ . The  $p_{\text{critical}}$  value was calculated to be 0.007917 and the null hypothesis was rejected as  $p_{\text{critical}} < \alpha$ . The cumulative probability for the alternative hypothesis to be true is 99.21%.